SCHOOL OF ENGINEERING AND APPLIED SCIENCE

CHEMICAL REACTION ENGINEERING LABORATORY

REPORT FOR THE PERIOD

June 1, 1988 - May 31, 1989

WASHINGTON UNIVERSITY / ST. LOUIS / MISSOURI 63130

REPORT

June, 1988 - May, 1989

CHEMICAL REACTION ENGINEERING LABORATORY

Department of Chemical Engineering

Washington University

St. Louis, Missouri 63130

Dr. M. P. Duduković

Director of the Laboratory

INTRODUCTION

Our Chemical Reaction Engineering Laboratory (CREL) remains committed to excellence in graduate student education through research, and to advancing the reaction engineering methodology in processing and preparation of materials and chemicals. We are indebted to all participating companies for supporting us in the above goals and in helping us establish CREL as a unique place for reaction engineering research.

There are several features that make CREL unique. So far we have not focussed all our activities into a very narrow field. Rather, our students are pursuing a broad spectrum of industrially relevant problems that involve transport-kinetic interactions. Through our weekly meetings and informal seminars all our students gain considerable breadth, well beyond the narrow boundaries of their own project. However, the breadth of our activities in no way has impaired the depth of our research. Not only that each thesis produced in CREL results in publication in top quality refereed journals but in many of the areas studied (e.g. fluidized bed for silicon growth, Czochralski crystal growth, trickle-beds, rotating packed beds, composites, etc.) our contributions have been recognized as being at the leading edge of current research. This fact that we do so many things, and do them all very well, should be considered our unique strength. We could not have achieved this without the steady support of our industrial sponsors. The breadth of our research reflects the diversity of their interests. The depth of our research reflects our commitment to fundamentals and represents a significant payback to the companies that have seeded the ideas for a particular project.

In summary, we are committed to excellence in reaction engineering and to maintaining a mutually beneficial partnership with our industrial sponsors. Only through such a partnership can we buffer the whims of federal funding and maintain a steady course and leadership in reaction engineering which is the cornerstone of chemical engineering.

TABLE OF CONTENTS

SUMMARY OF MAIN ACTIVITIES

During the period from June 1, 1988 through May 31, 1989 research activities in CREL were concentrated in the following three main areas:

1. Multiphase reactors
2. Preparation of new materials
3. Expert systems and control

The underlying theme is the improved understanding and quantification of transport-kinetic interactions through modeling and experimentation resulting in safer, faster and more accurate reactor selection for scale-up and design.

Here, we will briefly summarize the highlights of each area leaving it to the individual projects to emphasize the specific objectives and accomplishments.

1. Multiphase Reactors

Our research in this field spans a variety of projects from the traditional trickle-bed and bubble column reactors, through novel rotating packed beds, pulse reactors, etc., to the currently glamorized area of reactors for mammalian cell growth.

Our main goals are:

i) to invent, introduce, develop and quantify novel experimental techniques for measurement of flow and/or transport characteristics;

ii) to emphasize the use of first principles in the development of hydrodynamic and/or reactor models;

iii) to invent and investigate novel reactor types.

Our main accomplishments during the past year in the above area were as follows:

i) We have established a computer aided radioactive particle tracking (CARPT) facility and shown that valuable information on liquid recirculation and turbulence can be obtained in bubble columns (N. Devanathan). The use of the technique allows proper evaluation of different distributors and column designs. The technique can be extended to other reactor types. A new interpretation for tracer data of nonadsorbing and adsorbing tracers was developed in assessing maldistribution of the external fluid in packed beds and successfully demonstrated on experimental trickle beds (P. Hanratty). An appropriate, molecular flow, model has been developed for interpretation of adsorption-desorption measurements in the novel TAP reactor (B. S. Zou).

ii) A fundamentally based, phenomenological model was developed for the low gas-liquid interaction flow regime in trickle-beds. The model, with no adjustable parameters fitted to two-phase flow data, predicts well pressure drop, liquid holdup and transition to pulsing (R. Holub). A model that involves first principles has been developed for a DC plasma reactor (S. Pirooz).

iii) Significant progress has been made in characterizing the liquid structure in rotating packed beds where a fundamental model predicts well liquid holdup data collected with a novel implementation of impedance measurements (A. Bašić). A novel reactor has been successfully developed for growth of mammalian cells on novel matrix supports (V. Kalthod). This effort has progressed well in full collaboration with our Medical School (Dr. W. Pierce) and with our Biotechnology Laboratory (Dr. A. Prokop).

We have initiated three new projects in this area. An external loop, recycle packed bed reactor, is being developed (M. Al Dahhan) for studies of gas-solid catalyzed reactions at low to moderate pressures ($<$ 10 atm) and moderate to high temperatures (25°C to 600°C). It is in this operational range that basket type reactors are often unsatisfactory due to inadequate elimination of external mass transfer resistance, or due to failure to approach the perfect mixing limit. This project has the full support of Autoclave Engineers who are modifying and donating the necessary hardware. Potential uses of heat regenerators with phase change materials are being investigated (H. Erk) as well as the regenerator-reactor concept. Finally, we are approaching the problem of NO_x abatement from stationary sources (J. Turner) by developing a generic methodology of catalytic reactor design. We are attempting to provide a rationale and guidance for design of catalytic channels that must maximize mass transport to the wall while minimizing pressure drop.

2. Preparation of New Materials

The projects in this area focussed on the problems in new materials preparation that could profit the most from implementation of reaction engineering principles in handling transport-kinetic interactions. Our goal is the implementation of reaction engineering in such processes in order to speed up scale-up and technology transfer to manufacturing.

The problems studied varied from production of polycrystalline silicon to manufacture of high performance long-fiber reinforced thermoplastic composites. A complete model has been developed to describe silicon particle growth via agglomeration in aerosol ("free space") reactors for silane pyrolysis (Y. B. Yang). The model indicates that growth of large particles ($>$ 20 μm) is possible only in a multistage system with interstage dilution of the particle number concentration. A model for oxygen transport and incorporation into silicon has been developed for the Czochralski crystal growth technique (D. Dorsey). A variant of this model, to be implemented on a PC, should allow the practitioners to regulate their oxygen content at a desired level. The role of oxidation rate in determination of particle size and morphology in preparation of iron oxide particles for magnetic recording media has been better understood and quantified and should help in improved operation of the process (D. O'Connor).

Modeling of the process cycle of thermoplastic composites (I. S. Yoon) and modeling of volatiles removal in such composites (Y. B. Yang) has resulted in a better fundamental understanding of the long fiber composites manufacturing process. This in turn leads to an improved ability to select correct processing conditions for composites of different thickness.

3. Expert Systems and Control

We are making sure that our students get exposed to the constant advances in computer technology and provide them with opportunities to utilize and modify these by applying them to problems of reactor design and materials preparation. Our goal is to investigate the potential of expert systems in a number of situations and develop the most promising ones into useful engineering tools. How to implement knowledge based control in catalytic reactor design (P. Hanratty) and in manufacture of composites via the autoclave process (H. T. Wu) are studies in progress. Other studies involve application of genetic algorithms and neural networks (F. Wang), development of automatic knowledge acquisition procedures (D. Shieh) and investigation of the effect of model inaccuracies on model based control (K. Kage).

Regarding other news about graduate students, we can report that Yubo Yang successfully completed his D.Sc. thesis entitled "Transport-Kinetic Effects in Manufacture of Polycrystalline Silicon" in December 1988. Yubo's work demonstrated the need for fundamentals. Had first principles been followed by many who attempted to grow large silicon particles in a "free space" reactors, they would have realized that this cannot be accomplshed in a single stage unit. This realization alone would have saved them millions of dollars! Yubo has remained as a post-doctoral fellow in training at CREL and has shifted his work to composite modeling where he has already accomplished a major task by completing a devolatilization model.

Donald Dorsey completed his D.Sc. thesis entitled "Oxygen Transport in Czochralski Growth of Single Crystal Silicon" in December 1988. Don joined the Air Force Materials Laboratory at the Wright Patterson Air Force Base in Dayton, Ohio, where he is currently pursuing modeling of molecular beam epitaxy (MBE). CREL training proved invaluable since in less than 6 months at the Air Force, Don has already contributed a major scientific paper on MBE! Dan O'Connor, S. Pirooz and B. S. Zou defended successfuly their D.Sc. proposals during the 1988/89 academic year. Mr. Richard Holub got married in Spring, 1988 to one of our ex-undergraduates (Sandra MacKellar) and upon planned graduation in Summer 1989 will take a post with the Ethyl Corporation in Baton Rouge. We are happy to welcome M. Al Dahhan, H. Erk, K. Kage, D. Shieh and F. Wang as new CREL graduate students. We wish well to S. J. Choi who after having contributed significantly to our composites modeling effort, left to pursue other goals.

We would also like to welcome Autoclave Engineers to the family of our industrial sponsors. Their additional support of the recycle reactor project is particularly appreciated.

CREL remains involved in cooperative research efforts with the Biotechnology Laboratory, Gasche Laboratory, Materials Research Laboratory and our Medical School. During the past 12 months we remained active in publishing the results of our research. CREL's productivity in doctoral degrees granted, number of graduate students and papers published, is shown in Table 1. To keep things in perspective one should compare CREL's degrees with the total for the department and whole engineering school over the same time period which are also given in the same Table. CREL's funding is summarized in Table 2. Three professors, M. P. Dudukovic, B. Joseph and P. A. Ramachandran continue to channel their research activities through CREL.

TABLE 1

CREL PRODUCTIVITY

DOCTORAL DEGREES GRANTED FOR WORK IN CREL:

1986-87: 4	R. DAVE	-	COMPOSITES (JOINTLY WITH MRL)
	S. S. JANG	-	ON-LINE CONTROL
	S. MUNJAL	-	ROTATING PACKED BED
	K. MYERS	-	BUBBLE COLUMN
1987-88: 3	E. BEAUDRY	-	TRICKLE BEDS
	S. LAI	-	FLUIDIZED BED - SILICON
	B. THOMAS	-	ELECTROCHEMICAL REACTORS
1988-89: 2	D. DORSEY	-	CZ CRYSTAL GROWTH OF Si
	Y. YANG	-	AEROSOL REACTOR FOR Si GROWTH

TOTAL DOCTORAL DEGREES GRANTED	86/87	87/88	88/89
CREL	4	3	2
CHEMICAL ENGINEERING	5	4	3
SCHOOL OF ENGINEERING	15	16	18

NUMBER OF CREL GRADUATE STUDENTS (RESEARCH ASSOCIATES)

YEAR	84/85	85/86	86/87	87/88	88/89
NUMBER	9(1)	12(2)	10(3)	10(2)	16(1)

CONTRIBUTIONS TO THE LITERATURE

	84/85	85/86	86/87	87/88
CREL JOURNAL PUBLICATIONS	15	14	18	21
ChE DEPT. TOTAL JOURNAL PUBLICATIONS	40	29	37	31
ENG. SCHOOL - TOTAL PUBLICATIONS	175	157	150	161

TABLE 2

CREL FUNDING

	84/85	85/86	86/87	87/88	88/89
INDUSTRIAL FEES	120,000	130,000	122,500	120,000	120,000
INDUSTRIAL FELLOWSHIPS	35,000	35,000	35,000	-	25,000
JPL	144,000	55,000	-	-	-
EPRI		70,000	70,000	70,000	57,240
NSF	43,000	-	-	123,880	133,200
	342,000	290,000	227,000	313,880	335,440

INDUSTRIAL PARTICIPATION FEES ARE VITAL TO THE CONTINUITY OF THE CREL CONCEPT WHICH IS UNIQUE IN CRE.

LISTING OF ACTIVE PROJECTS

Projects active during the period June 1, 1988 through May 31, 1989 are classified into three categories of multiphase reactors, preparation of new materials and expert systems with control. The projects working titles and graduate students involved are listed below:

Area I. MULTIPHASE REACTORS

Name		Title: key words
N. Devanathan	1.	Investigation of Liquid Hydrodynamics in Bubble Columns via a Computer Automated Radioactive Particle Tracking Facility: New experimental technique for monitoring of liquid recirculation and turbulence as a function of design and operating parameters.
R. Holub	2.	Hydrodynamics in Trickle-Bed Reactors: New diagnostic model for assessment of liquid maldistribution with experimental verification. New pressure drop-holdup model proposed and tested against data. Transition to pulsing predicted.
P. Hanratty	3.	Tracer Studies in Trickle-Bed Reactors: Novel way of tracer data interpretation confirmed experimentally to lead to assessment of external liquid flow pattern.
A. Basić	4.	Hydrodynamics and Mass Transfer in Centrifugal Gas-Liquid Contactors: Novel three phase reactor. Experimental study of liquid holdup confirms new developed model.
B. S. Zou	5.	Quantification of the Mass Spectrometer Measured Responses of a Pulse, Catalytic Microreactor (The TAP Experiments): Monte Carlo simulations of mass spectrometer and responses and microreactor modeling lead to interpretation of pulse responses for nonadsorbing, adsorbing, and reacting tracers.
S. Pirooz	6.	Modeling of DC Plasma Reactors: Calculation of electron and ion densities in various plasma regions.
H. Erk	7.	Modeling of Cyclic Processes: Heat Regenerators Utilizing Phase Change Materials: Determination of optimal efficiencies for regenerators with phase change materials. Periodic operation of reactor-regenerators for exo-endothermic reactions.

J. Turner

8. Optimal Catalytic Reactor Design:
Chemical Reaction Engineering Aspects of NO_x Abatement:
Optimal honeycomb and tube configurations that maximize transport to the wall at minimum pressure drop.

M. Al-Dahhan

9. Design of a Recycle Reactor System:
External recycle system with monitored flows for low to moderate pressure operation (0.1 to 10 atm) and high temperatures (25° to 600°C).

V. Kalthod

10. Novel Porous Carrier and Reactor for Mammalian Cell Cultures:
(Joint Project with Medical School and Biotechnology Laboratory)
High density growth of anchorage dependent mammalian cells on new support material in a novel reactor of high volumetric productivity.

Area II. PREPARATION OF NEW MATERIALS

Y. B. Yang

1. Modeling of the Aerosol Reactor for Production of Polycrystalline Silicon:
Population balances, method of moments and fractals combine in arriving at a model that simulates well experimental evidence.

D. Dorsey

2. Oxygen Transport During Single Crystal Growth by the Czochralski Method:
Simulation of heat transfer, forced and free convection and magnetic field effects on oxygen mass transfer and crystal incorporation rates.

D. O'Connor

3. The Crystal Growth of α-FeOOH (Goethite) in Aqueous Solution at High pH:
Effect of oxygenation rate on product morphology.

I. S. Yoon

4. Modeling the Process Cycle of Thermoplastic Composites with Experimental Verification:
(Joint Project with MRL)
Measurement of resin pressure profiles in time and of devolatilization rates in quantifying the resin flow and devolatilization models.

Y. B. Yang

5. Modeling of Devolatilization of Thermoplastic (Polyimide) Composites:
(Joint Project with MRL)
Completion of computer algorithms for prediction of devolatilization rates as function of prepreg thickness and curing cycle parameters.

Area III: EXPERT SYSTEMS AND CONTROL

P. Hanratty

1. Structure and Implementation of a Knowledge-Based System for Catalytic Reactor Design:
Prototype expert system for above task under development.

H. T. Wu

2. Knowledge-Based Control in Manufacture of Composite Materials:
(Joint Project with MRL)
Testing of a prototype C-shell based expert system control. Knowledge base extracted from model simulation.

F. Wang

3. Application of Genetic Algorithms and Neural Networks in Process Controls:
Review of genetic algorithms and neural networks. Prototype developed for simple control task.

D. Shieh

4. Automatic Knowledge Acquisition Procedures for Process and Quality Control Using Routine Data:
Developing machine learning techniques in eliciting knowledge from routinely collected data. Linking machine learning modules with knowledge base module.

K. Kage

5. Model Accuracy Considerations in Model-Based Control:
Development of criteria for improvement of model accuracy based on statistical methods.

REVIEW OF ACTIVE RESEARCH PROJECTS

AREA I. MULTIPHASE REACTORS

The emphasis is on developing an improved understanding of the operation of various types of multiphase reactors. Models based on first principles are developed as well as novel experimental techniques.

The goal is safer, faster and more accurate scale-up and design of multiphase reactors and rational selections of multiphase reactors for new processes.

INVESTIGATION OF LIQUID HYDRODYNAMICS IN BUBBLE COLUMNS VIA A COMPUTER AUTOMATED RADIOACTIVE PARTICLE TRACKING (CARPT) FACILITY

A. Problem Definition

Liquid circulation or gulf streaming is a phenomenon commonly encountered in bubble columns caused by nonuniform holdup profiles. It is primarily responsible for liquid phase mixing. The assumption of complete backmixing can lead to overdesign if high conversion is desired or to reduced selectivity in the case of complex kinetics.

How this gulf streaming is affected by column size (diameter and height), column and distributor design, physical properties of the gas-liquid mixture and operating conditions (superficial velocities) is presently not well understood. Neither a theory based on first principles nor abundant data are available. The inviscid models (1-2) make use of the single phase vorticity transport equations which are not applicable for two phase flow. The "principle" of minimization of maximum vorticity used to close the problem has no physical basis. Joshi and Sharma (2) proposed multiple circulation cells in tall columns without experimentally confirming their existence. In addition, they assigned the same clockwise rotation to cells above each other, which is physically impossible. Information on the existence of such cells is vital for model development for liquid mixing. Liquid circulation has also been described by 1-D momentum balances for gas and liquid phase (3). The model requires as inputs the eddy viscosity and the gas holdup profile. The predictions of the 1-D model can be significantly improved by a) developing a suitable relationship for eddy viscosity and its dependence on column geometry and operating conditions and b) introducing a gas phase continuity equation. To determine the eddy viscosity values it is necessary to measure the Reynolds' stresses for the liquid phase.

Liquid mixing in bubble columns is caused by a) convection b) turbulent dispersion c) bubble wakes and by d) molecular diffusion (which is negligible). These mechanisms are usually lumped into a single effective axial dispersion coefficient in the widely used dispersion model. It has been argued (4) that at least in the churn - turbulent regime, the dispersion model is without theoretical basis. Models capable of accounting for the pertinent mechanisms listed above have to be developed.

B. Research Objectives

The overall objectives of this research are to test a novel experimental technique for determining liquid velocities in bubble columns, to examine its capability in providing liquid turbulence parameters and utilize the data obtained in improving the models for liquid circulation and backmixing. The research consists of a two prong approach as outlined below:

1. Experimental:

    - Development of noninvasive CARPT facility for measurement of local liquid velocities and turbulence parameters.

- Assessment of the effect of column diameter and operating conditions.
- Development of constitutive equations for a priori prediction of eddy viscosity and turbulent dispersion coefficients.

2. Theoretical:

   - Development of 1-D model for liquid circulation and comparison of model predictions with experimental data.
   - Solution of a convection-diffusion model for spread of a non-volatile tracer. Experimental verification using CARPT facility by the introduction of liquid radioactive tracer.

C. Research Accomplishments

Principle of CARPT: A single radioactive particle emitting gamma radiation of constant energy, which is dynamically similar to the recirculating liquid, is introduced into the column. As it moves along with the liquid, the particle is tracked using an array of strategically located scintillation detectors. The frequency of gamma rays arriving at each detector decreases with increasing distance between the tracer and the detector. The photon count rate obtained at each detector (the intensity) is related to the distance between the source and the detector using pre-established calibration. The instantaneous position of the tracer is then accurately calculated from the distances using an optimized linear regression scheme. Prudent use of the purposely introduced redundancy in distance measurements helps overcome the problem of intrinsic noise associated with the quantized nature of gamma emission. Time differentiation of the displacement yields local velocities. Ensemble averaged velocity profiles and other turbulence quantities can be computed after acquiring data for a sufficient length of time.

The Radioactive Particle: It was made by embedding a Scandium cylinder (machined from solid Scandium at the Ames Laboratory, Iowa) in a polypropylene particle as illustrated in Figure 1. The final particle density was 1.01 g/cc. The particle was then sent to the Reactor Research Facility, University of Missouri, Columbia for irradiation to the desired activity of 250 μCi. Experimental Results with Tap Water: Results are presented here for the air - water system in a 11.5in bubble column. A 3/16" porous plate with an average pore size of 25 μm was used as the distributor. The static liquid height was 23" giving an aspect ratio of 2. The air superficial velocity was 10.57 cm/s. Under these conditions, the liquid height was 28" yielding an average bed void fraction of 0.18.

Calibration and Dynamic Run: A calibration was carried out by positioning the tracer in 185 different spatial locations in the column and recording the intensities in the 16 detectors. A sampling frequency of 33 Hz. was used. A polynomial fit was used to relate the recorded intensities and the corresponding distances. A typical fit is shown in Figure 2. Once the calibration was completed the particle was dropped into the

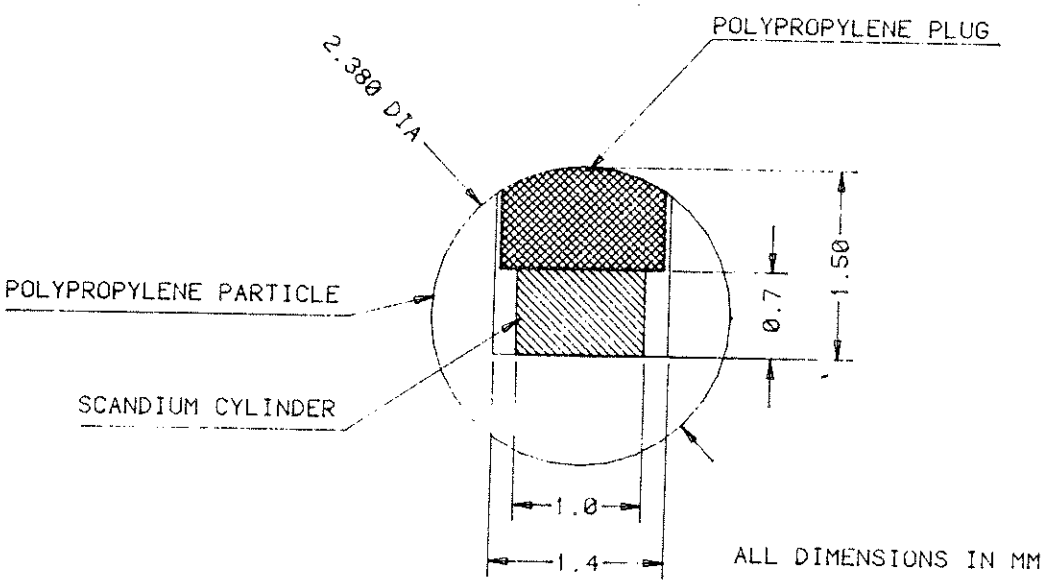

Figure .1: Radioactive Tracer Particle

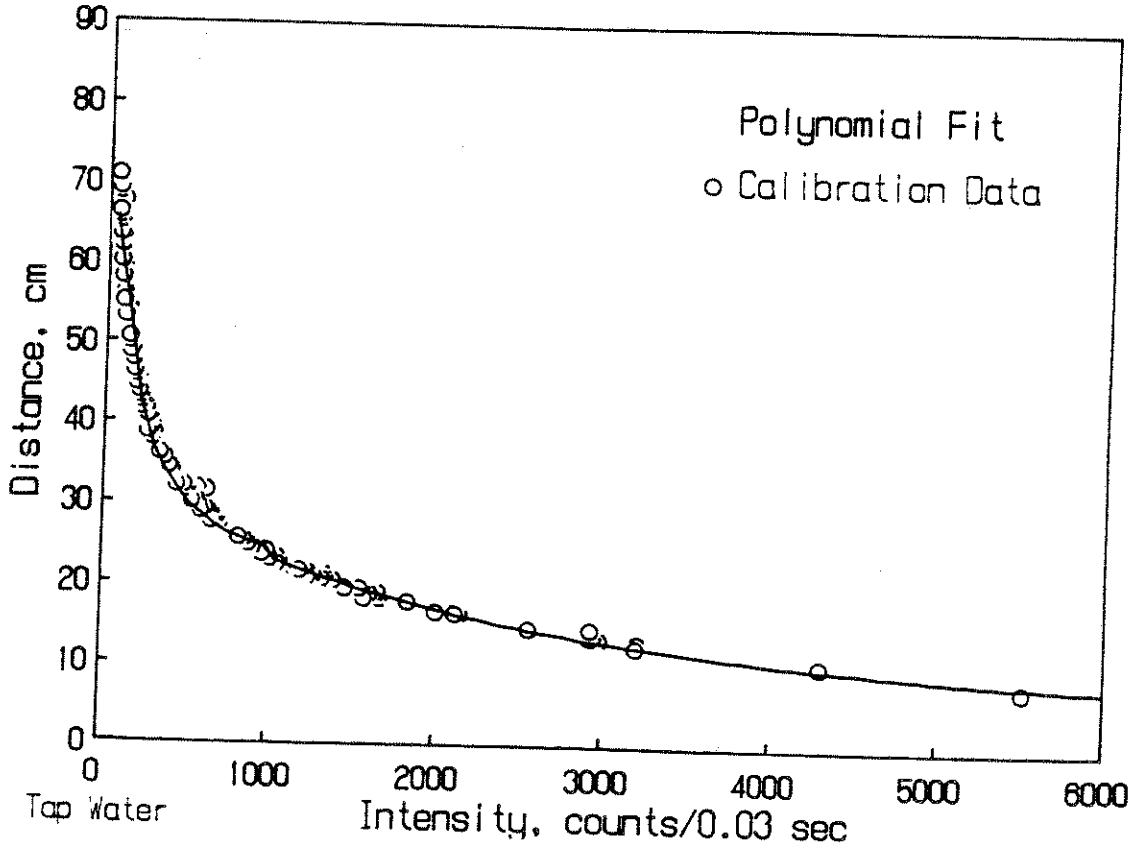

Figure .2: Calibration Data and Polynomial Fit for Detector 7

column and a 4 hour dynamic run was conducted at the same sampling rate of 33 Hz. The raw intensity data were stored in the hard disk of the computer for subsequent processing.

Data Processing: The program LOCATE was used to calculate the successive tracer locations from the raw counts data. To compute the velocity, the column was divided into 10 radial divisions, 16 azimuthal divisions and 50 axial divisions resulting in a total of 8000 compartments. The grid sizes were 1.5 cm in the r direction, 22.5 degrees in the θ direction and 1.55 cm in the z direction. The program VELOCITY then computed the mean velocity profiles and the tracer occurrence distribution. The program CIRCVEL was used to perform circumferential averaging of data. Program STREAMFN was then called to calculate the stream functions by integration of the velocity data.

Mean Recirculation Profiles: Figure 3 shows the recirculation pattern in the column. It is clearly seen that there exists a single recirculation cell with the liquid ascending along the column center and descending along the wall. The corresponding velocity vector plot is also shown in Figure 3. The starting point of these arrows correspond to the centers of the sampling compartments. The size of the arrow represents the magnitude of the velocity while its direction represents the direction of liquid flow. The maximum velocity occurs at the column center at a height of 58 cm and is 52 cm/s. Figure 3 also shows the tracer occurrence distribution (number/cc). It is relatively high close to the distributor and also the free surface and indicates relatively stagnant fluids in these regions.

Figure 4 shows the radial variation of the axial velocity at various z locations. Previous investigators (5,6) measured these velocity profiles only at one z location (usually close to the column mid plane). It is clear that the profiles flatten close to the distributor and the free surface, regions were flow reversal takes place. Figure 5 shows the axial variation of the radial velocities at various radial locations. For most part of the column, the radial velocities are typically less than 3 cm/s indicating that the flow, for all practical purposes is one dimensional. But close to the distributor and the free surface the radial velocities are higher and in opposite directions depicting the flow reversal of a single recirculation cell in the column. The data also confirms that in general flow is not axisymmetric in bubble columns; however, circumferential averaging is useful to present the data in a more readable form.

Presently one-dimensional models offer the maximum potential in describing the liquid circulation in bubble columns (7). Such an analysis is applicable to tall bubble columns in which the end effects can be neglected. In order to obtain useful information from CARPT data for modeling, the circumferentially averaged data have to be averaged in the axial direction also. From figure 4 it is clear that the entry region extends to a height of 35 cm, and thereafter the profile does not change until the free surface is approached. The averaged velocity profile is shown in fig. 6. The profile and the transition point agree well with the previous data reported by Hills (5) and Yang et al. (6). The Reynolds stress is shown in figure 7. The maximum shear is found at the transition point. The corresponding profile for single phase flow also shows a maximum but closer to the wall (8). The eddy viscosity profile was calculated from the

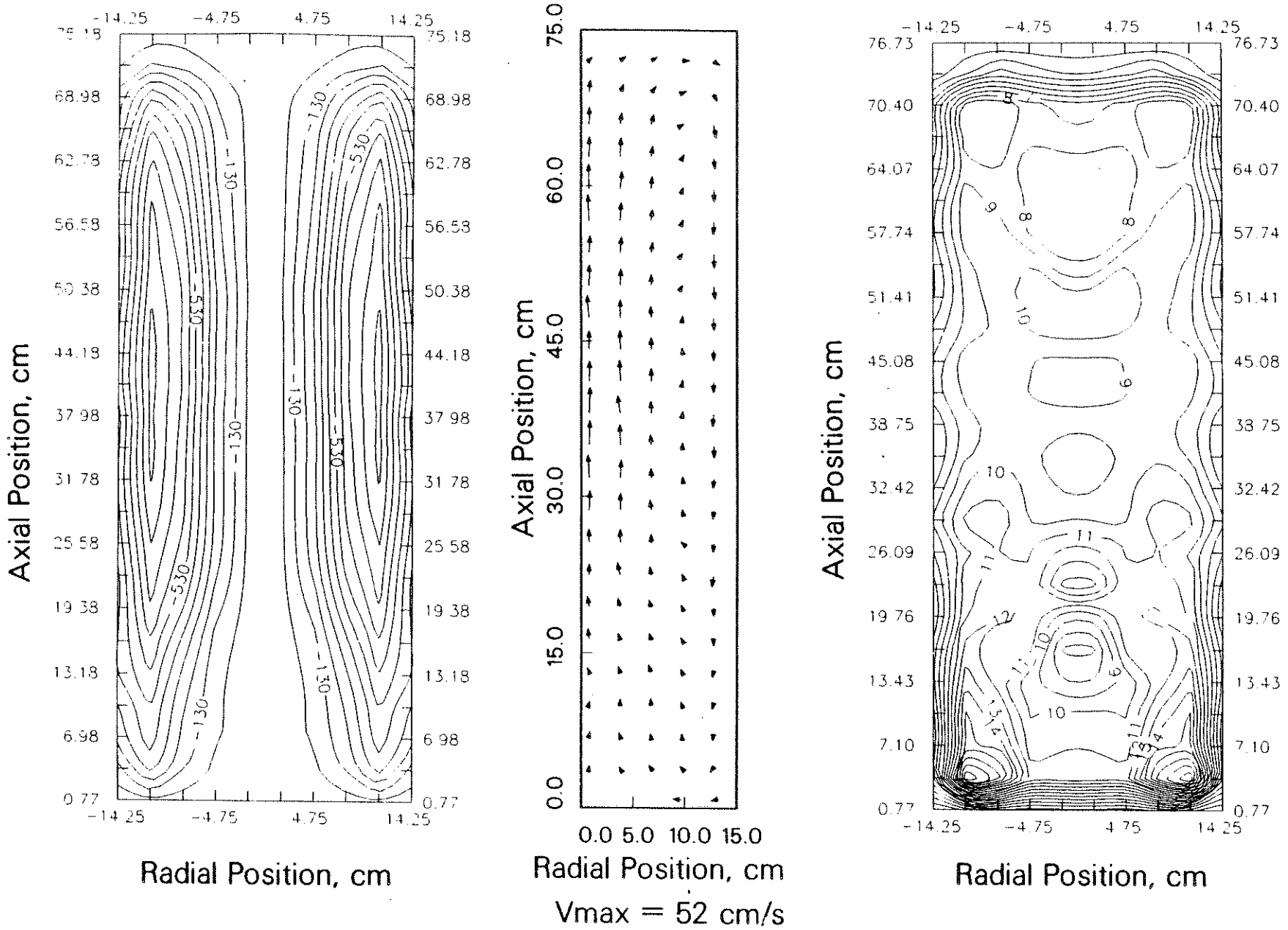

Figure 3: Streamlines, Velocity Vector Plot and Tracer Occurrence Distribution (Tap Water, $U_o = 10.57$ cm/s)

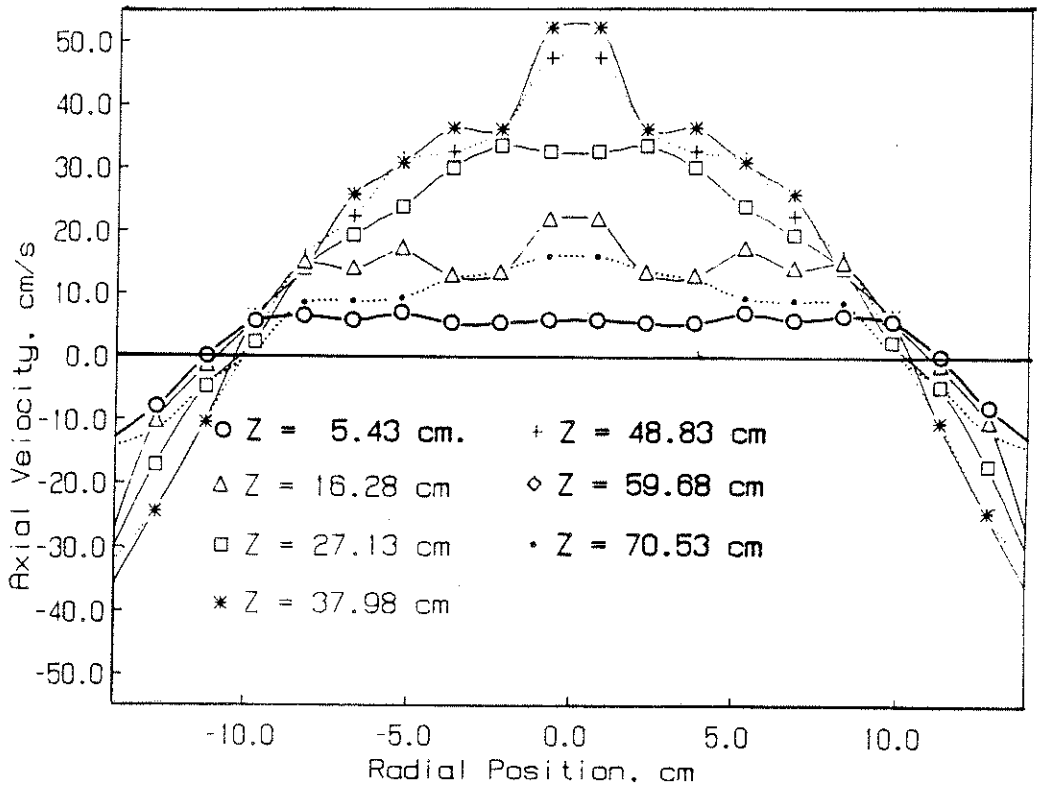

Figure 4: Radial Variation of Axial Velocity at Various z Locations

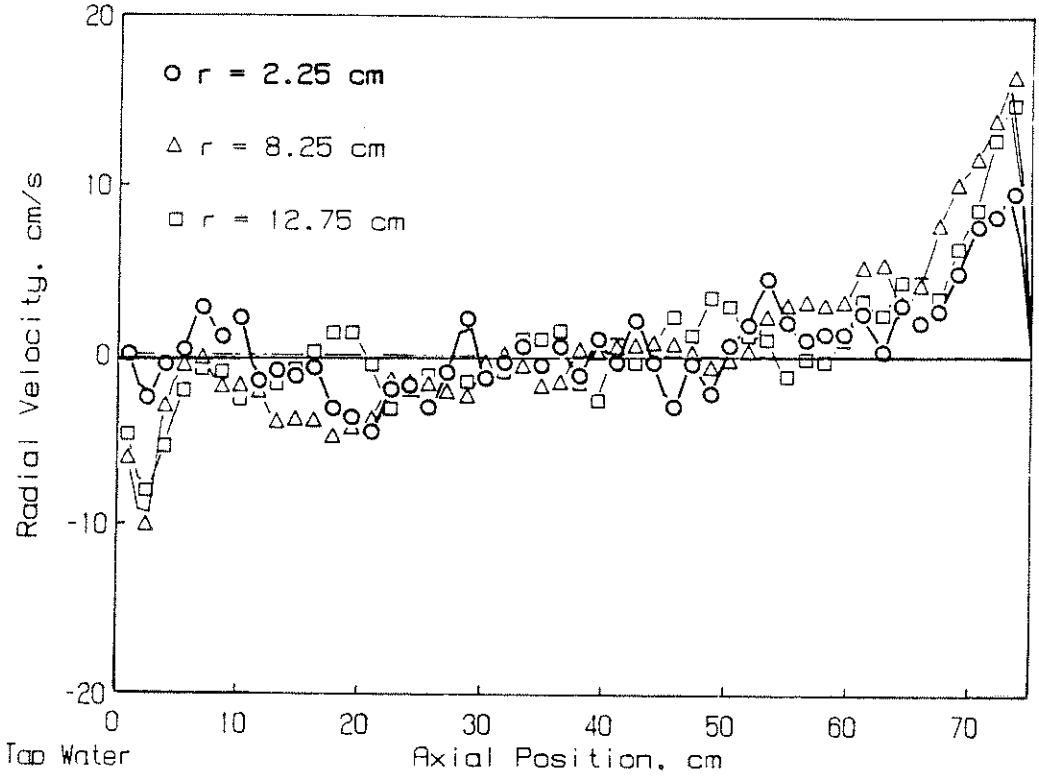

Figure 5: Axial Variation of Radial Velocity at Various r Locations

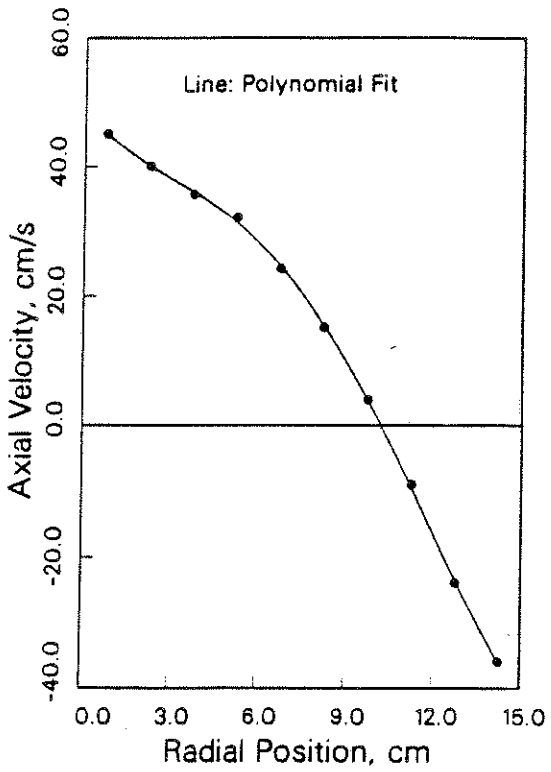

Figure 6: Axially Averaged Liquid Velocity Profile

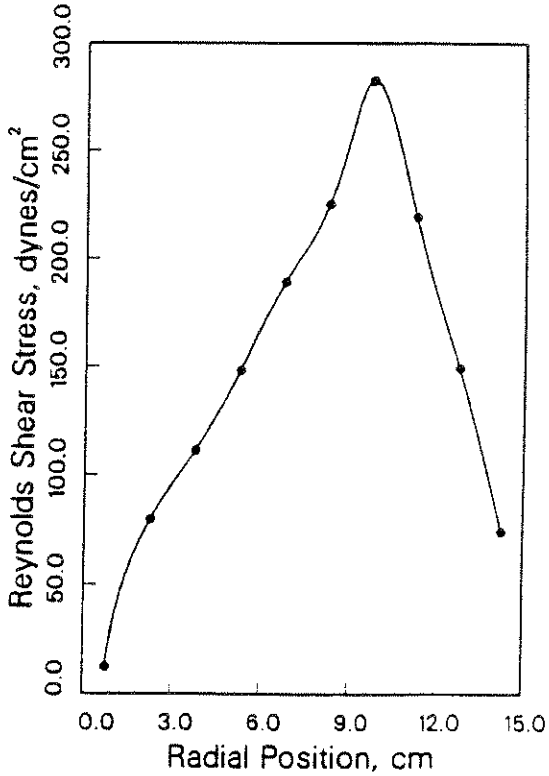

Figure 7: Axially Averaged Reynolds Shear Stress

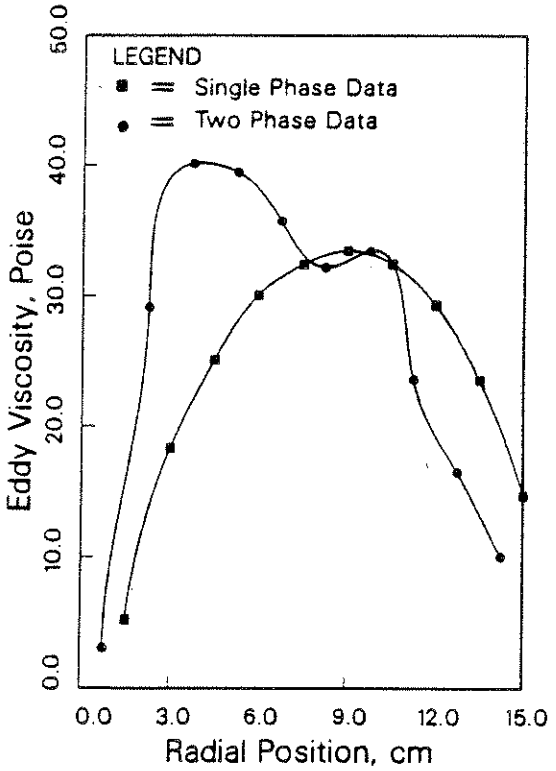

Figure 8: Turbulent Eddy Viscosity Profiles

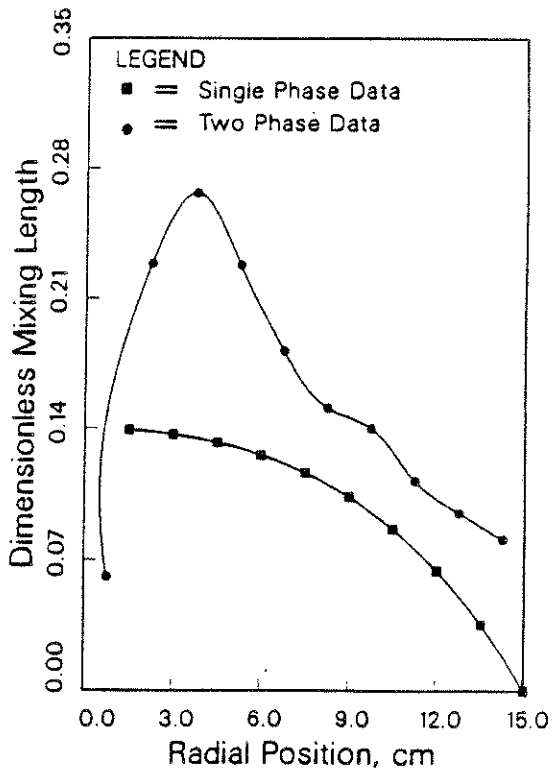

Figure 9: Mixing Length Profiles

velocity - stress data (a polynomial fit of the velocity data was differentiated to obtain the gradient). It goes through a peak as shown in figure 8. Nikuradse's data for single phase flow (9) for a Reynolds Number of 1.1 $\times 10^6$ is also shown in the same figure. The similarity in behavior is remarkable given the heterogeneous nature of two phase flow. Figure 9 also shows a comparison of Prandtl mixing lengths for single and two phase flows. In the case of two phase flow the mixing length peaks close to the axis while that for single phase flow shows monotonic decrease as the wall is approached.

In addition to mean circulation profiles a number of turbulence parameters were also computed from the data. These include the rms velocities, the kinetic energy of turbulence, the Lagrangian autocorrelation coefficients and the turbulence dispersion coefficients. Details of these can be found in reference 10.

D. Future Work

The research work to be accomplished is briefly outlined below:

1. The mean recirculation profiles and turbulence parameters will be determined for four different superficial gas velocities in the 12" column and also in 8" and 5" columns. The measured data will enable us to assess the role of diameter and superficial gas velocity.

2. A correlation will be developed for the prediction of the radial variation of the eddy viscosity. It will be used in the 1-D model for liquid velocity profile developed earlier. Model predictions will be compared with experimental results.

Bibliography

1. Freedman, W. and Davidson, J. F., Trans. Inst. Chem. Engrs., 47, 251 (1969).
2. Joshi, J. B. and Sharma, M. M., Trans. Inst. Chem. Engrs., 57, 244 (1979).
3. Ueyama, K. and Miyauchi, T., AIChE J., 25, 258 (1979).
4. Myers, K. J., "Liquid Phase Mixing in Churn-Turbulent Bubble Columns," D.Sc. Thesis, Washington University, St. Louis, MO.
5. Hills, J. H., Trans. Inst. Chem. Engrs., 52, 1 (1974).
6. Yang,Z., Rustemeyer, U. and Buchholz, R. and Onken, U., Chem. Eng. Commn., 25, 243 (1986).
7. Devanathan, N., "Investigation of Liquid Hydrodynamics in Bubble Columns Via a Computer Automated Radioactive Particle Tracking Facility," D.Sc. Thesis Proposal, Washington University, St. Louis, MO.
8. Bird, R. B., Stewart, W. E. and Lightfoot, E. N., Transport Phenomena, John Wiley, New York, 1960, p. 158.
9. Schlichting, H., "Boundary Layer Theory," McGraw-Hill, New York, 1979, pp. 596-611.
10. Moslemian, D. and Dudukovic, M. P., "Investigation of Liquid Hydrodynamics in Bubble Columns Via a Computer Automated Radioactive Particle Tracking (CARPT) Facility," NSF Progress Report, March 31, 1989.

HYDRODYNAMICS IN TRICKLE BED REACTORS

A. Problem Definition

The hydrodynamics of cocurrent, gas-liquid downflow in packed beds is an important, yet poorly understood phenomenon. Flow regime transition, pressure drop, liquid holdup, and gas-liquid-solid contacting efficiency are several important factors in trickle bed design and scale-up.

Flow regime prediction is accomplished using empirically developed maps or expressions which were derived from relatively small diameter beds. Sundaresan [1] observed the onset of pulsing in large beds as occurring locally (i.e the pulses did not span the entire bed). He conjectured that the transition point to pulsing across the entire bed is a function of the bed diameter. Chou *et al.* [2] observed a dependence of flow regime transition on bed porosity. The dependence of the transition to pulsing on bed properties has not been adequately explained in any of the flow regime maps or empirical models. Hydrodynamic models of the transition to pulsing based on the governing equations of two phase flow in porous media have been proposed in the literature [3,4]. The predominant approach is to attribute the onset of pulsing to a balance of surface tension and inertial forces. While the preliminary results of this approach seem promising, the model relies on empirical hydrodynamic models and an accurate knowledge of the capillary forces in the bed. Capillary forces have never been measured in trickle beds due to their small magnitude. The capillary pressure functions assumed in the models have not been justified. A fundamentally based theory of the transition to pulsing which incorporates both hydrodynamics and bed characteristics has not yet been established.

Pressure drop and liquid holdup are predicted using empirical correlations to phase flowrates, phase properties, and bed parameters [see 5, 6, 7 for review]. Several authors [8, 9, 10] have used empirically modified forms of the Ergun equation for each phase by accounting for the volume occupied by the other flowing phase. The Ergun equation for single phase flow in packed beds is based on single phase flow through an assumed pore scale geometry. The modified forms of the Ergun equation for two phase flow have not been derived from pore scale hydrodynamics but from empirical reasoning. Sweeney [8] and Specchia and Baldi [9] claim that the modified Ergun equation models do not require fitted parameters for two phase flow if the correct Ergun equation constants (obtained from single phase flow experiments) are used. Differences exist in the form of the modified Ergun equation due to differences in empirical reasoning used in the development by the different authors [8, 9, 10].

Gas-liquid-solid contacting efficiency on the bed scale (phase distribution) is an important factor in trickle bed design, scaleup and operation. The contacting efficiency is determined by the complex relationship between flow regime, pressure drop, liquid

holdup, and bed history. Bed history is an important factor based on the findings of Kan and Greenfield [11], Levec *et al.* [12], Christensen *et al.* [13], and Lazzaroni *et al.* [14] concerning multiple hydrodynamic states corresponding to different bed histories. These multiple hydrodynamic states have been qualitatively explained by different macroscale gas-liquid-solid contacting patterns [13]. Liquid-solid contacting efficiency has been modeled with network representations of bed geometry. The random walk models, Herkowitz *et al.* [15], and the percolation models, Crine *et al.* [16, 17, 18] and Ahtchi-Ali *et al.* [19, 20], derived on this basis require a knowledge of the contacting efficiency and are only useful for representing the experimental data and lack predictive ability. The bed of spheres model of Ng [21, 22] relies on liquid film spreading criterion developed for nonporous flat plates [23, 24] and on empirical rules for splitting liquid rivulets at sphere contact points. Ng's model can only be expected to represent large, nonporous packing particles. Since trickle beds do not conform to this constraint in practical applications, the usefulness of this model is not clear. Anderson *et al.* [25, 26] has proposed a phase distribution model based on the hydrodynamic model proposed by Sáez and Carbonell [10]. The driving force for phase redistribution is the capillary pressure gradient. Preliminary results are promising, but the capillary pressure curve must be assumed since experimental data are not available, as explained previously. The unknown capillary pressure and the empirical constants appearing in Sáez and Carbonell's correlation cause an undetermined inaccuracy in the model predictions. A predictive model of gas-liquid-solid contacting efficiency should be based on a sound hydrodynamic model which is free of parameters determined by fitting two phase flow data.

B. Research Objectives

The objectives of this project are:

1) Develop a general model of uniform two phase flow in packed beds for the trickle flow regime based on existing models of two phase flow in a single void.

2) Validate the model and determine any unknown factors by comparison to experimental data from trickle beds obtained in our laboratory and by other investigators.

3) Evaluate the transition from low to high gas-liquid interaction regime on a hydrodynamic basis using the hydrodynamics model of objectives 1 and 2. Develop a transition criterion which includes bed properties as well as phase properties and flowrates.

4) Develop and test a diagnostic model of macroscale phase distribution using the hydrodynamic model of objectives 1 and 2 as a base. The diagnostic model must rely on easily measured quantities of operating trickle beds.

5) Develop a model of phase distribution as determined by a minimum in the rate of energy dissipation. The hydrodynamic model of objectives 1 and 2 is used as a base.

C. Research Accomplishments

A model of the low gas-liquid interaction regime has been developed assuming complete catalyst contacting and uniform phase distribution. The void scale model is based on two phase flow in a crack or slit. A phenomenological view is that of a gas core flowing over liquid films which are contacting the wall. Turbulent effects were included in both phases using the universal velocity profile which is based on the mixing length theory. The development parallels that of Dukler *et al.* [27] for the liquid film and Pike [28] for the gas core. Slit and bed variables were related by equating phase volumes and specific solids surface area of a bed with a system of slits. The resulting model equations took the form of a modified Ergun equation where the two constants, E_1 and E_2, depend on bed, not phase, properties. Therefore, E_1 and E_2 can be determined from single phase flow experiments for each packing of interest. Two additional unknown parameters which characterize the extent of the phase interaction at the gas-liquid interface were used in the development.

The phase interaction parameters were determined to be zero in the low interaction regime by comparison of model predictions to 180 pairs of pressure drop and holdup data on beds with known single phase Ergun equation constants. The final form of the model contains no parameters determined from two phase flow experiments. Dimensionless gas and liquid pressure drop, see Nomenclature, are predicted by equations 1 and 2.

$$\Psi_G = \left(\frac{\varepsilon}{\varepsilon - \varepsilon_L}\right)^3 \left[\frac{E_1 Re_G}{Ga_G} + \frac{E_2 Re_G^2}{Ga_G}\right] \qquad (1)$$

$$\Psi_L = \left(\frac{\varepsilon}{\varepsilon_L}\right)^3 \left[\frac{E_1 Re_L}{Ga_L} + \frac{E_2 Re_L^2}{Ga_L}\right] \qquad (2)$$

These equations give a complete model of the trickle flow regime for determining pressure drop and holdup. Holdup is obtained first by equating the dimensional pressure gradients in the gas and liquid as shown in equation 3.

$$\Psi_L = 1 + \frac{\rho_G}{\rho_L}\left(\Psi_G - 1\right) \qquad (3)$$

Comparison of this model to pressure drop and holdup data showed an accuracy in model predictions comparable to existing correlations. This same functional form was developed by Sweeney [9] from empirical arguments and compared to pressure drop (only) data with the same conclusion. The absence of parameters fitted to two phase flow data makes the model applicable to any system in the trickle flow regime. Comparison of model predictions to pressure drop and holdup data are shown in Figure 1.

The universal velocity profile uses a pseudo Reynolds number, y^+, based on the shear stress and distance from the solid wall to characterize the degree of turbulence. In the liquid film model of the bed, the same pseudo liquid Reynolds number in terms of the bed variables has been found to have a characteristic value for each system at the transition to pulsing. The pseudo liquid Reynolds number of the bed, η_L, is related to the degree of turbulence in the liquid film by analogy to the equivalent factor in the universal velocity profile. The quantity, η_L, given by equation 4, is a function of the liquid flowrate and bed properties only since the phase interaction has been found to be negligible in the trickle flow regime.

$$\eta_L = \frac{1}{5\,(E_1)^{0.25}} \sqrt{E_1 Re_L + E_2 Re_L^2} \qquad (4)$$

The low to high interaction flow regime transition data of Midoux *et al.* [29], and Chou *et al.*[30] were used to generate values of η_L at transition. For non foaming systems, $\eta_{L,P}$ appears to be constant and independent of phase properties.

$$\eta_{L,P} = 5 \pm 0.5 \qquad 0.01 \le G \le 1 \ \frac{Kg}{m^2 s} \qquad (5)$$

For foaming systems $\eta_{L,P}$ decreases with decreasing surface tension.

$$\eta_{L,P} = 6.5\, e^{-0.4\lambda\psi} \qquad 0.01 \le G \le 1 \ \frac{Kg}{m^2 s} \qquad (6)$$

The criterion for nonfoaming systems agrees with the appearance of turbulent effects for single phase flow in pipes. The criterion for foaming systems is empirical. The parameters λ and ψ were chosen for convenience from flow regime maps based on Baker coordinates [29, 30]. The range of gas mass superficial velocities given for equations 5 and 6 indicates the trickle to pulsing (or foaming) flow regime transition. The trickle to dispersed bubble or spray flow regime transition is not considered in the criterion. Equations 4, 5 and 6 allow a simple solution for the critical liquid Reynolds number at

pulsing/foaming when the phase and bed properties (i.e. Ergun coefficients, particle diameter, and porosity) are know. This model is compared to several data sets available in the literature in Figure 2.

The diagnostic model for macroscale phase distribution has been developed and tested on data corresponding to the multiple hydrodynamic states obtained from different bed histories. The model, called the Three Zone Model, has been presented in detail [30, 31]. The model uses a measured bed pressure gradient to determine a quantitative estimate of the fraction of the bed occupied by three ideal zones. The three zones are: uniform gas-liquid distribution, liquid only flowing, and gas only flowing over wetted packing. The mass and momentum balances for each phase and the bed area balance form a set on nonlinear equations which can be solved for the flowrate of each phase in each zone and the fraction of the bed occupied by each zone.

Based on our work on modeling phase distribution in systems of capillaries [31,32], a model has been proposed for phase distribution in trickle beds based on a minimum in the rate of energy dissipation. Solution of the nonlinear, constrained minimization problem for several case studies is the focus of current and future work.

D. Further Research Plans

The results of this research effort in the hydrodynamics of trickle bed reactors is being prepared in a format suitable for publication and thesis requirements. Progress has been made in understanding the effect of bed parameters on the pressure drop, liquid holdup, and the trickle to pulsing flow regime boundary. The gas-liquid-solid contacting efficiency of operating trickle beds was addressed with the diagnostic, Three Zone Model. Future work in the area of gas-liquid-solid contacting efficiency will be focused on coupling the hydrodynamic model to detailed representations of the bed characteristics to give a predictive model of catalyst utilization.

E. Nomenclature

D_p = equivalent spherical diameter of the packing

E_1 & E_2 = constants of the Ergun equation for single phase flow on the packing of interest (describe bed tortuosity and roughness).

g = gravitational acceleration

Ga_α = the bed Galileo number of the α phase, $\dfrac{g D_p^3 \varepsilon^3}{\nu_\alpha^2 (1-\varepsilon)^3}$

G = gas mass superficial velocity = $\rho_G V_G$

L = liquid mass superficial velocity = $\rho_L V_L$

L_{Bed} = bed length over which pressure drop is measured

P = absolute pressure

Re_α = the bed Reynolds number of the α phase, $\frac{V_\alpha D_p}{\nu_\alpha(1-\varepsilon)}$

V_α = the bed superficial velocity of the α phase

y = distance measured from the slit wall in universal velocity profile

y^+ = pseudo Reynolds number used in the universal velocity profile

$$= \frac{\sqrt{\frac{\tau_\alpha}{\rho_\alpha}}\, y}{\nu_\alpha}$$

$0 < y^+ < 5$ Laminar flow

$5 < y^+ < 30$ Buffer Zone, some turbulent effects

$y^+ > 30$ Fully turbulent flow

Greek Letters

ε = bed porosity

ε_L = bed liquid holdup

η_L = psuedo liquid Reynolds number based on shear stress in the liquid and liquid holdup, reduces to equation 4 in terms of bed parameters and bed liquid Reynolds number.

λ = parameter defined on flow regime maps using Baker coordinates,

$$= \sqrt{\frac{\rho_G \rho_L}{\rho_{air}\rho_{water}}}$$

μ_α = viscosity of the α phase

ν_α = kinematic viscosity of α phase, $\frac{\mu_\alpha}{\rho_\alpha}$

ρ_α = density of the α phase

σ_L = surface tension coefficient of the liquid relative to the gas

τ_α = characteristic shear in the α phase

Ψ_α = dimensionless body force on the α phase $= \frac{1}{\rho_\alpha g}\left[-\frac{\Delta P}{L_{Bed}} + \rho_\alpha g\right]$

ψ = parameter from flow regime maps using Baker coordinates,

$$= \frac{\sigma_{water}}{\sigma_L}\left[\frac{\mu_L}{\mu_{water}}\left(\frac{\rho_{water}}{\rho_L}\right)^2\right]^{\frac{1}{3}}$$

Subscripts

α = general subscript meaning gas (G) or liquid (L)

G = gas phase

L = liquid phase

P = denotes the onset of the high interaction flow regime in equations 5 and 6

F.Bibliography

1. Sundaresan, S. "Mathematical Modeling of Pulsing Flow In Large Trickle Beds", AIChE Journal, 33, 455 (1987)
2. Chou, T.S., F.L. Worley Jr. , and D. Luss, "Transition to Pulsed Flow in Mixed-Phase Cocurrent Downflow through a Fixed Bed", Industrial and Engineering Chemistry, Process Design and Development, 16, 424 (1977)
3. Ng, K.M., "A Model for Flow Regime Transitions in Cocurrent Downflow Trickle Bed Reactors", AIChE Journal, 32, 115 (1986)
4. Grosser, K., R.G. Carbonell,and S. Sundaresan, "Onset of Pulsing in Two-Phase Cocurrent Downflow through Packed Beds", AIChE Journal, 34, 1850 (1988)
5. Ramachandran, P.A. and R.V. Chaudhari, *Three Phase Catalytic Reactors*, Gordon and Breach Science Publishers, NY, (1983)
6. Ramachandran, P.A., M.P. Dudković, and P.L. Mills, " Recent Advances in the Analysis and Design of Trickle Bed Reactors", Sadhana, Proceedings of the Indian Academy of Sciences, 10, 269 (1987)
7. Dudković, M.P., and P.L. Mills, *Encyclopedia of Fluid Mechanics*, Chapter 32 Gulf Publishing Company, Houston, Texas USA (1986)
8. Sweeney, D.E., "A Correlation for Pressure Drop in Two Phase Concurrent Flow in Packed Beds", AIChE Journal, 13, 663 (1967)
9. Specchia, V., and G. Baldi, "Pressure Drop and Liquid Holdup for Two Phase Concurrent Flow in Packed Beds", Chemical Engineering Science, 32, 515 (1977)
10. Sáez, A.E., and R.G. Carbonell, "Hydrodynamic Parameters for Gas-Liquid Cocurrent Flow in Packed Beds", AIChE Journal, 31, 52 (1985)
11. Kan, K. and P.F. Greenfield, "Multiple Hydrodynamic States in Cocurrent, Two-Phase Downflow through Packed Beds", Industrial and Engineering Chemistry, Process Design and Development, 17, 482 (1975)
12. Levec, J., A.E. Sáez, and R.G. Carbonell, "The Hydrodynamics of Trickling Flow in Packed Beds, Part II: Experimental Observations", AIChE Journal, 31, 369 (1986)
13. Christensen, G., S.J. McGovern, and S. Sundaresan, "Cocurrent Downflow of Air and Water in a Two Dimensional Packed Column", AIChE Journal, 32, 1677 (1986)
14. Lazzaroni, C.L., H.R. Keselman, and N.S. Figoli, "Trickle Bed Reactors. Multiplicity of Hydrodynamic States. Relation Between Pressure Drop and the Liquid Holdup", Industrial and Engineering Chemisty, Research, 28, 119, (1989)
15. Herskowitz, M. and J.M. Smith, "Liquid Distribution in Trickle Bed Reactors", AIChE Journal, 24, 439 (1979)

16. Crine, M., "Hydrodynamics of Trickle Bed Reactors: The Percolation Theory", paper presented at NATO Advanced Study Institute, Chemical Reactor Design and Technology, London, Canada, June 2-12, 1985
17. Crine, M., J.M. Asua, and G. L'Homme, "Axial Dispersion Processes in Liquid Trickle Flow through Packed Beds", The Chemical Engineering Journal, 25, 108 (1982)
18. Larson, R.G., L.E. Scriven, and H.T. Davis, "Percolation Theory of Two-Phase Flow in Porous Media", Chemical Engineering Science, 36, 57 (1981)
19. Ahtchi-Ali, B., and H. Pedersen, "Very Large Lattice Model of Liquid Mixing in Trickle Beds", Industrial and Engineering Chemistry, Fundamentals, 25, 108 (1986)
20. Ahtchi-Ali, B., and H. Pedersen, "Monte Carlo Simulations of Liquid Flow Patterns in Trickle Beds", Mathematics Computers and Modelling, 11, 38 (1988)
21. Ng, K.M., S.P. Zimmerman, C.F. Chen, and J.Y. Fores, "Liquid Distribution in Trickling Flow Trickle Bed Reactors", AIChE Annual Meeting, Chicago, Ill. November 1985, paper 131d
22. Ng, K.M., and C.F. Chu, "Trickle Bed Reactors", Chemical Engineering Progress, 83, 55 (1987)
23. Hartley, P.E. and W. Murghatroyd, "Criterion for the Breakup of Thin Liquid Layers Flowing Isothermally over Solid Surfaces", International Journal of Heat and Mass Transfer, 7, 1033 (1964)
24. Norman, W.S., and V. McIntyre, "Heat Transfer to a Liquid Film on a Vertical Surface", Transactions of the Institute of Chemical Engineers, 38, 301 (1960)
25. Andersen, D.H., and A.V. Sapre, "Use of Preconditioned Bi-conjugate Gradient Method in Modeling Two-Phase Flow in Porous Media", Mathematics Computers and Modelling, 11, 22 (1988)
26. Andersen, D.H., and A.V. Sapre, "Trickle Bed Reactor Flow Simulation" AIChE Annual Meeting, Washington, DC, November, 1988, paper 45e
27. Dukler, A.E., and O.P. Bergelin, "Characteristics of Flow in Falling Liquid Films", Chemical Engineering Progress, 48, 557 (1952)
28. Pike, J.G., "Influence of a Falling Thin Liquid Film Upon a Co-Currently Flowing Gas Stream in a Vertical Duct", Canadian Journal of Chemical Engineering, 267, October, 1965
29. Midoux, N., M. Favier, and J.C. Charpentier, "Flow Pattern, Pressure Loss, and Liquid Holdup Data in Gas-Liquid Downflow Packed Beds with Foaming and Nonfoaming Hydrocarbons", Journal of Chemical Engineering of Japan, 9, 350 (1976)
30. Holub, R.A., M.P. Duduković, and P.A. Ramachandran, "Hydrodynamics of Trickle Bed Reactors: A Diagnostic Model of Phase Maldistribution", AIChE Annual Meeting, Washington, DC, November, 1988, paper 45a

31. Holub, R.A., M.P. Duduković, and P.A. Ramachandran, "Hydrodynamics of Trickle Bed Reactors", Chemical Reaction Engineering Laboratory Annual Report, 1988, Washington University, St. Louis, Missouri, USA
32. Holub, R.A., M.P. Duduković, and P.A. Ramachandran, "Modelling Hysteresis Phenomena in Systems of Multiple Slits: Application of the Principle of a Minimum Rate of Entropy Production at Steady State", Mathematics Computers and Modelling, 11, 26 (1988)

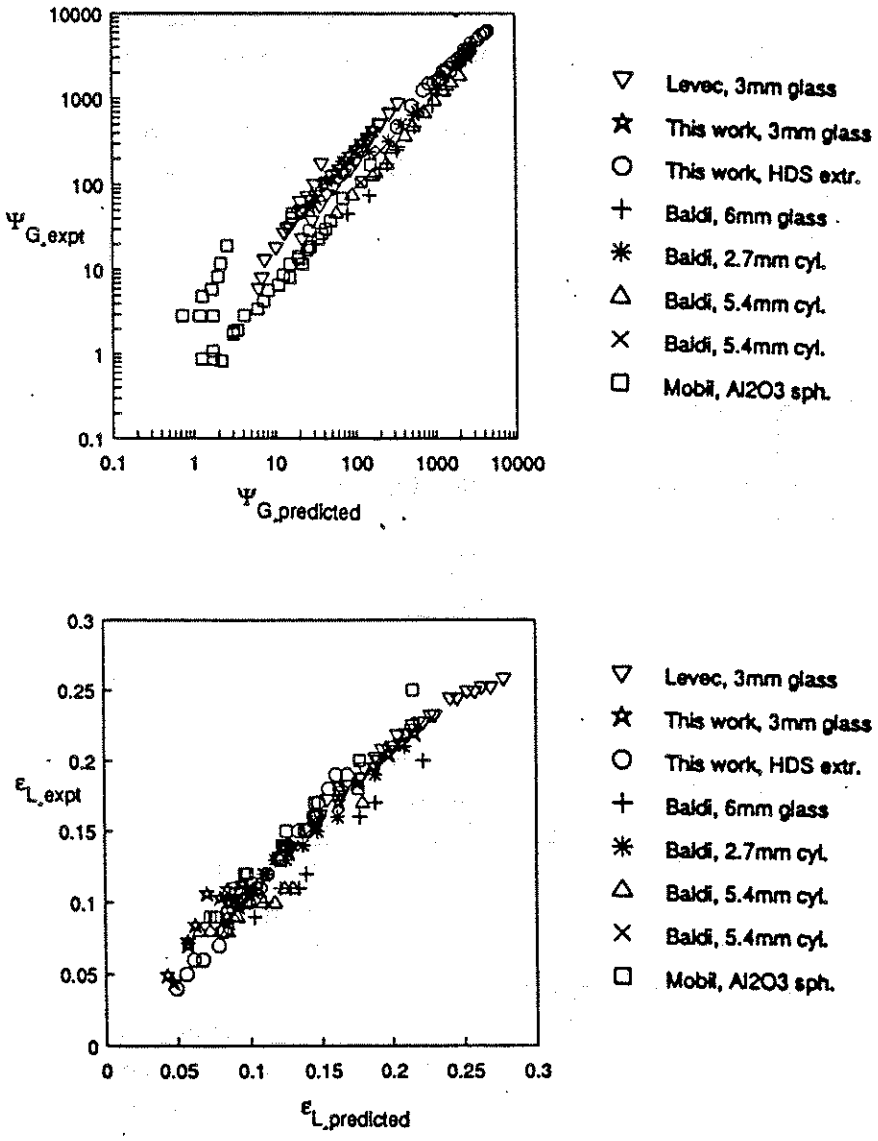

Figure 1 Comparison of Model Predictions and Data for Pressure Drop and Liquid Holdup

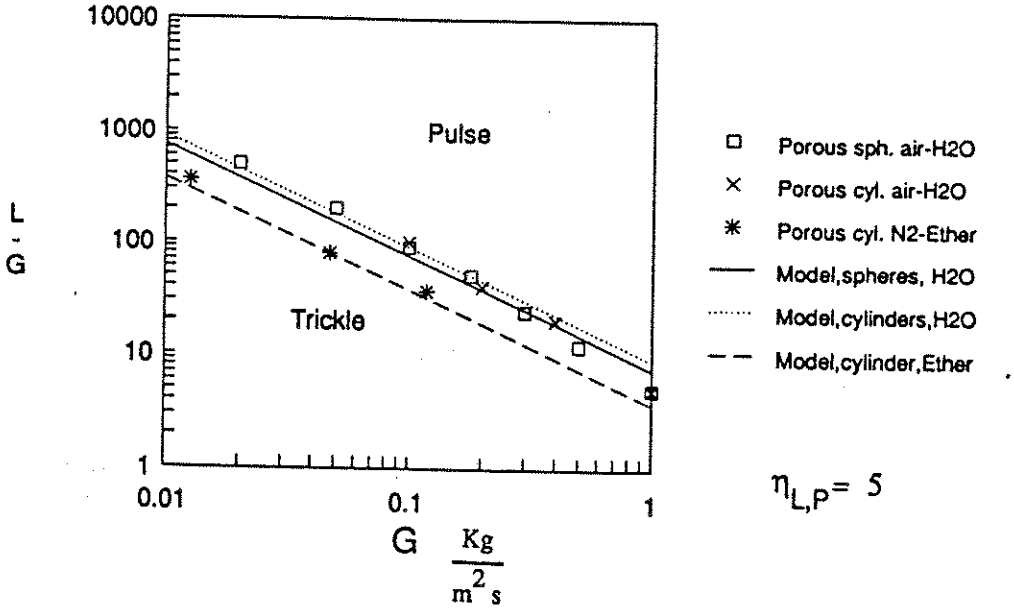

A. Nonfoaming Systems

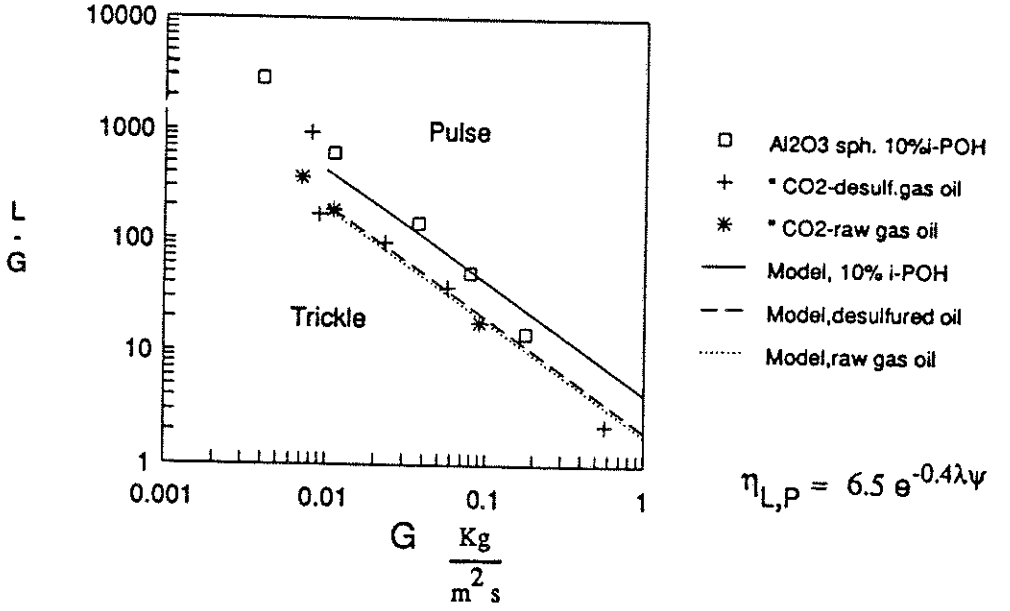

B. Foaming Systems

Figure 2 Comparison of Model and Predictions for the Trickling to Pulsing Flow Regime Transition for Nonfoaming and Foaming Systems. Predicted lines shift due to changing bed and phase properties.

TRACER STUDIES IN TRICKLE-BED REACTORS: EXPERIMENTAL VERIFICATION OF THE LT METHOD

A. Problem Definition

In last year's CREL Annual Report, a method was presented, now called the LT method, for the analysis of impulse tracer responses from packed bed reactors. Impulse tracer response curves are used often to assess flow maldistribution. Unfortunately, the response curve (E-curve) for packed bed reactors represent the combined effects of the flowing fluid and the fluid which enters the catalyst pore structure. To identify flow maldistribution in packed beds one wants only the response curve of the flowing fluid.

The LT method offers an approach by which to decouple the particle response from the overall response curve leaving the response curve of the flowing fluid. The procedure is illustrated in Figure 1. For the LT method, it is necessary to assume a particle transfer function (the transform from Figure 1b to 1c). Note that N different tracers will produce N different overall response curves for the packed bed (corresponding to Figure 1a) , but after applying the illustrated method the same response for flowing fluid should be obtained for all of the N tracers for the same gas and liquid flowrates if the correct particle transfer function is chosen.

Initially the LT method was tested using computer simulated curves for both well-distributed and maldistributed reactor response curves with superimposed error. The simulated response curves were used to test the viability of the LT method in the presence of reasonable experimental error, and to examine the commonly used methods of analyzing tracer data. The results of the simulation showed that the LT method produced the correct response curve of the flowing fluid for both the well-distributed and the maldistributed reactors, while the commonly used methods for analyzing tracer data were shown to have various shortcomings. This report shows the results of the LT method applied to experimental data.

B. Research Objectives

The objective of this project is to experimentally investigate the LT method for both well-distributed and maldistributed trickle-bed reactors.

C. Research Accomplishments

Experimental investigation of the LT method was carried out in three stages: first, the experimental determination of the needed particle tracer parameters; second, impulse tracer studies for well distributed trickle-bed reactors; and finally, impulse tracer studies for maldistributed trickle-bed reactors.

For the tracer experiments in trickle-bed reactors, hexane was used as the carrier liquid and nitrogen as the carrier gas. Heptane, cyclohexene, and benzene were used for the tracers and porous glass beads were used for packing. A column of 1.9 cm in diameter and 40 cm long was used for the reactor. A digital flow-through refractometer was used to monitor the tracer concentration from the reactor effluent. The unknown particle-tracer parameters, which were needed for the LT method, were measured in a separate reactor- a liquid-full (only liquid flow) packed bed.

The LT method was first experimentally examined for tracer data of a well- distributed packed column. Figure 2 illustrates typical refractometer output data (raw tracer data) for the impulse tracer studies. Figure 3 shows the normalized overall impulse tracer response curves for the data shown in Figure 2. Assuming a partially externally wetted sphere for the particle transfer function , the LT method was used to get the impulse tracer data. Figure 4 illustrates the final result of the LT method. The results demonstrate that approximately the same response curve is obtained for all three tracers (each of which had a different overall response curves, shown in Figure 2). The predicted response curve for the flowing fluid clearly exhibits that the column is well-distributed as expected. Therefore , the LT method has been experimentally shown to generate the correct response curve of the flowing fluid in a packed bed reactor with well-distributed liquid flow.

Next, the LT method was examined for tracer data from an experimentally maldistributed reactor. Maldistributed flow in the packed column was obtained by tilting the column 10 degrees off the vertical. Tilting the reactor causes liquid to preferentially flow in one region of the column because of the gravitational forces. Therefore tilting the column should produce liquid by-passing. Figure 5 illustrates the difference between the tilted and the non-tilted column response curves for the same gas and liquid flowrates using the same tracer. The response curve of the tilted column is shifted to earlier times suggesting that there is liquid by-passing present (as expected). Figure 6 shows the overall response curves of the tilted reactor for all three tracers. Applying the LT method (using the same particle transfer function and tracer-particle parameters as used for the well-distributed column) yields the final result shown in Figure 7. The LT method was not able to reduce all three of the overall impulse response curves to just one response curve for the flowing fluid. Therefore, one or more of the assumptions corresponding to the particle transfer function and/or to the method development must have been violated. Since for the well-distributed reactor the method was shown to work (Figures 2-5) the violated assumptions must be related to the flow maldistribution. Therefore, not being able to generate a single response curve for the flowing fluid indicates that there is some form of gross liquid maldistribution present in the reactor.

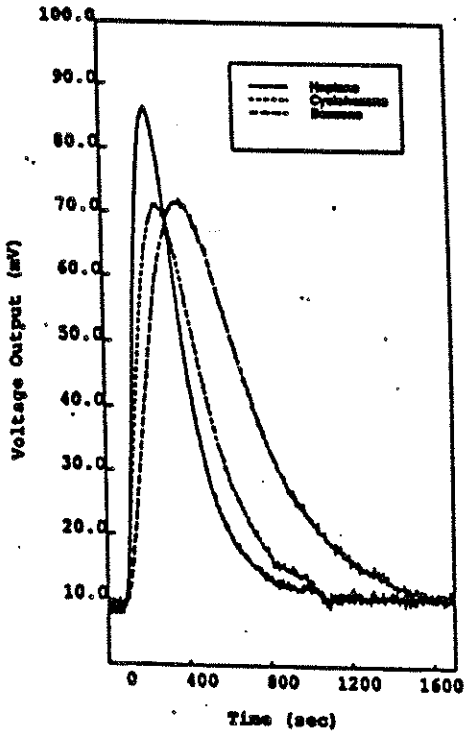

Figure 2 Voltage vs Time for Tracer Impulse Response in Trickle Beds for a Liquid Flowrate of 0.265 cm^3/sec and Gas Flowrate of 3.5 cm^3/sec

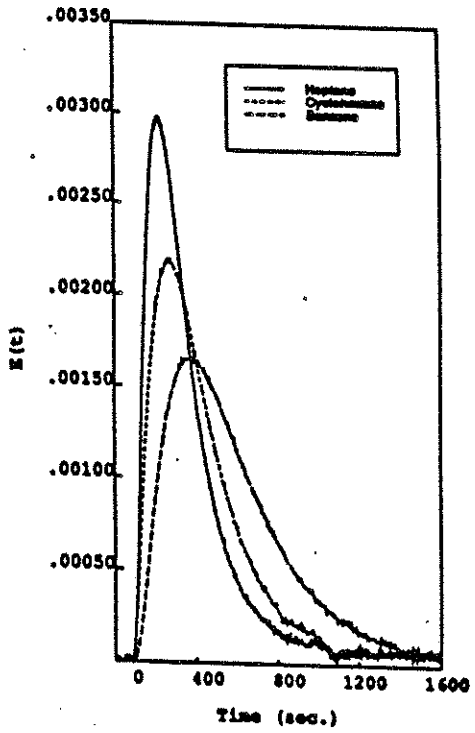

Figure 3 Normalized Impulse Response for Various Tracers in Trickle Beds at a Liquid Flowrate of 0.265 cm^3/sec and Gas Flowrate of 3.5 cm^3/sec

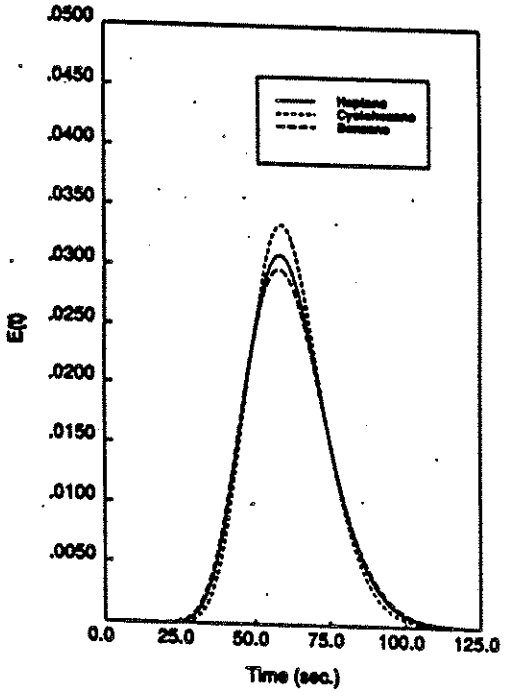

Figure 4 Estimated Impulse Response , E(t), of Fluid External to Particles Obtained by Using the LT Method on Responses of Figure 3

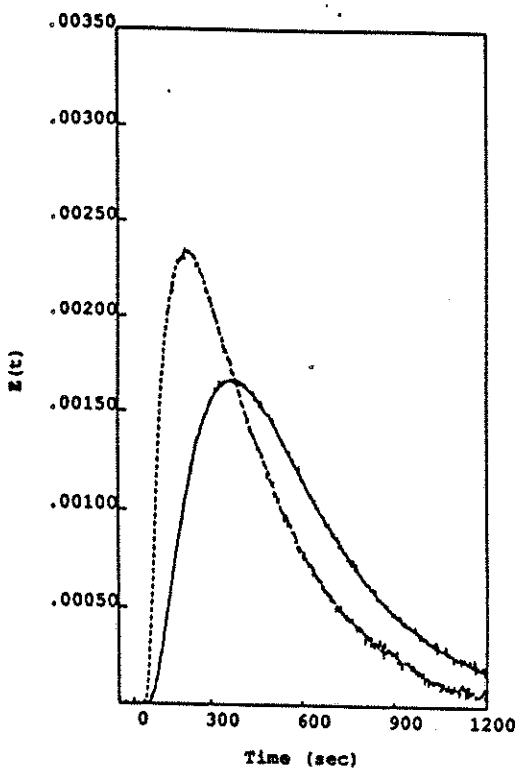

Figure 5 Normalized Impulse Response for a Vertical and a Tilted Trickle Bed

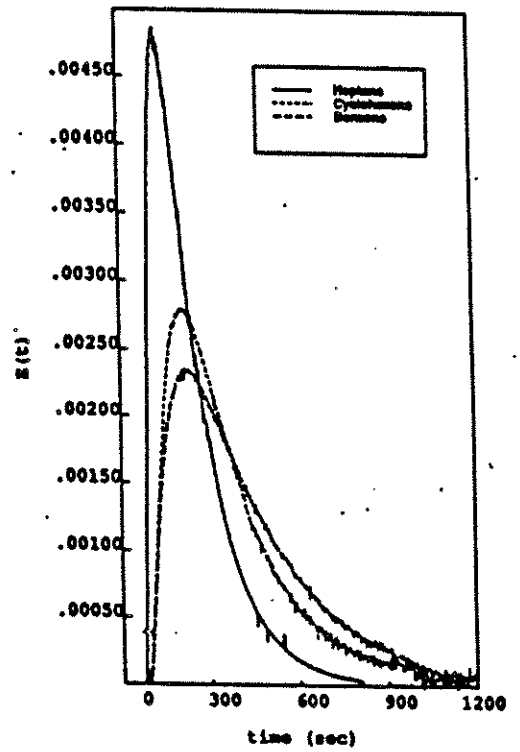

Figure 6 Normalized Impulse Response of Various Tracers in a Tilted Trickle Bed for a Liquid Flowrate of 0.198 cm^3/sec and a Gas Flowrate of 3.5 cm^3/sec

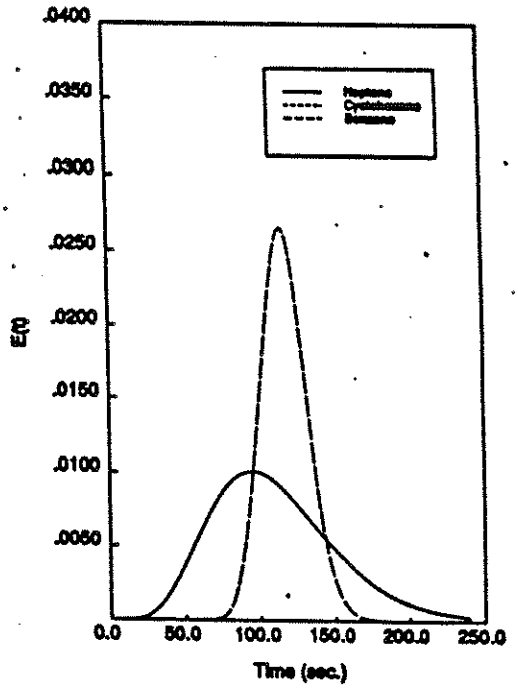

Figure 7 Application of the LT Method for Responses of Figure 6 (Inability to Achieve a Single E(t) Curve Points to the Assumptions of the Model Not Being Satisfied (Indicates Non-homogeneity)

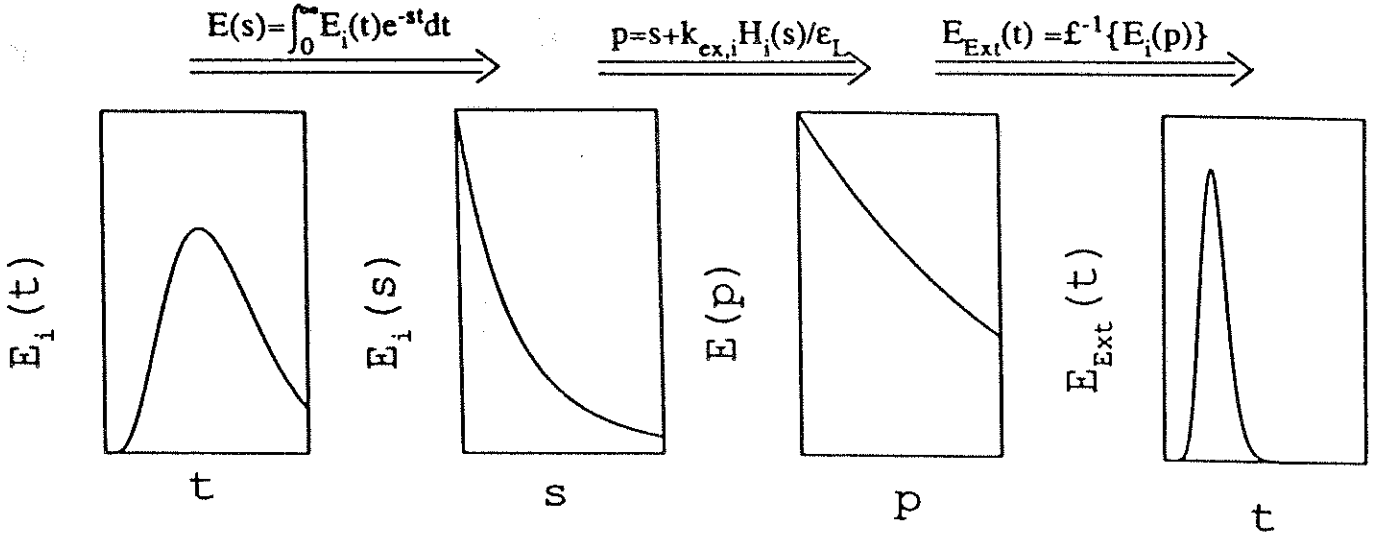

Figure 1a Impulse Response Curve

Figure 1b Laplace Domain Response Curve

Figure 1c Laplace Domain External Response Curve

Figure 1d External Response Curve

Figure 1 Demonstration of the Procedure for the LT Method

HYDRODYNAMICS AND MASS TRANSFER IN CENTRIFUGAL GAS-LIQUID CONTACTORS

A. Problem Definition

Rotating gas-liquid contactor is a device in which centrifugal force is employed as an adjustable drive for flow of liquid through a porous medium countercurrently to pressure difference driven gas flow.

Interphase transport of momentum and mass in the rotating porous medium (the rotating packed bed - RPB) are the phenomena which govern the performance of centrifugal contactors. An understanding of these processes is necessary for developing a theoretical basis for description of centrifugal contactors. Such a theory should explain the high performance of these devices in mass transfer operations. It should also indicate the feasibility of their use in other processes, for example such as involve three phase systems with chemical reactions. Finally, such a theory should provide a sound basis for reliable design and scale-up of centrifugal contactors.

Development of a theory to fill these need is the motivation for this project which addresses the problem of transport phenomena inside the RPB.

B. Research Objectives

We hypothesize that liquid phase present in the rotating packed bed is in the form of thin films which cover the surface of the packing. To verify this hypothesis we are developing a model of liquid holdup which is based on particle scale hydrodynamics and follows a statistical approach. The following tasks were set:

- Develop a statistical model which allows the irregular surface of the packing to be treated as a collection of randomly oriented but regular elements.
- Analyze the hydrodynamics of film flow on elementary surfaces defined in this way. Develop a model of holdup for RPB based on this, particle scale, flow analysis.
- Obtain experimental information about liquid holdup and the state of distribution of the liquid phase in the RPB. Use this information to develop the model further.

In addition to the experimental and theoretical work on the RPB, we studied mathematical problems of mass transfer in laminar liquid films.

C. Research Accomplishments

1. Liquid Holdup Measurement and Prediction

For of detection of liquid structure and measurement of liquid holdup in the RPB we use a method based on measurement of electrical resistance. When liquid is the only conducting phase in the system, it can be shown that the electrical resistance measured across the bed is a function of both the amount of liquid present and the state of its distribution in the bed. A simple model was developed which gives the relationship between the resistance of the bed and liquid holdup and distribution.

The cross section of one half of our RPB unit is represented in Figure 1. The main parts of the device are marked, as well as the added electrical elements which make up the circuit for electrical measurements.

Two kinds of resistance measurements are possible. In radial experiments we measure the resistance between the cylindrical wire mesh electrodes (1 in Figure 1) which bound the bed radially an enable us to impose a radial potential drop across the bed. In axial experiments cylindrical electrodes are removed and the insulating sheets (10) are replaced by plate electrodes on both top and bottom surface of the rotor. This measurement gives the resistance of the bed when potential difference is applied axially.

The resistances measured radially (in the direction of flow) and axially (in the transverse direction) should contain information about the possible anisotropy of the liquid distribution. This can be argued because the anisotropy effects, if they exist, will most likely be manifested as different connectedness of the liquid phase in the radial and axial direction.

So far we have successfully completed a series of radial measurements without gas flow.

In the development of the theoretical model we used Davidson's statistical approach [7]. In this method the surface of the packing is described as a collection of flat elements, or facets of random orientation and size. When applied to the geometry of the RPB this analysis gave rise to facets of more than one type. Different types could be defined according to different orientations of the surface with respect to the radius vector and the axis of symmetry. Figure 2 is a schematic representing the elementary surface which is named the rotating blade. The rotation axis of the bed is perpendicular to the plane of the drawing at point **O**. The rotating blade is the shaded element - a plane of random length, parallel to the bed axis and at a random orientation, θ, with respect to the radius vector, **r**. Under the assumption that the radial distance, r, at which the blade is found is much larger than the average blade size, the centrifugal acceleration on the blade, $g_x = r\omega^2 cos\theta$, can be considered constant. Film flow on a rotating blade defined in this way is analogous to gravity film flow on an incline.

Hydrodynamics of films on facets of other types, in which the facet plane is not parallel to the bed axis are extremely complicated. We hoped that the forces which

determine the holdup could be appropriately accounted for by an analysis limited to rotating blades. The model which we developed includes only these elements and in that respect it is analogous to particle scale models of liquid holdup for gravity packed beds ([2], [5], [7], [13]), in which the elementary surface is the incline. Different descriptions of hydrodynamics on facets were used in these works. Davidson [7] postulated laminar films at terminal velocity. Buchanan [5] used this situation only as the low Reynolds number limiting case and called it the viscosity-gravity regime. The limiting situation for high Reynolds number was defined as a balance of gravity and inertial forces. In that case film thickness is the result of thickening at facet joints due to the kinetic energy loss there and their thinning away from the joint points due to acceleration by gravity. Bemer and Kalis [2] used developed turbulent films. Yilmaz and Brauer [13] developed a correlation based on the numerical solution of laminar film flow down an incline including the entry region of accelerating flow.

There is no indication of appropriateness of any one of these descriptions alone for film flow on facets inside the RPB. We developed a semiquantitative model for film thickness which is is based on superposition of entry and asymptotic effects on every facet. The entry effects are the loss of kinetic energy and thickening of films immediately after the leading edge *i.e.* the joint with the preceding blade. This effect was quantified by introducing a coefficient ξ, which has the physical meaning of the head loss coefficient used in the Bernoulli equation. In analogy to flow in elbows, the coefficient ξ was assumed dependent on the angle ϕ, between two adjoining facets and was defined as:

$$\xi = k(\pi - \phi)^2. \tag{1}$$

The factor k is a function of only the shape of packing elements and is the only adjustable parameter of the model.

Farther down the blade the film is accelerated and thinned towards an asymptotic thickness which it would reach if the blade were infinitely long. Five different correlations were used for for the asymptotic film thickness. One of them was Nusselt's formula for developed laminar films and the other four were different correlations for developed turbulent films ([3], [4], [8], [9]).

The inclination of the blade with respect to the radius, θ, the joint angle between blades, ϕ, and the blade length are assumed random variables with uniform probability density distributions. They assume values in the ranges $[0, \pi/2]$, $[0, \pi]$ and $[0, d_p]$, respectively, d_p being the maximum dimension of the packing element. With further assumptions of the uniform distribution of liquid onto all packing elements and perfect wetting, it is possible to calculate the average of the mean film thickness and the local liquid saturation of the void space.

In our model of bed resistance a liquid holdup equivalent of the radial resistance is defined. This quantity, denoted by $\langle\beta\rangle$ and termed the radial mean holdup, is an across-the-bed integral average of the local liquid saturation of voids. Although it is a function different from the overall liquid saturation of the bed, it is a good measure

of the overall saturation. The radial mean holdup was used as a basis for comparison of the experimental data and model predictions.

The plots in Figure 3 show the comparison of the experimental data and model predictions of the radial mean holdup, $\langle\beta\rangle$. The data was obtained in a radial experiment without gas flow, with 3 mm glass beads as packing and with tap water as the liquid phase. The maximum relative error of the experimental data is 1.6% and the mean is 1.1%. The solid curves were obtained when the turbulent film correlation of Brötz [4] was used as the asymptotic film form in our model. This correlation gave the best prediction among all tried. The model predictions obtained with other asymptotic film forms are shown in broken lines and for the sake of clarity are given only for the highest rotational speed. The predictions at lower rotational speeds show discrepancies with the experimental data of the same magnitude and trend.

The good agreement between the model and the data in the entire range of flow rates and rotational speeds is achieved by selecting a value 0.7 for the only unknown parameter, k, which is characteristic of the packing. The five correlations for asymptotic film thickness all have different dependencies on the the liquid flow rate, the exponent ranging from one third for laminar films to two thirds for the turbulent film form [4]. Experimental data agrees well with the model in both the slops and magnitude only when one asymptotic film form is used and with a single value of the parameter k. This is evidence both of sensitivity of the experimental method and the accuracy of the proposed model. Furthermore we are led to believe that the regime of film flow in the RPB is a turbulent one - the regime described by correlation [4].

2. Mass Transfer Model

In the theoretical work on the mathematics of mass transfer in laminar liquid films we have been able to find a new convenient solution for a situation with short contact time. Such short penetration solutions are a class of approximate solutions of the problem of mas transfer in laminar liquid films. Different short penetration solutions arise as asymptotic forms of the full description of mass transport between a liquid film and either a solid surface or gas phase. An extensive survey of the literature pointed to an important case of short penetration problem for which a simple solution did not exist. This is the problem of liquid-solid mass transfer in developed laminar flow over a reacting surface. The problem is limited to the entry region, where a linear profile of liquid velocity can be assumed and to first order kinetics of the heterogeneous reaction.

For negligible diffusion in the direction of flow (high Péclet number), the mathematical model takes the form of the familiar Lévêque equation with Robin boundary condition. In dimensionless form,

$$y\frac{\partial C}{\partial x} = \frac{\partial^2 C}{\partial y^2} \tag{2}$$

$$
\begin{aligned}
x = 0, \quad y \in [0,\infty) : \quad & C = 1 \\
x \in (0,\infty), \quad y = 0 : \quad & \frac{\partial C}{\partial y} - Da\, C = 0 \\
x \in (0,\infty), \quad y \to \infty : \quad & C \to 1.
\end{aligned}
\tag{3}
$$

x and y denote the distance from the leading edge and from the solid surface, respectively, and C is the concentration of the solute. The length $PeY = bY^3/\mathcal{D}$ was used for characteristic length in the x direction, where Y is the characteristic transverse distance (film thickness for film flow), b is the gradient of velocity at the solid surface and $\mathcal{D}$ is the binary diffusivity of the solute. Based on a first order surface reaction rate constant, k_s, the Damköhler number is $Da = k_s Y/\mathcal{D}$. Concentration is normalized with respect to its value at the inlet. Of practical importance are solutions for the interface concentration, $C_0(x) = C(x,0)$ and for the interface flux, $[\partial C/\partial y]_{y=0} = Da\, C_0(x)$.

This problem has been addressed by several authors ([1], [10], [11], [12]). In these studies the solution for the interface concentration function, $C_0(x)$, is given in integral form and the full solution, $C(x,y)$, is given in the form of the formal convolution or contour inverses of the Laplace transform.

We would like to express the solution of this problem in the following convenient form. If we define the mass transfer coefficient, $k(x)$, as the ratio of the interface flux and the inlet concentration, then the local Sherwood number can be defined by:

$$
\frac{Sh(x)}{Da} = \frac{k(x)}{k_s} = \frac{1}{Da}\left.\frac{\partial C}{\partial y}\right|_{y=0} = C_0(x). \tag{4}
$$

The average Sherwood number over a length L is:

$$
\frac{\overline{Sh}(L)}{Da} = \frac{\overline{k}(L)}{k_s} \stackrel{\text{def}}{=} \frac{1}{L}\int_0^L C_0(x)dx \tag{5}
$$

The problem was solved by Laplace transform. An analytical solution in terms of incomplete gamma functions was found for the surface concentration, $C_0(x)$. An explicit form for the full solution, $C(x,y)$, was found as a series with good convergence properties for values of the arguments corresponding to short distances from the solid surface.

Local and average interface fluxes, equations (4) and (5), are the quantities of engineering interest. However, their calculation entails evaluation of the interface concentration, $C_0(x)$. Although our solution for $C_0(x)$ is more explicit than the one previously reported, it is still too cumbersome for design purposes.

By using Churchill's [6] method for function approximation we have been able to find convenient approximate formulas for interface fluxes. These formulas are simple, two term expressions and they approximate the fluxes to within 1%. The approximate formulas can be simplified even further to give the following expressions which contain no adjustable parameters:

$$\frac{1}{Sh(x)} = \frac{1}{Da} C_0(x) \approx \frac{1}{Da} + 1.857\, x^{1/3} \tag{6}$$

$$\frac{1}{\overline{Sh}(L)} \approx \frac{1}{Da} + 1.238\, L^{1/3} \tag{7}$$

The error of the above formulas is 2% for the average flux and 6% for the local flux.

Our approximate formulas provide convenient solution for this short penetration problem which has so far been lacking. The accuracy of the approximate formulas is adequate for most design and experimental applications. Examples of possible applications of these solutions are modeling of multiphase reactors in the film flow regime and analysis of kinetic data in experimental reactors with liquid films.

D. Future Work

The presented results of the study of liquid holdup in the RPB demonstrate the merit of the developed measurement method and of the theoretical model. However, more experimental data is necessary in order to establish that the assumptions used in the model describe the physical situation in the RPB.

First we will perform more radial measurements and add more data points to the existing experimental data base. Gas flow will be added as an additional operating parameter.

Axial measurements will be made and the results analyzed for the effects of anisotropy.

According to our model, the coefficient k, used to account for the kinetic energy losses on the particle scale, is a quantity dependent only on the shape of packing elements. For a given packing this coefficient should not depend on the physical properties of the liquid. This assumption will be tested by using liquids of different viscosity and packing of different types.

The assumption of complete wetting of the packing surface will be tested with liquids of different surface tension.

Electrical parts installed to our RPB unit, namely the leads and the slip ring (11 and 18 in Figure 1), are a very valuable asset for further experimental studies of the rotating porous medium. Because the leads are drawn all the way to the packing, any quantity relating to the packed bed which can be transformed into an electrical signal can be measured with very little end effects. This makes our unit a unique

experimental reactor for the study of transport processes in rotating porous media. Two of such studies can be suggested.

Pressure transducers mounted on the inner and outer support ring of the bed (2), will allow the measurement of pressure drop across the packing alone. Some preliminary measurements across the entire system which were made in our Laboratory indicated that pressure drop of the RPB was favorably low. By more accurate measurements, free of end effects, the pressure drop behavior of the RPB can be characterized more precisely for a variety of packing types. The advantages of low pressure drop may be exploited in some applications through the use of packings with high specific surface area and low porosity.

Study of the global mixing characteristics of the RPB is another experiment made possible in our equipment. Cylindrical wire mesh, like the one used in radial experiments (1), can be used to line the inner and outer support ring (2). In this way thin cells for in situ pulse generation and detection can be made. Transient conductivity measurements in that system would provide the residence time distribution characteristics of the packed bed alone.

D. Nomenclature

b	gradient of the velocity distribution at the solid surface
C	dimensionless solute concentration
C_0	dimensionless solute concentration at the solid surface
$\mathcal{D}$	binary diffusivity of solute
Da	Damköhler number, $k_s Y/\mathcal{D}$
d_p	maximum dimension of the packing element
g	centrifugal acceleration, Figure (2)
g_x	component of g in the direction of flow, Figure (2)
h	film thickness, Figure (2)
k	parameter in the coefficient of local kinetic energy loss, eq. (1); mass transfer coefficient, eq. (4)
$\overline{k}$	average mass transfer coefficient, eq. (5)
k_s	rate constant for the first order heterogeneous surface reaction
L	dimensionless distance along the solid surface
Pe	Péclet number, $bY^2/\mathcal{D}$
r	radial position in the packed bed, Figure (2)
Sh	Sherwood number, eq. (4)
$\overline{Sh}$	average Sherwood number, eq. (5)
x	dimensionless distance from the leading edge of the solid surface
y	dimensionless distance from the solid surface
Y	characteristic distance in the direction y

Greek Symbols

$\langle\beta\rangle$ radial mean holdup
θ angle of the inclination of blade with respect to the radius, Figure 2
ξ coefficient of local kinetic energy loss, eq. (1)
ϕ joint angle between two blades
ω rotational speed

E. Bibliography

1. Apelblat A., 1980, *Chem. Eng. J.*, vol. **19**, p. 19.
2. Bemer G. G. and G. A. J. Kalis, 1978, *Trans. Instn. Chem. Engrs. L.*, vol. **56**, p. 200.
3. Brauer H., 1965, *VDI Forschungsheft*, No **481**, Düsseldorf.
4. Brötz W., 1954, *Chem. Ing. Tech.*, vol. **26**, p. 470.
5. Buchanan J. E., 1967, *I. E. C. Fund.*, vol. **6**, p. 400.
6. Churchill S. W. and R. Usagi, 1972, *AIChE J.*, vol. **18**, p. 1121.
7. Davidson J. F., 1959, *Trans. Instn. Chem. Engrs. L.*, vol. **37**, p. 131.
8. Feind K., 1960, *VDI Forschungsheft*, No **481**, Düsseldorf.
9. Ganchev B., V. Zozlov and V. Lozovetskiy, 1972, *H. Tr. Sov. Res.*, vol. **4**, p. 102.
10. den Hartog H. J. and W. J. Beek, 1970, *App. Sci. Res.*, vol. **A19**, p. 338.
11. Friedman I. E., 1976, *AIChE J.*, vol. **22**, p. 407.
12. Ghez R., 1978, *Int. J. H. M. Tr.*, vol. **21**, p. 745.
13. Yimaz T. and H. Brauer, 1973 *Chem. Ing. Tech.*, vol. **45**, p. 928.

1. Stainless wire mesh screens
2. Perforated steel support rings
3. The packed bed
4. Stainless steel rotor base
5. Insulation plate
6. Retention grooves
7. Plexiglass spacer ring
8. Rotor wall
9. Rotor cover
10. Adhesive insulating foil
11. PVC insulated leads
12. Lead withdrawal hole
13. Caulk
14. Wire duct
15. Gas inlet pipe
16. Slip ring connection cup
17. Stationary slip ring piece
18. Rotating slip ring piece
19. Stationary terminals of the in-rotor part of the circuit
20. Liquid introduction nozzles
21. Liquid introduction pipe
22. Liquid seal
23. Rotor casing
24. Continuous liquid disk
25. Mounting table
26. Liquid film
27. Drain pipe
28. Rotor casing attachment bolts
29. Gasket

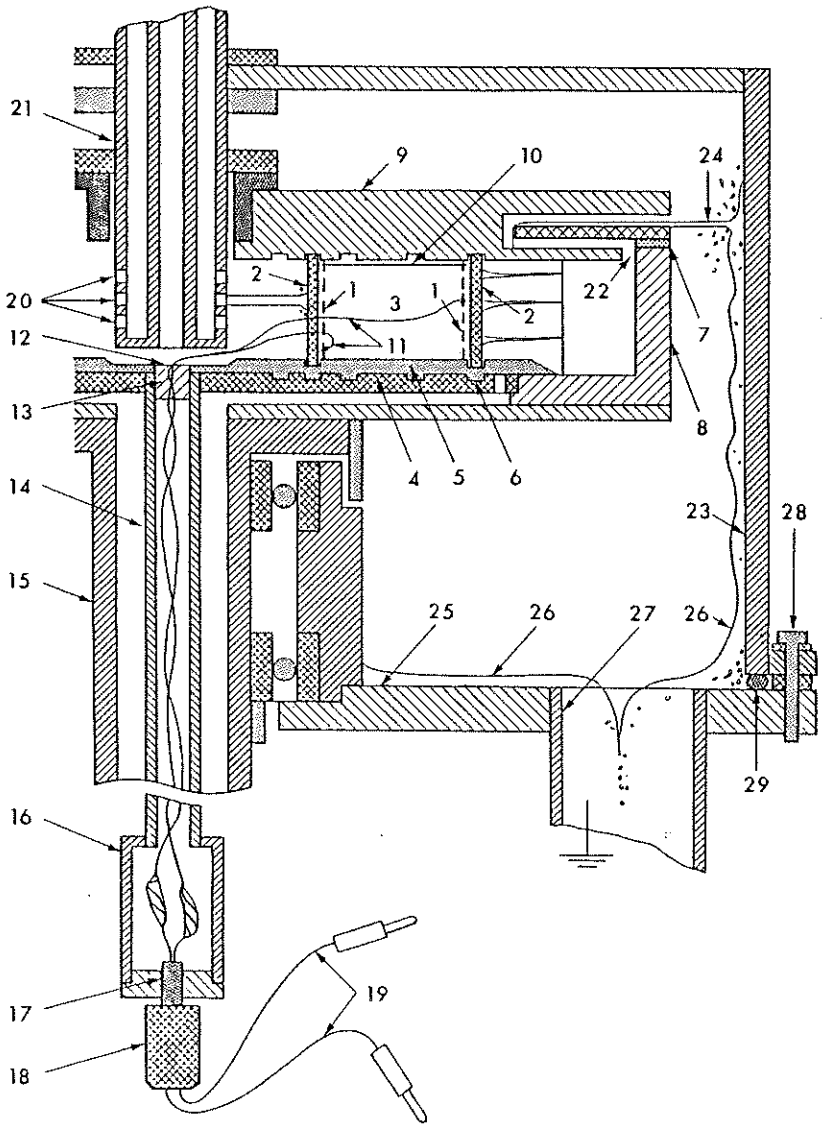

Figure 1. Cross section of the RPB with parts of the electrical circuit. Not to scale.

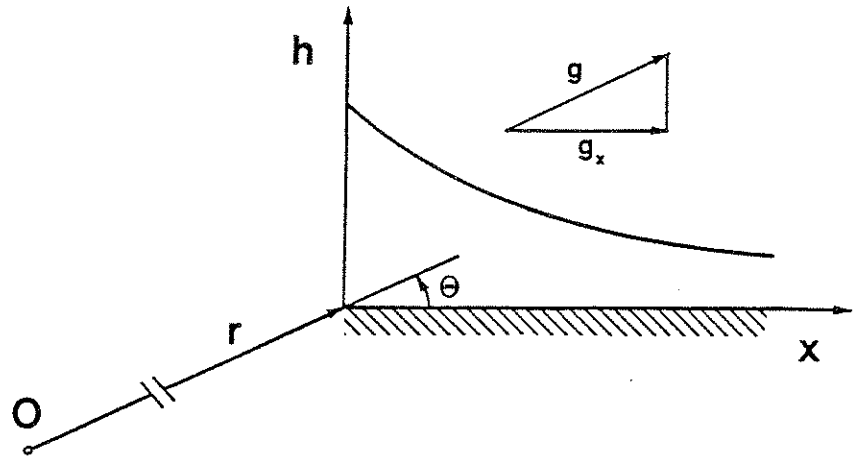

Figure 2. Schematic of the rotating blade. The system rotates around the axis of the bed, perpendicular to the plane of the drawing at point O. h is the film thickness.

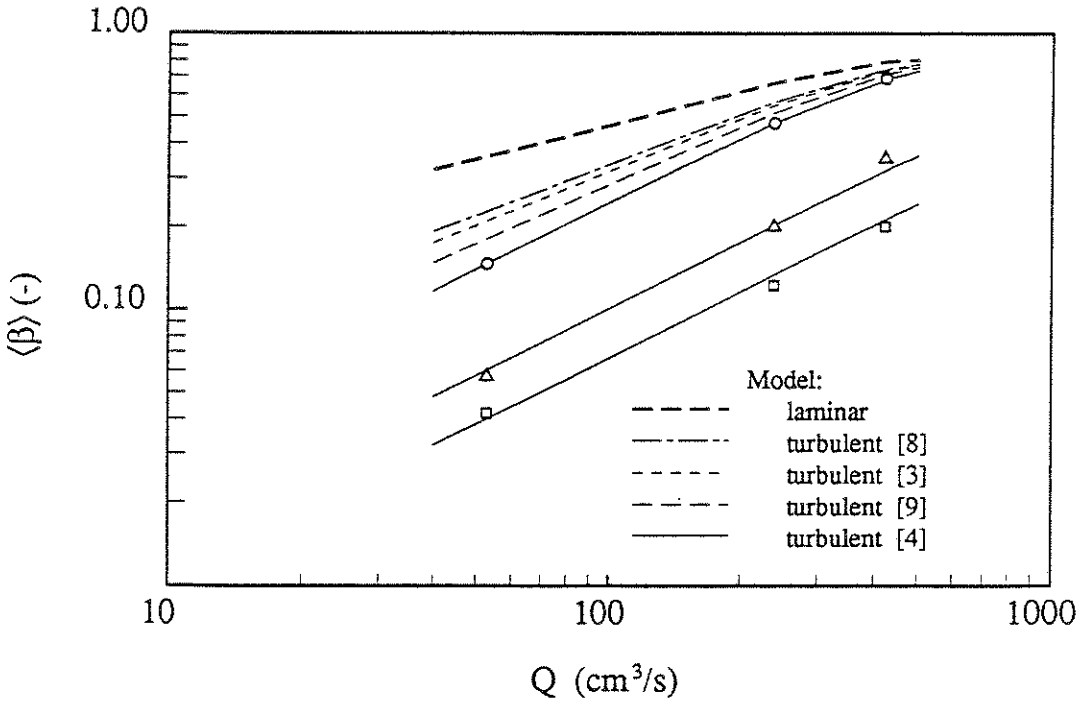

Figure 3. Comparison of the experimental data and the model for the radial mean holdup. 3 mm glass beads, porosity 0.335, bed radii 3.1 to 8.5 cm, bed height 2.54 cm, tap water, no gas flow. Circles - 314 rpm, triangles - 946 rpm, squares - 1584 rpm. $k = 0.7$ for all lines.

QUANTIFICATION OF THE MASS SPECTROMETER MEASURED RESPONSES OF A PULSE, CATALYTIC, MICROREACTOR (THE TAP EXPERIMENTS)

A. Problem Definition:

If we knew what happens on the catalyst surfaces during reactions and which were the active/selective phases, we could develop better strategies to improve catalyst performance, i.e., selectivity, activity or rate. The TAP system, Temporal Analysis of Products, lets us approach this goal a little better[1].

The TAP reactor system consists of a microreactor, a high speed pulse gas injection manifold(both contained in an ultra-high vacuum system), and a computer-controlled real time mass detector, see Figure 1. The gas pulses which are introduced by the high speed valve move through the catalyst bed and emerge with an encoded history of the reactions taking place between the reactant molecules and the catalyst surface. This history is analysed by the mass spectrometer and it gives a unique view of the catalytic reaction sequences, adsorption/desorption phenomena, and fleeting reaction intermediates.

The TAP reactor system has some unique properties. Most of the surface science techniques can obtain information only from idealized conditions and on a microscopic scale. TAP is capable of handling actual catalysts and achieving rapid screening of new catalyst formulations. It can be used to study some heterogeneous catalytic reactions which have lower reaction probabilities than what are required for the single crystal surface experiments.

The interpretation of the many types of TAP experiments is still in the development stage. Although TAP experiments that have been done before gave results which are unobtainable by other types of experiments, the results can only be explained by qualitative arguments. The quantitative treatment of these results is desirable so that the TAP technique will meet its full potential.

B. Research Objectives:

1. Develop quantitative models of the four main components of the TAP device. These are:

- the fast pulse gas delivery system;
- the catalyst micro-reactor;

- the high vacuum system;
- the real time detector system.

2. Perform experiments to verify the quantitative models. Suggest the methodology for performing experiments which will assure that data can be obtained correctly.

C. Research Progress and Results:

1. Based on the assumptions that in the catalyst microreactor the number of gas-solid collisions are much greater than the number of gas-gas collisions we arrive at the conclusion that the gas molecules will be emitted from the catalyst bed with isotropic angular distribution and with some velocity distribution determined by gas solid interaction. The mass spectrometer is a concentration sensitive device and the observed response curve reflects the change of the number density with time in the measuring zone of the mass spectrometer head. Knowing that molecules are in the molecular flow regime with some type of velocity distribution, $f(v)$, usually Maxwellian velocity distribution, and that the mass spectrometer measures concentration, the following formula can be derived which relates the flux at the reactor outlet, N_j^e, to the response curve measured by the mass spectrometer, $R(t)$:

$$R(t) = C \int_0^t N_j^e dt_i \int_{\frac{L_m}{t-t_i}}^{\frac{L_m+d_m}{t-t_i}} f(v)dv \qquad (1)$$

here $R(t)$ is the response curve recorded by the mass spectrometer, C is the scaling factor, d_m is the effective length of the mass spectrometer detector, f_v is the velocity distribution density function, L_m is the length from the reactor outlet to the mass spectrometer, t and t_i is time, v is the velocity of the molecule, N_j^e is the total flux of component j at the outlet of the microreactor.

2. A simple Knudsen diffusion model is proposed to describe the flow phenomena in the microreactor catalyst bed. In this model we solve the diffusion and reaction problem in the reactor with glass beads packed in front of the catalyst bed. We found the analytical solution of the governing partial differential equation. The first and second moment of a simple diffusion and adsorption equation is obtained which can be used to extract adsorption rate parameters from the experimentally measured response curve. The flux curve predicted by our model and the application of the Equation 1 are shown on Figure 2. The curve with the dashed line is the flux vs time curve obtained by linear operator theory for diffusion, adsorption and desorption; the curve with the solid line is the response curve measured by the mass spectrometer after applying Equation 1. We can see that the shape of the curve

does not change very much due to Equation 1, but the time shift of the curve is not negligible.

D. Future Work:

1. Use various methods to verify our assumptions and models. For example, pack glass beads inside the reactor and study how the response curve changes with the change of the glass beads diameter, pulsing gas molecular weight, reactor temperature, and packing method, etc. We can see whether the change of the response curve is consistent with the model prediction.

2. Study the possibility and the necessity for the direct proof of the model. For example, whether it is necessary and possible to install fast ionization gauge in the reactor chamber and the mass spectrometer chamber. Whether it is possible to put such ionization gauge in the microreactor. If it is necessary and possible, how can we construct such fast ionization gauge. This may help us learn more precisely how the gas molecules flow in the various components of the TAP system.

3. Try to put the TAP system of our Laboratory together.

4. Investigate the flow of gas molecules in the front part of the microreactor. If the full solution of the problem cannot be obtained, it will also be helpful to get a qualitative description of the flow phenomena.

E. References

1. J. T. Gleaves, J. R. Ebner, And T. C. Kuechler, *Temporal Analysis of Products [TAP] - A Unique Catalyst Evaluation System with Submillisecond Time Resolution,* Catalysis Review - Science and Engineering, 30(1), 49-116 (1988).

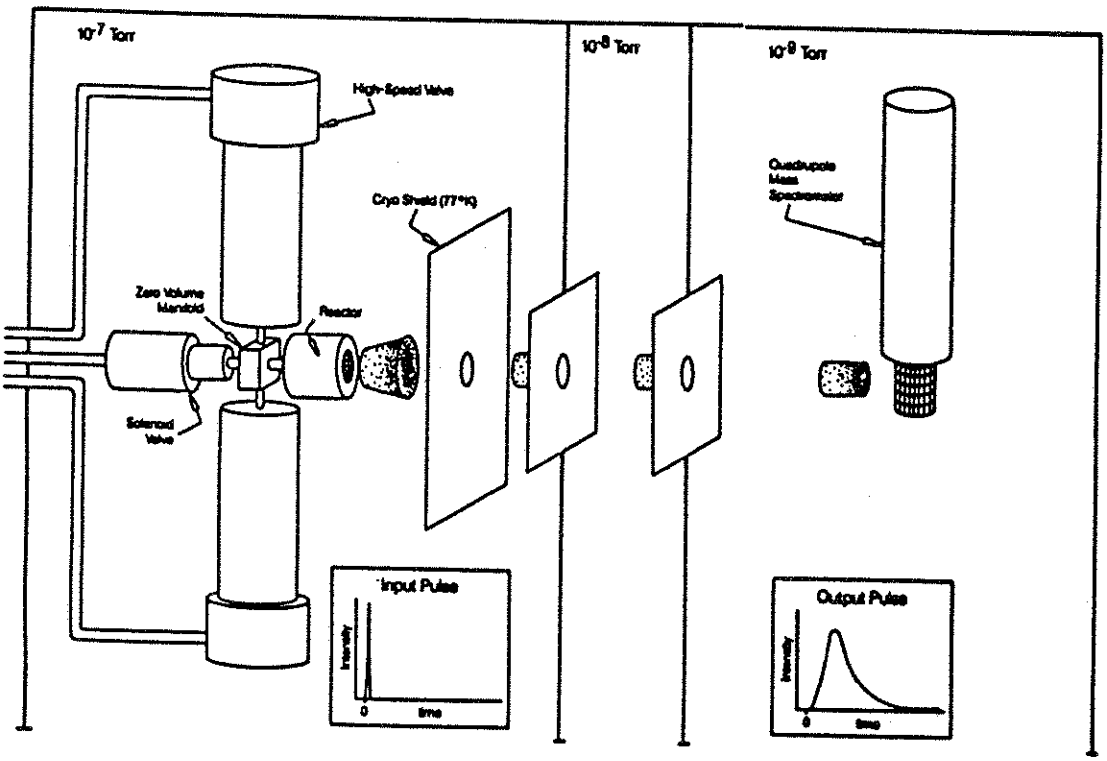

Figure 1: TAP System

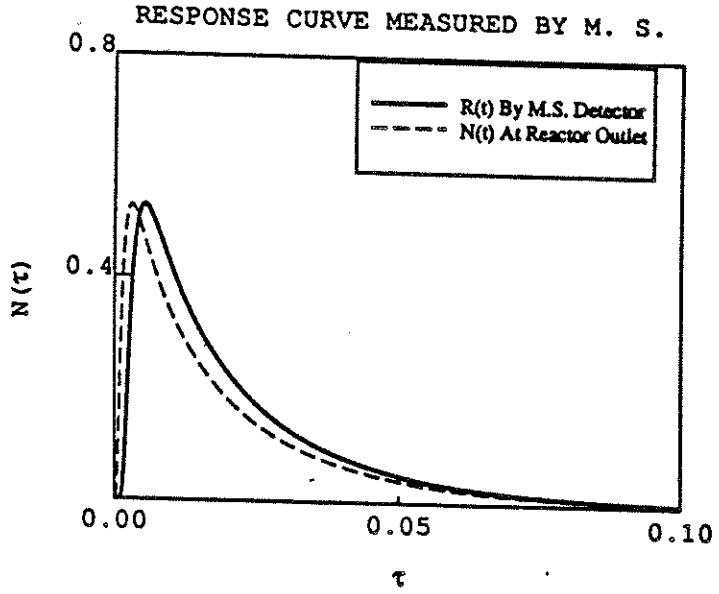

Figure 2: The Response Curve Predicted By Our Model

MODELLING OF DC PLASMA REACTORS

A. Problem Definition

Plasma processes, despite their increasing role in deposition and etching of thin films, are still an art and few modeling studies have appeared. The considerable interest in plasma deposition is driven by the ability to grow films at relatively low process temperatures, combined with special material properties that can not be realized in conventional thermally driven processes. The applications of plasma processing can be divided into two categories: deposition of material and removal of material.

Considerable experimental studies have been done on plasma reactors and the results were interpreted, for the lack of detailed models, on the basis of qualitative reasoning. Thus, plasma processing techniques have been developed empirically for the most part and the dependence of processes on certain measurable parameters may be known only very approximately. In addition, such knowledge is not fundamentally based. What is needed are quantitative models that predict the process parameters such as deposition or etching rate, film composition, etc. as a function of operating and design variables. The modeling required in this field can be subdivided into two major categories: (1) modeling of the chemical effects and (2) modeling of the electrical effects. The modeling of chemical effects includes the identification of reactions and mass transfer for the precursor, and of diffusion, thermophoretic movement, and deposition of the product species. Reaction engineering techniques can have a major impact here as revealed by some recent studies in this area. The modeling of the electrical effects is needed in order to determine the electron density(concentration) and electron energy levels(plasma physics). These plasma parameters are then used in a proper model of chemical reactions driven by the electron activation of relatively inert species. Thus, the modeling of the glow discharge needs to be coupled with the classical chemical reaction engineering methodology (plasma chemistry).

The proposed research is aimed at developing a model for plasma reactors which is both detailed and computationaly effective.

B. Research Objectives

1. To determine self-consistent models of one-dimensional dc discharges used in plasma processing and solve them by mixed numerical and analytical methods. Specifically we are seeking:
   - Development of a two-region model with generalized ambipolar approximation for the negative glow region and the numerical integration of the cathode sheath region.
   - Development of three- and four-region models which include in addition to the regions above the collisionless part of the cathode region (region very close to the cathode) and the anode sheath, respectively.

2. Calculation of electron and ion densities, electron temperature, and electric field with spatial dependence in dc plasmas.

   - Numerical integration by Gear's routine for the collisional part of the cathode region.
   - Development of approximate analytical experssions for the bulk plasma region and the collisionless cathode region.

3. Developement of a mass transfer model, by incorporating the electronegative and neutral species into the discharge model, and computation of deposition rate for the mass transfer model.

4. Verification of the model using suitable experimental data.

C. Research Accomplishments

A two region model has been developed which simplifies the computations for a dc glow discharge plasma between two parallel plates. The model consists of equations for electron and ion continuity, Poisson's equation for the electric field, and electron energy. Electron thermal diffusion is neglected based on the analysis of Lorentz models for gases. The glow discharge is divided into a cathode sheath and a bulk plasma. The anode sheath is ignored in the computations. The bulk plasma is assumed quasineutral and supports ambipolar diffusion. To link the sheath region and the bulk region, the classical ambipolar analysis is modified to include a net total current in the plasma. In the sheath region the plasma variables are determined by numerical integration of an initial-value problem by Gear's routine. The sheath region solution is obtained by integrating from the cathode toward the anode, with the ion current fixed and with the cathode electric field iterated upon until a complete solution is found. The sheath-bulk boundary occurs at that distance from the cathode where the electron and ion densities are nearly equal (sheath thickness is automatically obtained); matching conditions on the plasma varibles are imposed here.

The second region in the computation is the bulk plasma where the approximation of electroneutrality leads to an analytical solution. The matching of the electric field, particle densities and the electron temperature at the cathode sheath - bulk plasma interface completes the problem and also leads to a direct prediction of sheath thickness. In addition, as the total current is fixed, the continuity of fluxes of ions and electrons is automatically satisfied at this point. The model leads to prediction of electron and ion densities, electron temperature and electric field with the total current density and the interelectrode gap as the input variables. Exploration of discharge properties was also performed and the effect of pertinent parameters was qualitatively calculated.

The structure of the model is shown in figure 1. Figure 2 is the plot of the ion and electron densities. The electron density is almost zero in the sheath (the lower curve in figure 2) and both ion and electron densities peak in the bulk. In the bulk region,

following the ambipolar approximation, the values of the ion and electron densities are equal. The electron density is orders of magnitude smaller in the sheath than its value in the bulk, but the Gear's routine calculates it sufficiently accurately. This is one of the advantages of the initial value method used here. The method resolves a widely different concentration range for ions and electrons. The electron temperature distribution in the sheath is shown in Figure 3. The temperature rises almost linearly close to the cathode due to the acceleration of the electrons by the electric field. As the endothermic ionization starts to take place the temperature starts to drop off. An average electron temperature is computed in the bulk. This temperature is calculated by balancing the energy requirements between the sheath and the bulk. Figure 4 represents the spatial dependence of the electric field. The field increases linearly in the cathode sheath; then it becomes almost zero in the bulk and finally positive as it gets close to the anode sheath. Since the effect of the anode region is neglected, the solution of the electric field is only valid up to the 0.1 centimeter of the anode (0.1 centimeter is chosen as the anode sheath thickness for lack of better information). The potential distribution in the sheath is plotted in Figure 5 and it rises monotonically in the sheath to its most positive value in the bulk. Even though the potential drop seems small here, within the limits of our model the potential distribution seems reasonable. A detailed analytical computation was performed to find the bounds on the potental drop in the sheath and it was observed that the obtained numerical solution is well within the bounds.

For the region near the cathode (collisionless sheath) analytical solutions are possible (Mobility Limited Model). This region is assumed to be collisionless and therefore the fluxes of ions and electrons are constant. There are strong electric field effects in this region and therefore the migration term is dominant and the diffusional effects are neglected. The mobility limited model was compared with the initial value problem approach. Since the ionization is very small in the initial portion of the cathode sheath, up to 0.03 centimeter (for our computations) from the cathode, there is good agreement between this two approaches. Therefore it could be advantagous to use the analytical apporoach of the mobility limited model for calculation close to the cathode sheath. Thus the numerical solution is needed only for the collisional part of the sheath.

One of the advantages of the multi-zone model is the possible incorporation of additional important phenomena (e.g. addition of the equations for the negative and neutral species) in the model and ease of numerical stability analysis as opposed to that for the global simulation. The two-region model aids our understanding of the physics of the discharge and can be coupled with the chemistry to complete the picture of glow discharge modeling.

D. Future Work

1. Addition of the conduction term to the electron energy equation.

2. Addition of excitation reactions to the existing model.

3. Expanding the model to predict the deposition rates of thin films in plasma reactors.

Bibliography

1. B. Chapman, *Glow Discharge Processes.* New York, John Wiley & Sons, 1980.

2. G. Turban, and Y. Catherine, *J. Thin Solid Films*, 48, 57, 1978.

3. D. B. Graves and K. F. Jensen, *J. IEEE Trans. Plasma Sci.*, 14, 78, 1987.

4. S. Chapman and T. G. Cowling, *The Mathematical Theory of Non Uniform Gases.* Cambridge University Press, 1958.

5. C. W. Gear, *Numerical Initial-Value Problems in Ordinary Differential Equations.* Prentice-Hall, Englewood Cliffs, 1975.

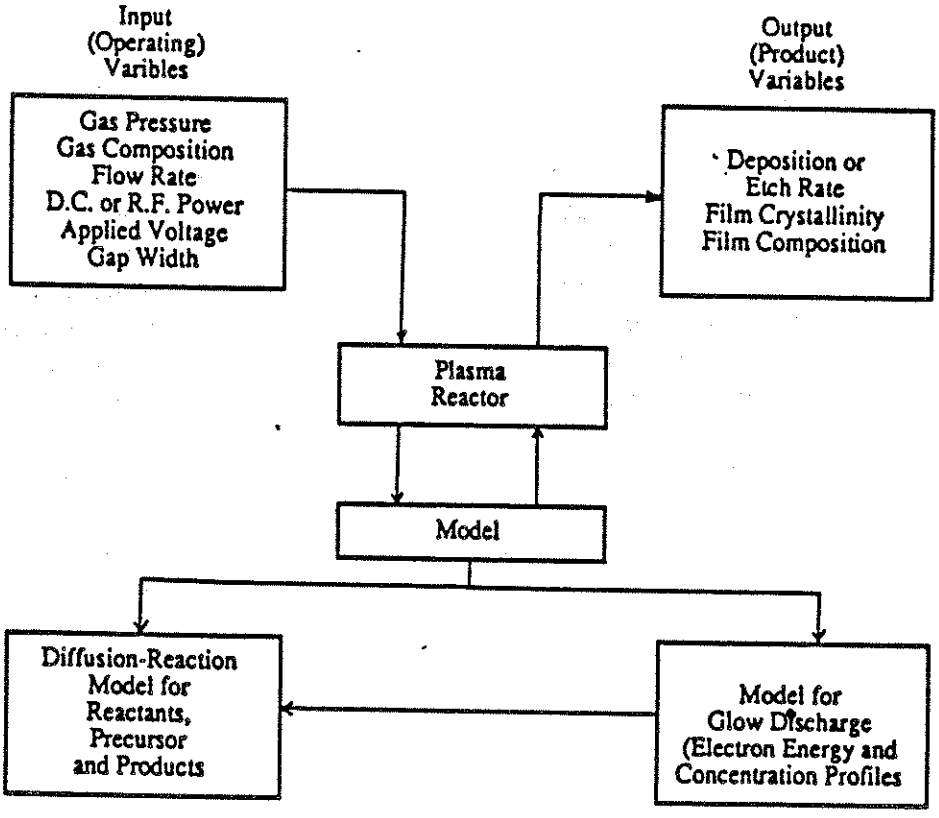

Figure 1: Interrelationship of the subtasks involved in plasma modeling

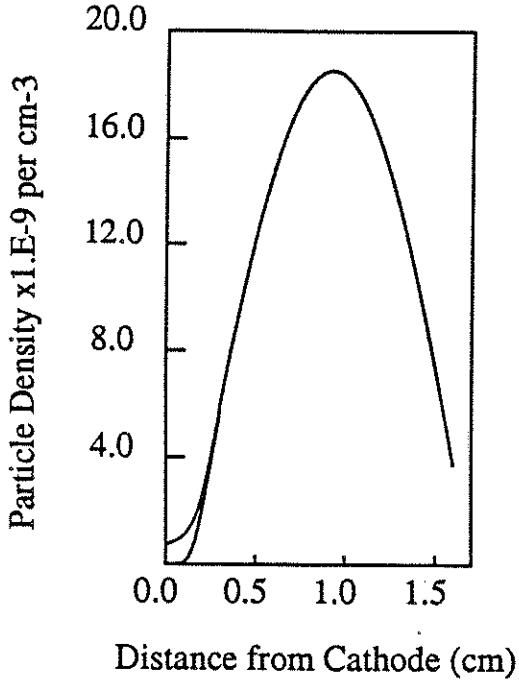

Figure 2

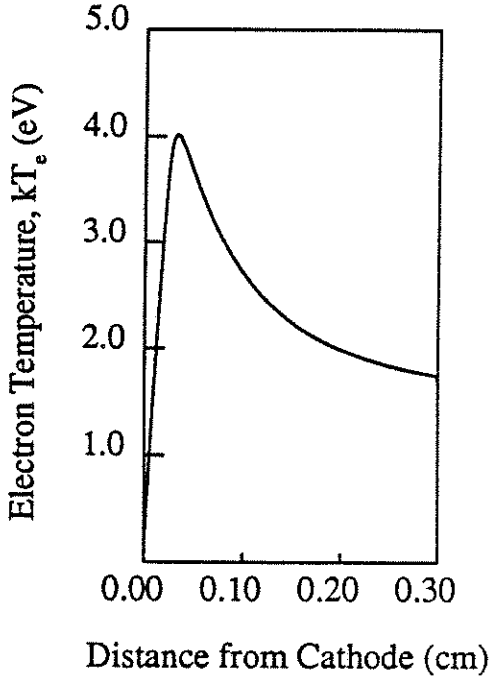

Figure 3

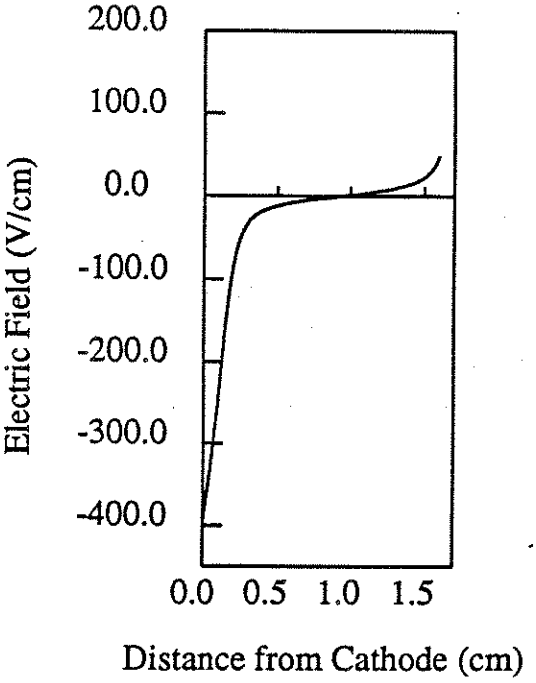

Figure 4

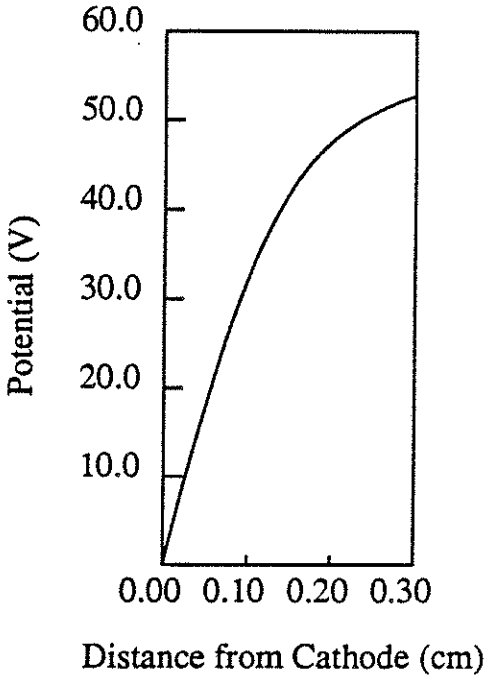

Figure 5

MODELING OF CYCLIC PROCESSES:

HEAT REGENERATORS UTILIZING PHASE CHANGE MATERIALS

A. Problem Definition

Energy consumers, such as the chemical process industry, are being forced to improve their overall thermal efficiencies. There are several factors responsible for the need to improve efficiencies:

- economic – nonrenewable, low-cost energy sources are being depleted, forcing a conversion to more expensive fuels;
- legislative – emission standards for pollutants such as SO_x, NO_x and CO, forcing a reduction in fuels burned;
- legislative – maximum temperature levels for exhaust/stack gas temperatures, forcing heat recovery from waste gasses;
- legislative – maximum temperature levels for steam condensate and cooling water, forcing heat recovery for waste heat streams.

Gunn [1] reports an estimate that approximately eleven percent of the energy consumed in the manufacturing sector is rejected as waste heat. The manufacturing sector can no longer afford this.

Heat regenerators and recuperators are often employed to recover and recycle thermal energy, thereby improving overall efficiency and reducing emissions. Recuperators are essentially heat exchangers which transfer heat from one stream to another. Recuperators cannot store energy, and consequently the heat extracted from the waste stream must be used immediately. For high temperature heat recovery, recuperators must be made of costly high temperature alloys or ceramics. Capital costs for recuperators may be high because of the intricate geometries; e. g. cross-flow, curved-plate counter-flow, as well as the shell and tube; see Reiter [2] and Reay [3]. In particularly dusty environments, recuperators may suffer from severe erosion.

Packed bed regenerators, on the other hand, are relatively simple in design; consisting of a tower packed with inert packing (e. g. stoneware) or checkerwork. They are capital inexpensive and very durable. In dusty environments regenerators do not suffer severe erosion, and any damage that may occur can be easily repaired by replacing the inexpensive packing. Regenerators store heat in the packing for use at a later time. In some applications this is an advantage since heat requirements tend to be cyclic; whereas in some continuous processing applications this is a disadvantage.

A variation of the packed bed regenerator is the rotary regenerator or Ljungstrom wheel [2], [3]. This regenerator combines the features of a recuperator with the heat storage capability of a regenerator. A wheel of packing or checkerwork rotates within a split duct. The hot stream flows through one side of the duct, while the cold

flows though the other side. Heat transfer can be regulated by varying the rotational speed of the wheel, as well as by use of dampers to regulate the flows of the streams. The Ljungstrom wheel is used in many industrial applications and finds some use in residential cooling applications in Europe. For cooling applications the rotary regenerator may be coated with a hygroscopic salt, e. g. LiCl. When warm, moist air passes over the hygroscopic packing, water condenses thus cooling and dehumidifying the air which is then fed into the building's air conditioning system. The stale, dry building air passing through the exhaust duct of the wheel carries the moisture which has been absorbed by the wheel away, thereby regenerating the hygroscopic surface. Thus the latent heat of vaporization of water has been used to improve the effectiveness of the rotary regenerator.

It would seem quite logical to extend the concept of using latent heat storage in regenerators. The calculations of Lai [4] and Schmidt and Willmott [5] show that as the regenerator packing thermal conductivity increases the effectiveness (or efficiency) also increases. In addition, as the heat capacity of the packing increases the amount of heat which can be stored per unit volume of regenerator increases. In other words, capital costs for a fixed regenerator capacity should be reduced as one uses regenerator packing with higher heat storing capacities.

Latent heat storage offers orders of magnitude higher heat storing capacity over sensible heat storage. Substantial amounts of energy are absorbed or released when a material undergoes a phase change. Table 1 lists some compounds comparing heat capacity and latent heat of fusion. A regenerator packed with encapsulated phase change material could potentially serve as a highly effective and economical heat storage device. It is of interest to note that besides within CREL, the concept of using encapsulated phase change material has been independently proposed by Mulligan [6].

B. Research Objectives

The objective of this project is to model regenerators which contain encapsulated phase change materials. We wish to gain insight into how they may be potentially utilized. Specifically, there are three major tasks to accomplish:

1. Develop a model for packed bed and rotary regenerators using encapsulated phase change materials. Establish the effectivenesses of these units.

2. Examine whether such a regenerator which is cycled in a periodic fashion is stable in time, i. e. does the regenerator have single or multiple operating states? What values of parameters guarantee a single stable state.

3. Explore cases where reactions are conducted in regenerators. Can regenerators serve as packed bed reactors? Can isothermality be maintained, at least in semi-batch operation, in regenerators packed with encapsulated phase change material?

C. Research Accomplishments

Initial efforts have focused upon modeling encapsulated phase change material. This problem is referred to as the Stefan problem. For finite geometries an analytical solution does not exist (Carslaw and Jaeger [7]). Consequently numerical solutions must be employed. Crank [8] and Furzeland [9] describe techniques for numerical solution. One technique is to immobilize the moving boundary between the liquid and solid phases via a numerical transformation. Once this is accomplished the highly nonlinear partial differential equations describing heat flow in the liquid and solid phases may be numerically integrated along with the equation describing the freezing/thawing front velocity.

Assuming the particle scale dynamics can be obtained, one needs to consider the regenerator bed scale. Initial attempts to incorporate a dispersion model, see Wen and Fan [10], were unsuccessful because of the nonlinear nature of this model and coupling with the nonlinear Stefan problem on the particle scale. Recently the mixing cell model, see e. g. Butt [11], has been considered an appropriate model. Currently this model is being programmed.

D. Future Research Plan

1. Complete computer models for phase change regenerators. Simulate and examine performance. Compare effectiveness to that obtained in conventional regenerators.

2. Extend packed bed model to develop a model for Ljungstrom regenerators. Consider performance and effectiveness for this regenerator.

3. Establish mathematical criterion for uniqueness and stability of the phase change regenerators. Determine if multiple operating states exist. If so, establish regions guaranteeing uniqueness.

4. Extend models to consider conducting n-th order exothermic or endothermic reactions in packed bed regenerators. Examine issues of isothermality.

5. Explore techniques for fabricating encapsulated phase change materials.

6. Verify model predictions in an experimental apparatus.

Bibliography

1. Gunn, Marvin E., "Recovery of Industrial Waste Heat", in *Utilization of Reject Heat*, Chapter 2, Mitchell Olszewski, editor, Marcel Dekker, Inc., New York, (1980)
2. Reiter, Sydney, *Industrial and Commercial Heat Recovery Systems*, Chapter 4, Van Nostrand Reinhold Company, Inc., Cincinnati, (1983)
3. Reay, D. A., *Heat Recovery Systems – A directory of equipment and techniques*, Halsted Press, a Division of John Wiley and Sons, Inc., New York, (1979)
4. Lai, Shin-Ming, *Periodic Operation of Heat Regenerators: A New Method for Calculation of Thermal Efficiency*, Master of Science Dissertation, Washington University, St. Louis, Missouri, (1983)
5. Schmidt, F. W. and A. J. Willmott, *Thermal Energy Storage and Regeneration*, Hemisphere Publishing Corporation, New York, (1981)
6. Mulligan, J. C., *NASA Tech Briefs*, **13**, 4, p. 103, (1989)
7. Carslaw, H. S. and J. C. Jaeger, *Conduction of Heat in Solids*, Second Edition, Chapter XI, Oxford Press, Great Britain, (1959)
8. Crank, John, *Free and Moving Boundary Problems*, Oxford Press, Great Britain, (1984)
9. Furzeland, R. M., *J. Inst. Maths Applics*, **26**, pp. 411-429, (1980)
10. Wen, C. Y., and L. T. Fan, *Models for Flow Systems and Chemical Reactors*, Marcel Dekker, New York, (1975)
11. Butt, J. B., *Reaction Kinetics and Reactor Design*, Prentice-Hall, Englewood Cliffs, New Jersey, (1980)

Table 1
Heat Storage Data for Selected Compounds

Compound	Heat Capacity, kJ/kg °K	Heat of Fusion, kJ/kg	Melting Point, °C
H_2O	4.2	335.	0.
Na_2SO_4	1.9	254.	32.
P116 Paraffin	2.5	210.	47.
$Ba(OH)_2$	1.2	267.	78.
$MgCl_2$	1.7	165.	116.
Li	3.6	268.	179.
Fe_2Cl_6	0.3	264.	304.
B_2O_3	0.9	330.	450.
Al	0.9	398.	660.
KCl	0.7	360.	770.
KF	0.8	469.	875.
NaF	0.4	698.	992.

OPTIMAL CATALYTIC REACTOR DESIGN: CHEMICAL REACTION ENGINEERING ASPECTS OF NO_x ABATEMENT

A. Problem Definition

Nitrogen oxides (NO_x) emissions from anthropogenic sources are being subjected to stringent controls. Recent regulations for the Los Angeles Basin have targeted refineries for drastic NO_x emission reductions, and similar trends for other stationary sources are progressing on a national and international scale (more and less slowly, respectively). In the case of utility power plants, two options are available for reducing emissions – combustion modification and flue gas treatment. While the former is usually economically favorable, frequently the latter must also be employed to meet the emission standards.

The most common flue gas treatment technology entails selective catalytic reduction (SCR). In this case, ammonia is injected into the flue gas stream where the NO_x and ammonia-derived nitrogen is reduced to diatomic nitrogen over a suitable catalyst. The reactor type is usually a monolith with honeycomb or parallel plate passages. These designs feature low pressure drops (and thus less energy penalty on the overall plant thermal efficiency) relative to packed beds. To date, the United States has imported its SCR technology from Japan and Europe. It has not been demonstrated that optimal conditions for overseas systems coincides with optimal conditions for U.S.-based operations. Discrepancies may arise due to differences in fuel type and overall plant operating conditions. Indeed, relatively little attention has focused on the chemical engineering aspects of optimal reactor design. This leads to a key question – how does one select the optimal process, catalyst and reactor type for NO_x abatement? Also, on a more fundamental basis, this problem addresses the area of reactor design for mass transfer limited gas-solid catalytic reactions.

B. Research Objectives

We wish to study the design of reactors for gas-solid catalytic reactions. A *generic* approach is favored because the developments should be applicable to a broad range of systems encompassing industrial processing and pollution abatement. Key results will be demonstrated using suitable case studies such as SCR technology for NO_x abatement.

C. Research Accomplishments

This project is evolving from its embryonic stage. Preliminary work focused on developing a concise set of project goals. We subsequently built a firm understanding in the current status of NO_x abatement technology. Most recently, the literature concerning gas-solid catalytic reactions has been reviewed.

D. Future Research Plan

Objective functions will be defined for comparing reactor types. The functions will be based on economic principles. Dependent variables: may be selected by optimization of the objective function; or may appear as constraints in the problem statment. For example, in the case of NO_x abatement, minimum reactant conversion appears as a constraint set by current regulations. The objective function balances catalyst volume against pressure drop. Other processes may be subject to different objective functions. A key aspect of this work is the identification of the extent to which the results can be generalized to different processes.

The objective functions will be used to determine the performance of various traditional reactor types. We wish to determine how the optimal conditions differ: between various reactors for a given objective function; and between various objective functions for a given reactor type. The study will cover geometries such as channels, pipes and packed beds; both laminar and turbulent flow regimes will be investigated.

Next we will extend the analysis to assess the effects of various mass transfer enhancement devices such as wavy surfaces and turbulence promoters. This study will quantify the net gains achievable by such systems, and hopefully shed light onto novel structural designs. Upon embarking into the realm of novel structures, it will be necessary to conduct experimental mass transfer studies to verify the anticipated reactor performance.

Design of a Recycle Reactor System

A. Problem Definition

The majority of large scale processes in chemical and petroleum industries are based on heterogeneous catalytic reactions. Therefore, there is a need to have a reliable experimental system for measuring rate data in packed beds of catalyst particles under precisely controlled and known conditions.

An external recycle reactor, shown in Figure 1, is best suited for this purposes. The outstanding features of such a reactor are: direct measurement of the reaction rate, perfect mixing, isothermal operation, minimum error of analysis and direct measurement of fluid flow rate and its superficial velocity. The designed system should have the following features:

1. The ability to eliminate external mass and heat transfer resistances so that the kinetic rate, masked possibly only by internal diffusional effects, can be obtained.
2. The ability to achieve and measure superficial velocities typical of commercial reactors so that the effect of velocity on apparent kinetics can be studied in scale-up and scale-down applications.

Successful handling of this problem requires a combination of theoretical and practical expertise. The problem is addressed jointly with Autoclave Engineers.

B. Research Objectives

1. Design, construction, and operation of a recycle packed bed catalytic reactor which will allow:
   - Isothermal operation
   - Precise control and measurement of gas and solid temperature, net gas flow rate, recycle gas flow rate, inlet and exit gas composition.
2. Selection of a test reaction related to pollution abatement, conducting experimental studies and comparing the data obtained in the new recycle system to data from other systems.
3. Conducting experimental studies and analysis of data in preparing guidelines for the design and scale-up or scale-down applications..
4. Critical analysis of the desirable experimental reactors for scale-up or scale-down of reactions catalyzed by catalytic monoliths and packed-bed reactors.

C. Research Accomplishments

Comprehensive literature review of the currently available information on experimental packed-bed catalytic reactors, internal recycle reactors, external recycle reactors and other laboratory reactors was completed. Their advantages and disadvantages for operation have been summarized at high temperature and low to moderate pressure. From the review of the available external recycle reactors, it was found that the critical hardware problem

associated with the external recycle reactor is the recirculating pump, since there are no commercial pumps that satisfy the required pump features. Accordingly, ideas to modify and construct a new pump which could be operated at high temperatures up to 600C°, low to moderate pressures (1-10 atm) and at high recirculation flow rate have been specified and discussed with Autoclave Engineers Inc.

The design of a recycle reactor system that meets the objectives stated above has been accomplished. The Autoclave Engineers Micro-BTRS Oven Reaction System has been chosen for appropriate modifications. SO_2 oxidation is selected as a test reaction. The necesary calculations to evaluate the pressure drop throughout the reactor bed, heating and cooling requirements during the startup and steady state operation, the temperature drop throughout the recirculation loop and the required heating to bring the inlet flow to the reaction temperatures have been done by developing general computer programs. Calculations for different dimensions and operating conditions were performed for the chosen reaction system of SO_2 oxidation. Heating and cooling capacity, pressure indicator, temperature measuring device, valves, checkvalves, filters and flow rate measuring devices have been specified. Also the dimensions and sizes of the reactors and the system setup have been specified. Figure 2 shows the schematic drawing of the reactor. Figure 3 and Figure 4 show the front view and side view respectively of the recycle reactor system which is accomodated in the Micro-BTRS Oven. Figure 5 and Figure 6 show the pipes and instruments layouts of the system.

D. Future Work

1. Detailed specification of the instruments required for the system.
2. Analysis of the desirable experimental reactors for monoliths and packed-bed studies in scale-up or scale-down applications.
3. Construction of the recycle system and the experimental setup.
4. Testing the modified pump to prove its ability to meet the system objectives.
5. Testing the recycle reactor and the experiment of setup.
6. Studies of the kinetics of SO_2 oxidation.
7. Taking data oriented toward design and scale-up and developing the protocol for this purpose.
8. Demonstrating the ability of the new system and comparison with data from other reactor systems.

Bibliography

1. Akyurtlu, J.F.; Curtlin, D.J.; Sviatoslavsky, I.N. and Steware, W.E. Ind. Eng. chem. Fundam. Vol. 25, 290-292, 1986.
2. Berty, J.M., Plant/Operation Progress, Vol. 3 No. 3, 163, 1984.
3. Berty, J.M. and Berty, I.J., Alche. Annual Meeting, Nov. 1987, New York City.
4. Carberry, J.J., Industrail and Engineering Chemistry, Vol. 56, No. 11, 39, 1964.
5. Christoffel, E. G., Catal. Rev. _ Sci. Eng. Vol. 24 No. 2, 159-232, 1982.

6. Doraiswamy L. K., and Tajbl, D.G., Cat. Rev. _Sci. Eng. Vol. 10, No. 2, 177-219 1974.
7. Livbjerg H. and Villadsen J., Chem. Engr. Sci., Vol. 26, 1495-1503, 1971.
8. Perkins, T. K. and Raise, H.F., Alche. J. Vol.4 No. 3, 351, 1958
9. Serrano, C. and Carberry, J.J., Applied Catalysis 19, 119-139, 1985.
10. Weekman, V.W., Jr. Alche. J. Vol. 20 No. 5, 833, 1974.

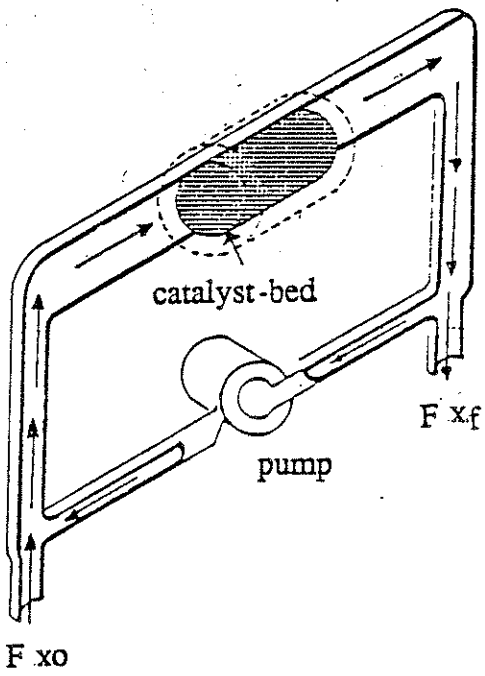

Figure 1: Schematic drawing of external recycle reactor system.

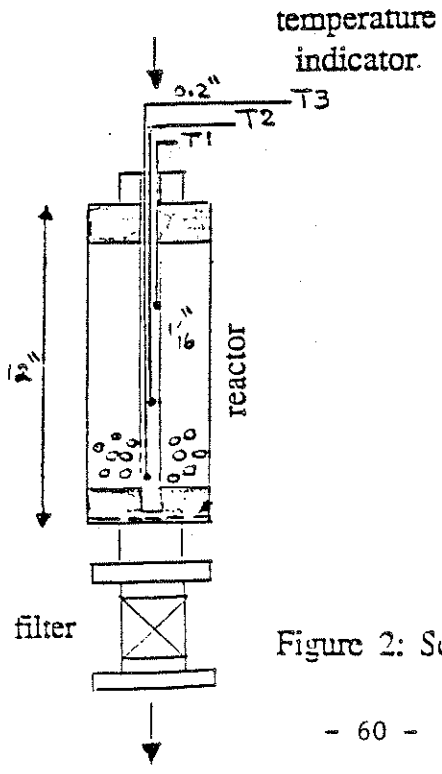

Figure 2: Schematic drawing of the reactor.

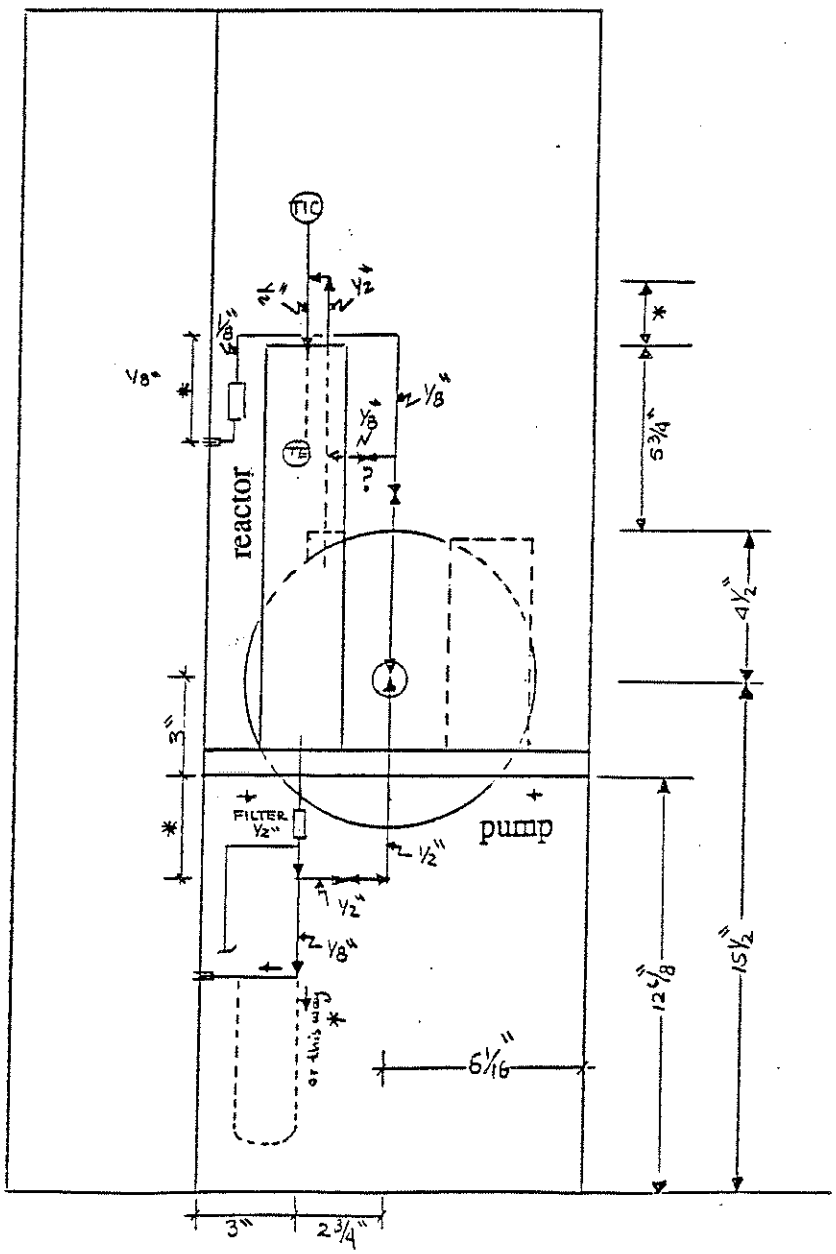

Figure 3: Front view of the external recycle reactor system.

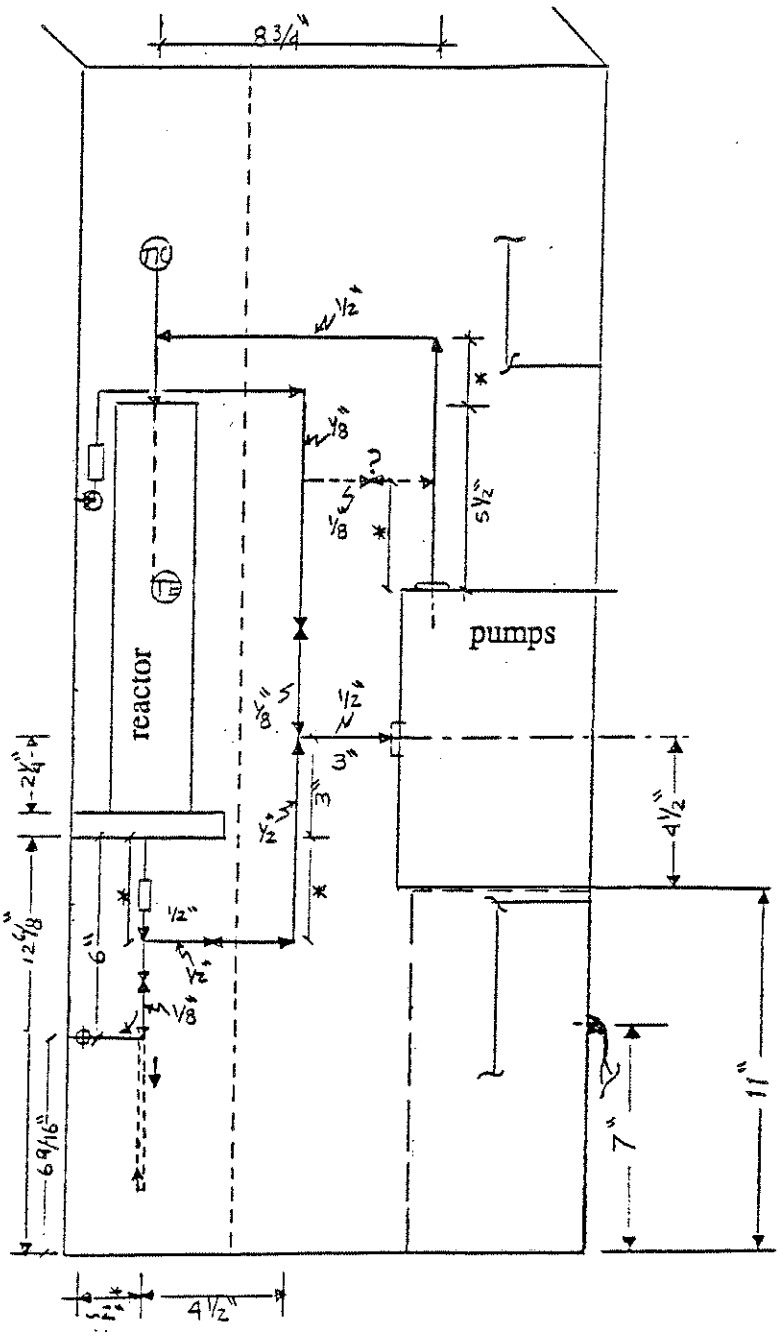

Figure 4: Side view of the external recycle reactor system.

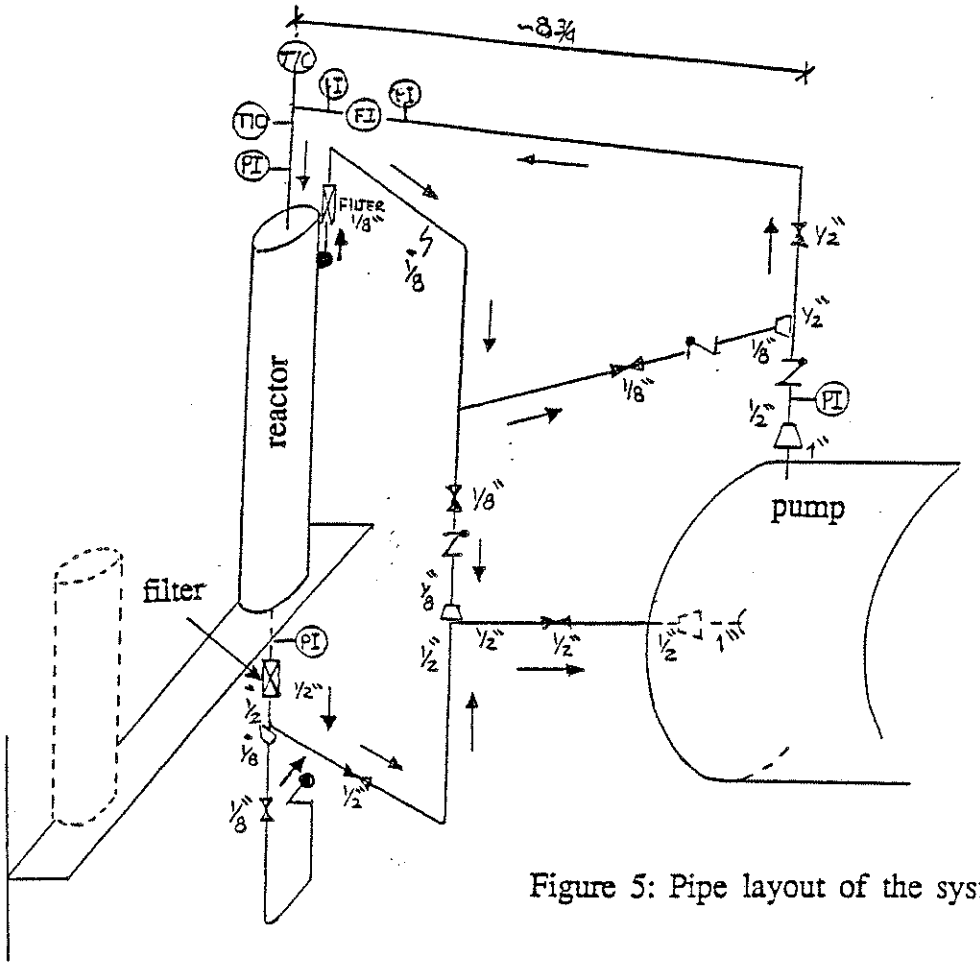

Figure 5: Pipe layout of the system.

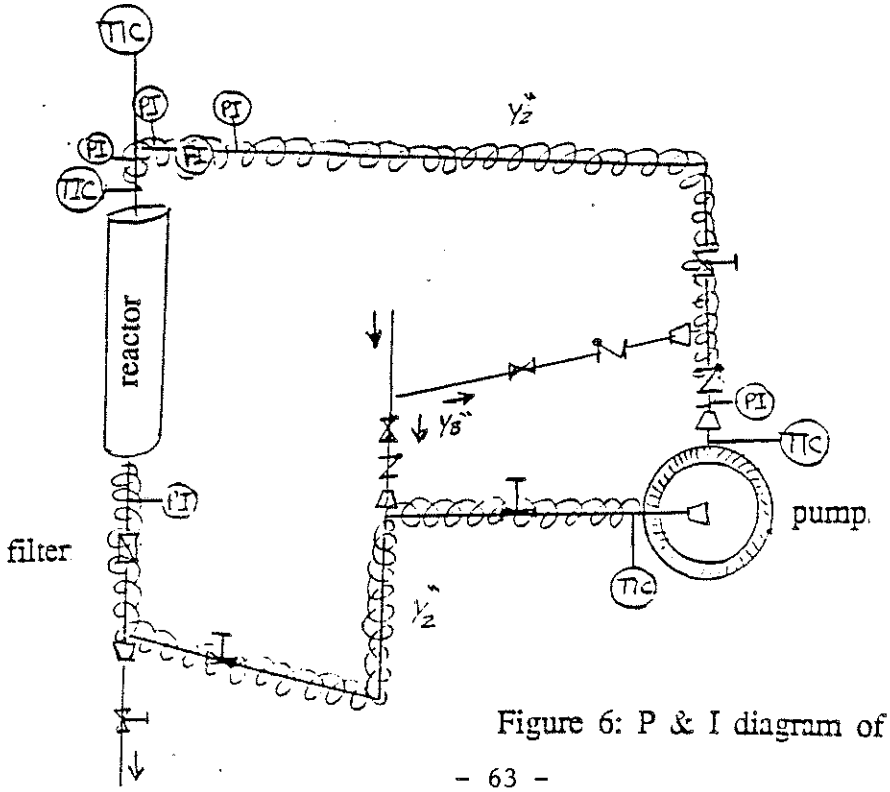

Figure 6: P & I diagram of the system.

NOVEL POROUS CARRIER AND REACTOR FOR MAMMALIAN CELL CULTURES

We regret that due to the desire of our Medical School colleagues to pursue a patent application we cannot at this time reveal the contents of this project. No CREL funds were used in support of this project. CREL community will get the information above as soon as possible.

AREA II. PREPARATION OF NEW MATERIALS

The emphasis is on introducing the reaction engineering methodology in describing transport-kinetic interactions involved in manufacture of new materials. Modeling, based on first principles and experimental work, is pursued.

The goal is rapid assessment of various technologies and rapid transfer of bench scale science to manufacturing.

MODELING OF THE AEROSOL REACTOR FOR PRODUCTION OF POLYCRYSTALLINE SILICON

A. Problem Definition

One attractive approach in producing bulk silicon particles, with the possibility of conveying silicon particles directly to the Czochrolski's crystal growth apparatus, is by homogeneous gas phase pyrolysis of silane in a series of aerosol reactors. Particle sizes as large as $10\mu m$ in mass mean diameter were produced at CalTech in a laboratory tubular reactor shown in Figure 1 using seed particles of $0.16\mu m$ in diameter. If the particles can be grown to larger sizes, for example 50 to $100\mu m$, this aerosol reactor would provide a very desirable means for commercial manufacture of polysilicon. In order to accomplish this goal, two steps are required: (1) Establish a basic theory of particle growth, set up a laboratory scale reactor, and experimentally demonstrate the feasibility of growing large size particles. (2) Apply the theory of particle growth together with the reaction kinetics and transport effects to formulate a detailed reactor model. An appropriate model could provide the necessary information on how to improve the laboratory scale reactor in order to grow the aerosol to super-micron size, and would present guidelines for design of large scale reactors.

Small particles grow by the following major mechanisms as illustrated in Figure 2: (1) agglomeration of fines on seed particles, (2) condensation of silicon vapor on particle surface, and (3) CVD reaction on particle surface. Successful growth of aerosol particles requires that the seed aggregates scavenge effectively the fines formed by homogeneous nucleation at a maximum decomposition rate of silane. Previous work on modeling aerosol reactors neglected the agglomeration of the aerosol which is very important for the system of interest. Therefore a model accounting for agglomeration had to be developed.

B. Research Objectives

The purpose of this research is to study the transport-kinetic effects in production of silicon particles. Specifically it is desired to model the aerosol reactor and to investigate the possibility of growing larger particles for commercial application. The research objectives are:

- Critical Evaluation of Union Carbide's and CalTech's attempts to grow silicon particles by condensation, agglomeration and CVD growth to $50-100\mu m$ sizes.
- Modeling the second stage of CalTech's aerosol reactor with seed particles. This will include the mass balances for both silicon vapor and silane, and population balances for fines and seed particles.
- Comparison of model predictions with the experimental results.
- Determination of whether one could, in a series of reactors, accomplish particles growth to $50-100\mu m$ and estimation of the required temperature profile.

C. Research Accomplishments

A rather involved mathematical model, based on first principles, has been developed to simulate the agglomeration, coagulation, condensation as well as CVD reaction occurring in a seeded aerosol reactor for production of silicon particles. Mass balances on silane and silicon vapor as well as population balances are considered. Although the mathematical formulation of model equations follows well established conservation laws, not only is there no analytical solution for the resulting integral-differential equations, but a straightforward numerical approach quickly runs into severe, practically prohibitive requirements on computer time and memory. Therefore, as an approximation, the population balances for the particles are reduced to dual moment equations for fines and seed aggregates with application of fractal dimension and parametized distribution functions. Two techniques are discussed in developing the moment equations. The first consists of approximating the collision frequency functions with effective values, and the second uses collision frequency functions to generate the moment equations.

The dominant particle growth mechanism in this system is scavenging of small fines, which initially have very small size and later are fused to a $0.1\mu m$ range. As illustrated in Figure 3, the agglomeration of small fines on seed aggregates accounts for 90% of the seed growth on average, while condensation of silicon vapor contributes about 10% and CVD reaction on seeds less than 2 %. This mechanism suggests that in order to grow the particles successfully the reactor should be designed so that the seed aggregates can always scavenge the fines effectively.

The model simulations are in good agreements with the available experimental results on particle mass distributions. Figure 4 shows the model predictions compared with the experimental data for 1% silane in the feed. Figure 5 shows the model predictions for 2% silane in the feed with breakage of agglomerates accounted for and without breakage accounted for. The simulations demonstrate that the detailed model with breakage describes the mass distribution of product particles well. Breakage of agglomerates becomes important only at SiH_4 concentrations higher than 1% which leads to formation of loose aggregates (lower fractal dimension).

The process parameters, such as feed silane concentration, seed number concentration, temperature profile along the reactor, gas flow rate etc. are related to the silane yield into product aggregates, mean product size, fines' loss as well as the size distributions of product aggregates and fines. Model predictions indicate that as the feed silane molar fraction increases, the yield decreases because more fines are generated at larger silane concentration and growing fines also scavenge the smaller fines. However, the mass mean diameter of aggregates increases with increasing silane fraction. The temperature profile employed in the experiment in the second stage of the reactor is:

$$T = 775(1 + 0.685 \times Z^n)^{0.5} \ ^oK \tag{1}$$

with $n = 1$, where Z is the dimensionless distance along the reactor.

If the temperature profile is changed by varying the power dependence n on reactor dimensionless length Z, the yield of seed aggregates is also changed as shown

in Figure 6. The best yield about 74 % is achieved for 1 % silane feed with $n = 0.75$ because of the balance of two rates – coagulation rate among fines and scavenging rate of fines by seeds.

After investigating the flow rate and seed number concentration effects on the yield, the optimal operating conditions are identified. If the flow rate is reduced by 50% and the seed number concentration is decreased by 20% with $n = 0.75$, the yield can increase to 78.9% and the mass mean diameter would be $7.0\mu m$ for 1% silane feed in nitrogen system. It is also indicated that using hydrogen as carrier gas would grow the particles up to $12\mu m$ in mass mean diameter with yield about 80 % for 1 % silane feed under optimal operating conditions, due to larger diffusivity of silicon vapor and larger collision frequency between fines and seeds in the hydrogen carrier system.

It is estimated that about 1000 reactors in a series, without diluting the seed number concentration from stage to stage, are required in order to grow dense particles to $50\mu m$ in diameter, if 1 % SiH_4 feed in hydrogen is chosen with the seed number concentration of $2.5 \times 10^4 \#/cm^3$ and with temperature profile shown in equation (1) with $n = 0.75$. However, if the seed number concentration is diluted by a factor of 1.2 from stage to stage, only 30 reactors in a series are needed for growing dense particles to $50\mu m$ in diameter.

D. Further Research Plan

- Modify the detailed model to take into account the process of fusing seed aggregates to dense particles that will be used as seeds in the next stage reactor.
- Experimentally verify the model prediction for the third stage of aerosol reactor.

Bibliography

1. Yubo Yang and M. P. Duduković, " Modeling of the Aerosol Reactor for Production of Silicon Particles Using Fractals", *AIChE 1988 Annual Meeting*, Paper No. *62j*, Washington, D.C., Nov. 27 – Dec. 2, 1988
2. Alam, M. K. and R. Flagan, " Controlled Nucleation Aerosol Reactor: Production of Bulk Silicon", *Aerosol Science and Technology*, **5**, 237-248, (1986)
3. Richter, R., L. M. Sander and Z. Cheng, " Computer Simulation of Soot Aggregation", *J. of Colloid and Interface Science*, **100**, 203-209, (1984)
4. Mountain, R. D., G. M. Mulholland and H. Bauss, "Simulation of Aerosol Agglomeration in the Free Molecular and Continuum Flow Regimes", *J. of Colloid and Interface Science*, **114**, 67-81 (1986)
5. Frenklach, M. and S. J. Harris, " Aerosol Dynamics Modeling Using the Method of Moments", *J. of Colloid and Interface Science*, **118**, 252-261 (1987)

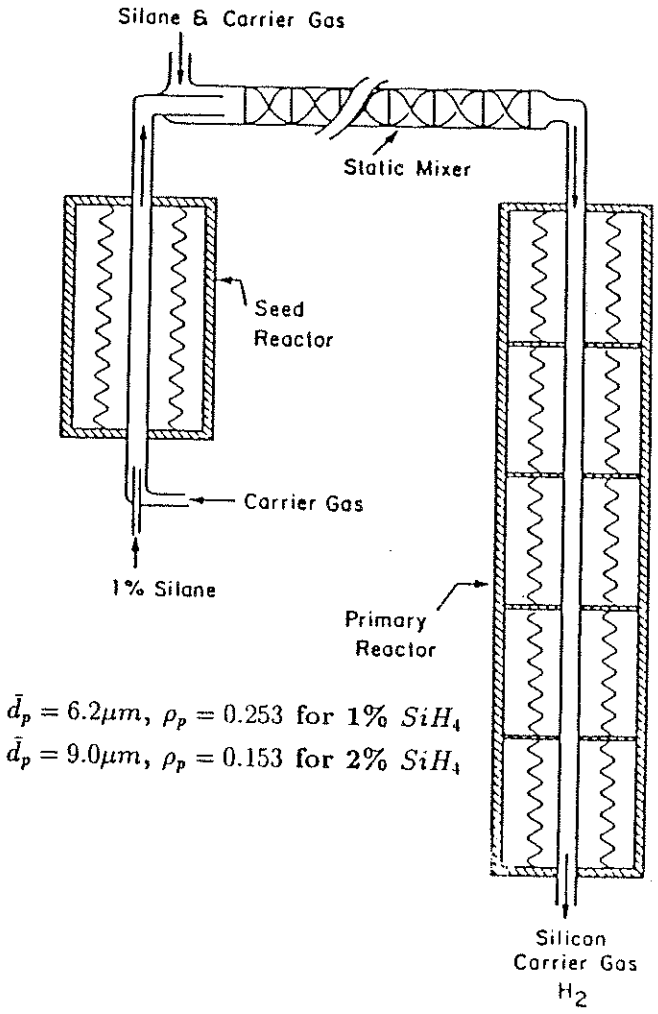

Figure 1. Two Stage Aerosol Reactor

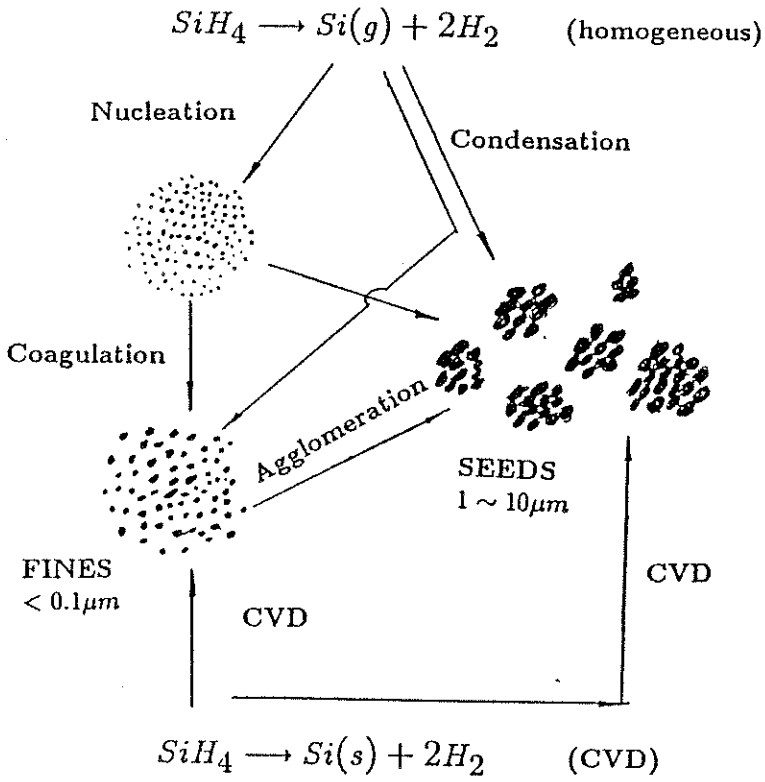

Figure 2. Particle Growth Mechanism

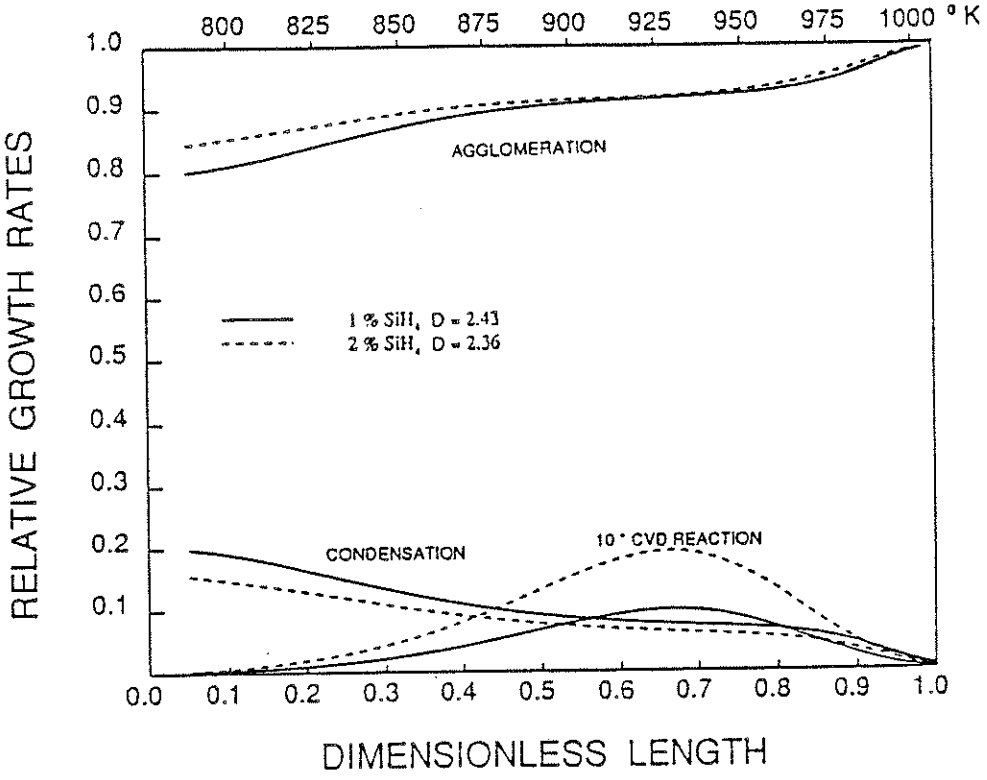

Figure 3. Relative Particle Growth Rates Along the Reactor

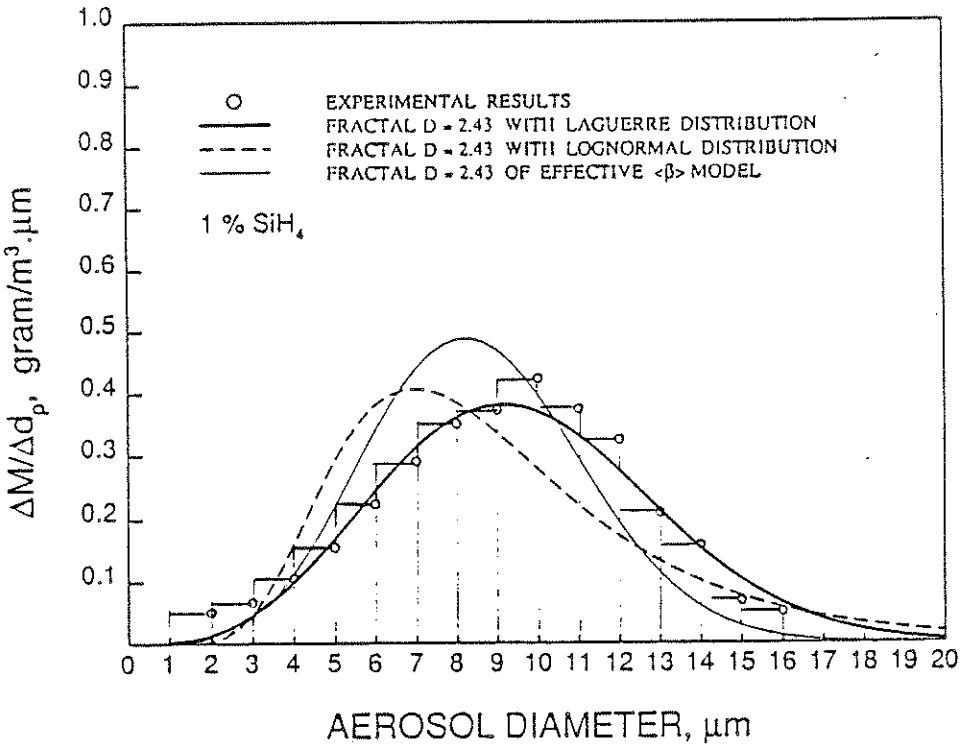

Figure 4. Model Predictions for 1% SiH_4 in the Feed

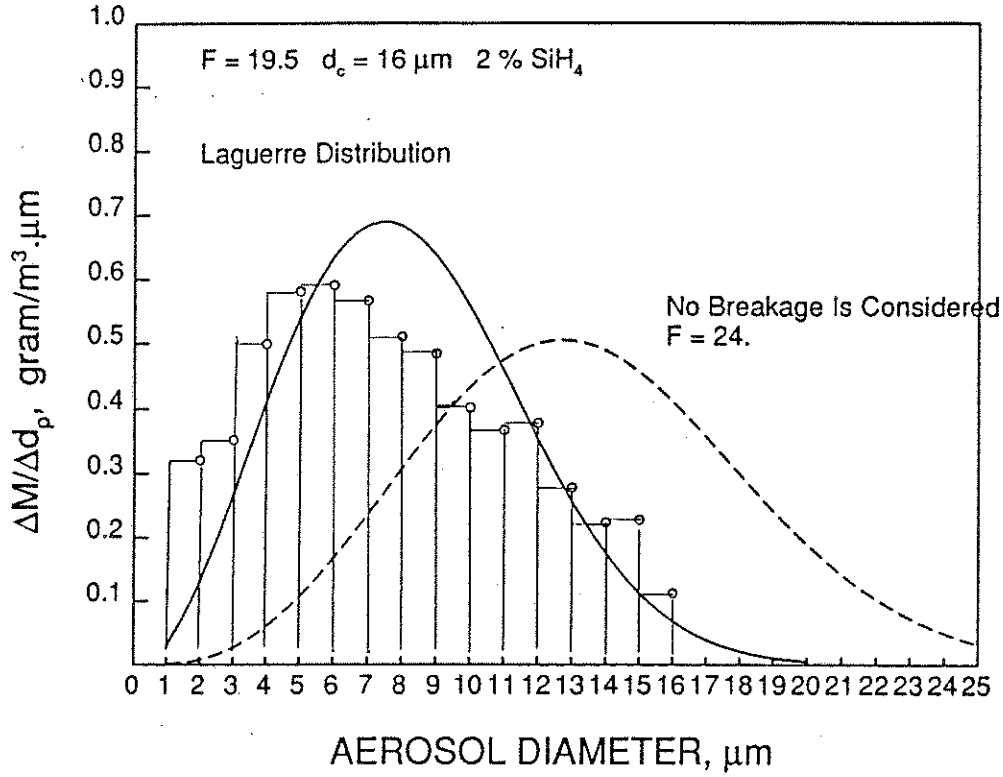

Figure 5. Model Predictions for 2% SiH_4 in the Feed with and without Breakage of Agglomerates Considered

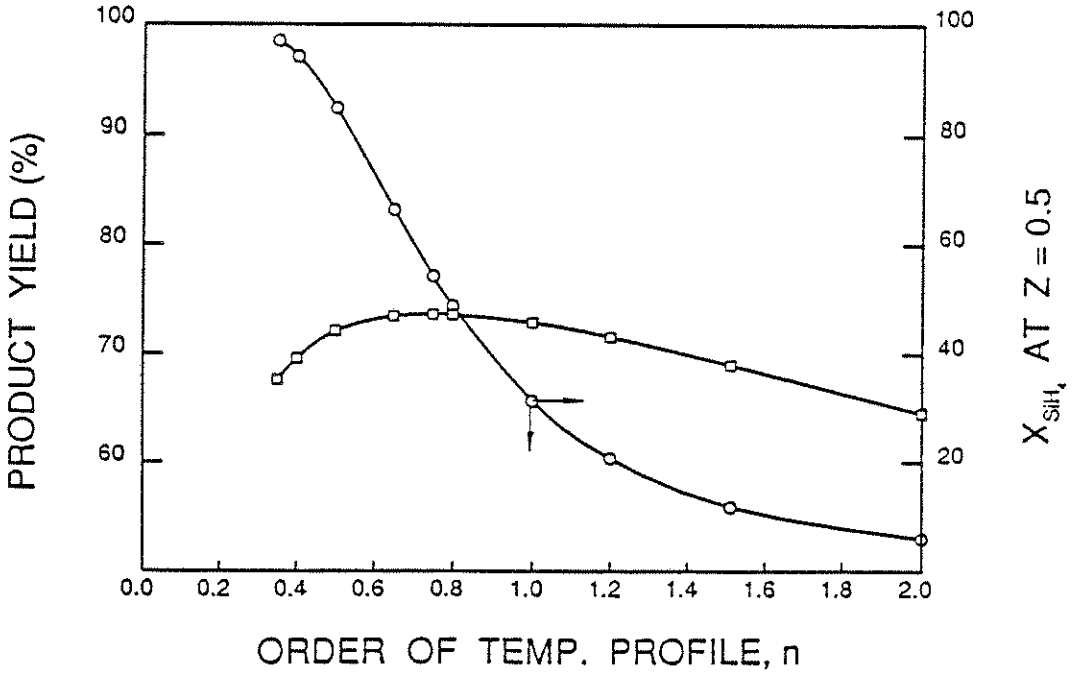

Figure 6. Product Yield as a Function of Temperature Profile

OXYGEN TRANSPORT DURING SINGLE CRYSTAL GROWTH BY THE CZOCHRALSKI METHOD

A. Problem Definition

Single crystal silicon with uniform electrical properties is required for many semiconductor applications. To obtain uniformity, dopants and oxygen must be evenly distributed throughout the grown crystal. For some applications (e.g. power devices), low oxygen contents are also required.

The Czochralski (CZ) technique is the predominant method for producing single crystal silicon from the melt. The CZ-apparatus is shown in Figure 1. The process is described in detail in a previous CREL annual report [1]. A brief summary is given below.

Polycrystalline silicon of high purity and any desired dopants (e.g. boron or phosphorous) are placed in a quartz crucible and heated to form a melt. A single seed crystal of appropriate crystallographic orientation is brought into contact with the surface of the melt. The pull rate of the seed and the heat input to the melt are manipulated to achieve and maintain growth at the desired diameter. The crucible is rotated so that the effects of any asymmetries in the heating of the melt are reduced. The crystal is also rotated, in order to generate flows which will favorably affect the heat and mass transfer in the melt.

Oxygen enters the melt because of the slow dissolution of the quartz crucible. Oxygen then leaves the melt either by evaporating from the free surface or by being incorporated into the growing crystal.

B. Research Objectives

The purpose of this work is to develop a model which describes the incorporation of oxygen during growth of single crystal silicon from the melt by the CZ-technique. The model should predict the oxygen distribution obtained in the grown crystal as a function of the CZ-puller geometry and of the operating conditions. Using this model, the possibility of employing an applied magnetic field during growth to obtain low oxygen content silicon will be investigated.

C. Research Accomplishments

A global oxygen transport model has been developed following the work of Carlberg, King and Witt [2]. In this model, perfect mixing in the bulk of the melt is assumed, and the only resistance to mass transfer exists in thin boundary layers adjacent to the crystal, crucible and free surface. Because of the slow growth rate (~ 1 in/hr), the system is assumed to be in a pseudo-steady state with respect to the oxygen concentration in the melt at any stage during crystal growth. A mass balance on oxygen therefore yields:

$$\text{Dissolution Rate} = \text{Evaporation Rate} + \text{Incorporation rate} \qquad (1)$$

Many models exist that relate the incorporation rate of a solute in the melt to the operating conditions, and these are particularly well established for the standard CZ-

process (in the absence of an applied magnetic field). Models for dissolution of the crucible and evaporation of oxygen from the free surface do no exist in the open literature. The approach here was to describe the evaporation and dissolution in terms of mass-transfer coefficients. The coefficients are related to the geometric and operating parameters through a boundary layer analysis. Due to space limitations, results obtained for the case of growth in the presence of an applied magnetic field will not be presented here.

C.1 Crucible Bottom Dissolution

The crucible bottom was modeled by an infinite disk rotating adjacent to a semi-infinite body of fluid (the melt). The boundary layer thickness is small enough relative to the crucible radius and melt height such that this is a valid approximation. It was determined that

$$Sh_{CB} = \frac{k_{CB}\sqrt{\nu\omega_C}}{D} = 0.62Sc^{1/3}; \quad Sc = \nu/D \tag{2}$$

where Sh_{CB} is the Sherwood number for crucible bottom dissolution, k_{CB} is the dissolution mass-transfer coefficient for the crucible bottom, ν is the kinematic viscosity of the melt, ω_C is the rotation rate of the crucible, D is the diffusivity of oxygen in molten silicon and Sc is the Schmidt number.

C.2 Crucible Vertical Wall Dissolution

The crucible vertical wall was approximated by an infinite, isothermal, vertical wall in rectangular coordinates adjacent to a semi-infinite body of fluid. Natural convection was the only flow mechanism considered in this boundary layer. The resulting expression for the average value along the wall of the Sherwood number was found to be

$$Sh_W = \frac{k_W H}{D} = 0.82Gr^{1/4}Sc^{1/3}; \quad Gr = \frac{\beta g \Delta T_e H^3}{\nu^2} \tag{3}$$

where k_W is the dissolution mass-transfer coefficient for the crucible vertical wall, Gr is the Grashof number (a measure of the strength of buoyant convection), β is the volume expansivity, g is the acceleration due to gravity, ΔT_e the temperature difference across the boundary layer and H is the melt height.

C.3 Evaporation from the Free Surface

Flow in the free surface boundary layer is dominated by the thermocapillary force which is introduced by the temperature gradient (and resulting surface tension gradient) across the melt free surface. This boundary layer was approximated by an ideal system of a semi-infinite fluid (in a rectangular geometry) which has a constant shear stress on the free surface (corresponding to a linear temperature profile) for $x > 0$, where x is the

downstream distance from the point where the shear stress is initially applied (the shear stress is zero for $x < 0$). A similarity solution was found for the fluid flow and mass transfer in the boundary layer. To our knowledge, this solution has not appeared previously in the open literature. The average value of the Sherwood number across the free surface was found to be

$$Sh_E = \frac{k_E L}{D} = 1.11 Sc^{1/2}\left(\frac{Ma}{Pr}\right)^{1/3}; \quad Pr = \frac{\nu}{\alpha}; \quad Ma = \frac{-\frac{1}{\mu}\frac{d\gamma}{dT}\Delta T L}{\alpha} \tag{4}$$

where k_E is the evaporation mass-transfer coefficient, L is the distance from the crystal edge to the crucible wall, Ma is the Marangoni number (a measure of the strength of the thermocapillary flow), Pr is the Prandtl number, μ is the viscosity, γ is the surface tension, ΔT is the temperature difference across the free surface and α is the thermal diffusivity.

The above equation underpredicts the evaporation rate because it does not take into account the enhanced mass transfer due to interfacial turbulence. Introducing the eddy diffusivity to the development yields the following result which is valid for large values of the eddy diffusivity parameter, a_D:

$$Sh_E = \frac{3\sqrt{\alpha_D}}{\pi}\left(\frac{Ma}{Pr}\right)^{1/3}; \quad \alpha_D = \frac{a_D}{D} \tag{5}$$

C.4 Results

Figure 2 gives the axial oxygen distribution predicted for the grown crystal for four different values of a_D with all other parameters held constant. Since the solubility limit of oxygen in molten silicon is 69 ppma, and the lowest oxygen contents obtainable by the standard CZ-process are ~ 10 ppma, the appropriate range for the eddy diffusivity parameter is 0.01 - 1.0 cm^2/s for this case. Using a value of $a_D = 0.1$ cm^2/s, the sensitivity of the results to uncertainties in the physical property data was examined. This is shown in Figure 3. Uncertainties in the surface tension coefficient ($d\gamma/dT$) and the solute diffusivity introduce large discrepancies into the simulation results.

Figure 4 shows the effects of various operating parameters on the predicted axial oxygen profiles in the crystal. The crystal growth rate and heat input rate are seen to have a small effect on the concentration profile, while the crucible rotation rate has a larger effect. The oxygen content is found to be much less sensitive to the crystal rotation rate than what is observed in practice. This indicates that some model refinements may be required.

C.5 Conclusions

A preliminary model was developed which predicts the axial distribution of oxygen in a CZ-grown silicon crystal as a function of the geometric and operating parameters. It has been shown that more accurate physical property data is needed in order to obtain precise

predictions from the model. The discrepancy between the model and experimental results for different crystal rotation rates indicates that some model refinement may be required. The results of this work and of published experimental studies yield that an applied magnetic field can lower the oxygen content obtained in the crystal only at the expense of introducing unacceptable nonuniformities in the distribution of dopants and oxygen.

D. Future Work

1. The existing computer code is being adapted into a form such that it can be used by crystal growth practitioners (i.e. a user-friendly version is being developed).
2. The effect of the crystal rotation rate on the predicted oxygen profiles must be more accurately modeled. Because the flow due to crystal rotation directly opposes that due to Marangoni convection, it will have the effect of reducing the evaporation rate. The enhanced mixing in the melt caused by the crystal rotation can be modeled by splitting the melt into two perfectly mixed compartments (an inner core under the crystal and an outer core under the free surface). An exchange coefficient, which increases with increasing crystal rotation rate, describes the exchange of mass between the two compartments.

E. Bibliography

1. CREL Annual Report, June 1, 1987 - May 31, 1988
2. Carlberg, T., T.B. King and A.F. Witt, J. Electrochem. Soc., 129, 189 (1982)

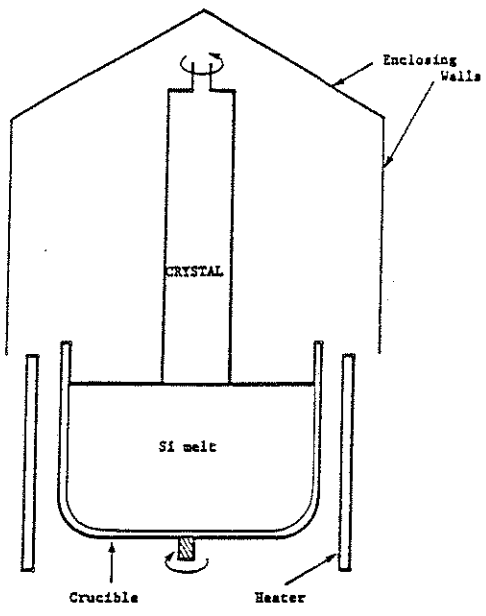

Figure 1. Schematic of the Czochralski crystal pulling apparatus.

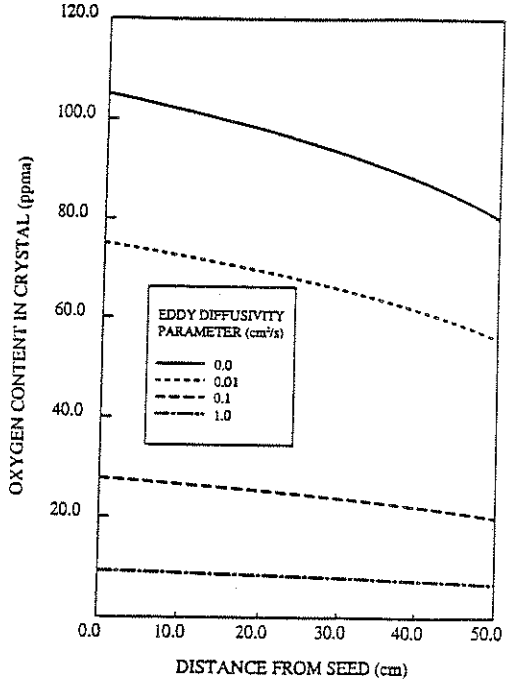

Figure 2. Effect of the eddy diffusivity parameter on the predicted value of the oxygen content in the grown crystal

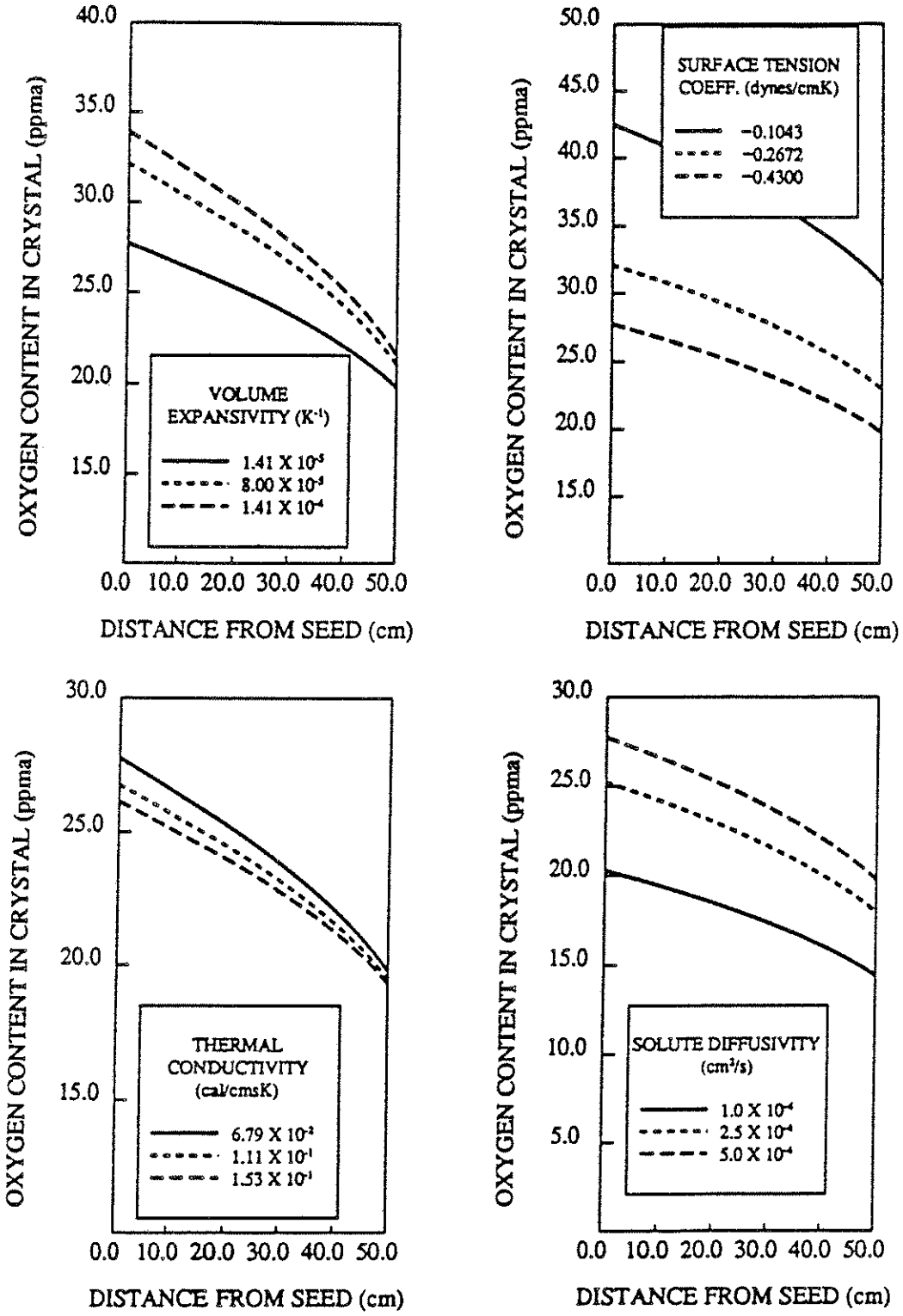

Figure 3. Effect of the uncertainty in physical property data on the model results.

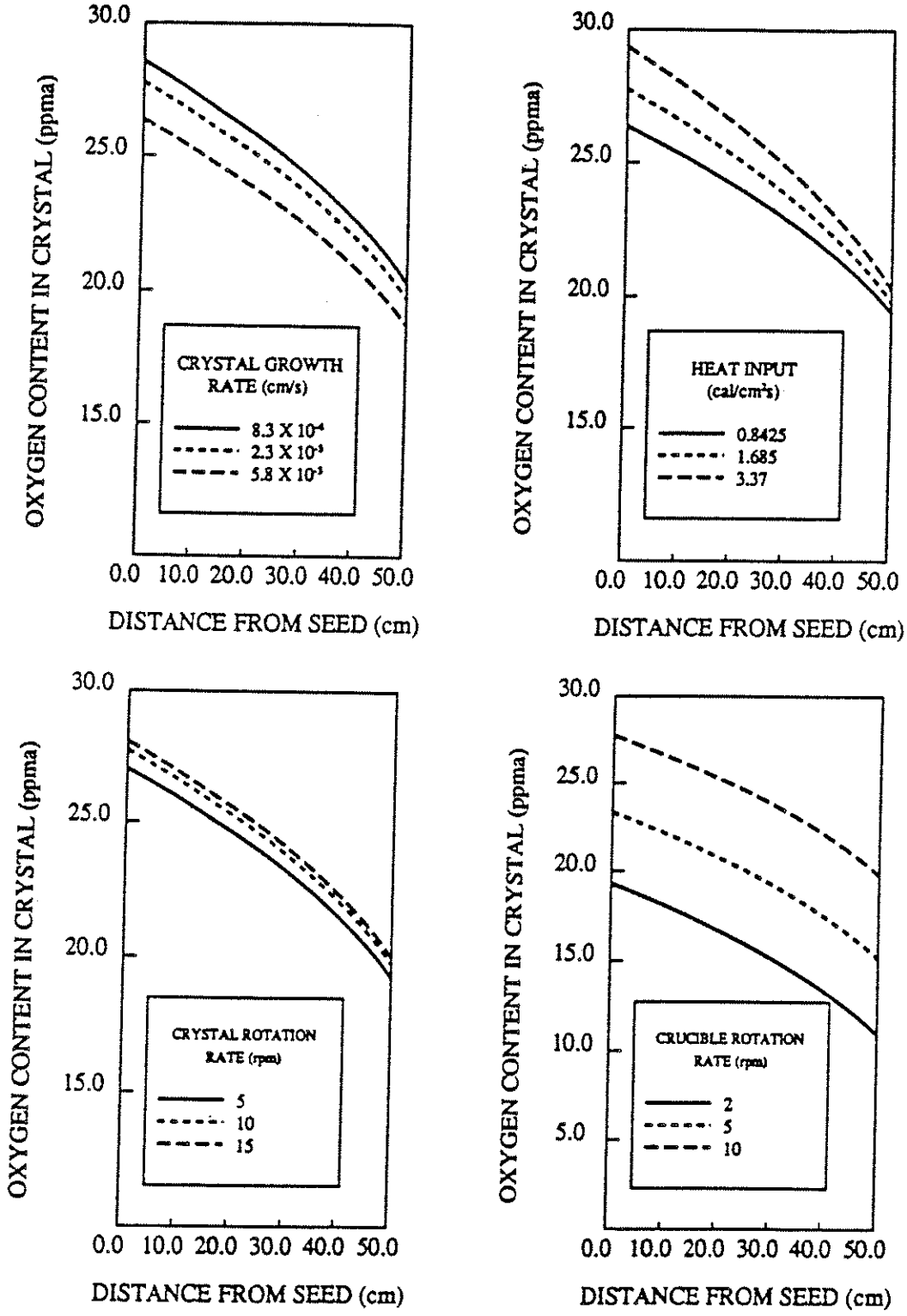

Figure 4. Effect of the operating parameters on the predicted oxygen content in the grown crystal.

predictions from the model. The discrepancy between the model and experimental results for different crystal rotation rates indicates that some model refinement may be required. The results of this work and of published experimental studies yield that an applied magnetic field can lower the oxygen content obtained in the crystal only at the expense of introducing unacceptable nonuniformities in the distribution of dopants and oxygen.

D. Future Work

1. The existing computer code is being adapted into a form such that it can be used by crystal growth practitioners (i.e. a user-friendly version is being developed).
2. The effect of the crystal rotation rate on the predicted oxygen profiles must be more accurately modeled. Because the flow due to crystal rotation directly opposes that due to Marangoni convection, it will have the effect of reducing the evaporation rate. The enhanced mixing in the melt caused by the crystal rotation can be modeled by splitting the melt into two perfectly mixed compartments (an inner core under the crystal and an outer core under the free surface). An exchange coefficient, which increases with increasing crystal rotation rate, describes the exchange of mass between the two compartments.

E. Bibliography

1. CREL Annual Report, June 1, 1987 - May 31, 1988
2. Carlberg, T., T.B. King and A.F. Witt, J. Electrochem. Soc., 129, 189 (1982)

The Crystal Growth of α-FeOOH (Goethite) in Aqueous Solution at High pH

A. Problem Definition

The controlled production of iron oxide particles is important to their application as pigments and magnetic particles. Goethite is simply a form of iron oxide whose orthorhombic crystal structure results in a morphologic form suitable for further processing into magnetic particles. Its characteristic yellow color also makes it useful as a pigment.

There are many different morphological and crystalline forms of iron oxides along with a myriad of processes for producing them. A review of these processes is available elsewhere (1). Generally speaking, the solution conditions such as pH, temperature, pressure, ionic strength, types of ions, and transport effects control the properties of the final particles. The chemistry behind the oxide formation is complex and often not well understood. As a result, the formation of particles with the proper characteristics is difficult and a quantitative approach to modelling the particle growth is not available.

In magnetic particle applications, the particle size, shape, and crystal structure/composition control the magnetic properties of the particles. Although goethite particles are not magnetic, they are often produced as an intermediate product in processes used to manufacture γ-Fe_2O_3 magnetic particles. This is done because goethite particles can be grown in a desirable morphology (needle with aspect ratios larger than 8:1) and length (.2 - 1 μm). Goethite particles are generally formed in the three-phase slurry oxidation of aqueous ferrous hydroxide ($Fe(OH)_2$). The goethite intermediate is then transformed to γ-Fe_2O_3 through a series of gas-solid reactions. Although the internal crystal structure of the particles is changed, the external morphology essentially remains constant.

The primary objective of this work is to relate the conditions of particle growth to the morphology of the final product. This will be achieved through experimental identification of the key operating variables and subsequent modelling of their effects.

B. Research Objectives

There are three main objectives of this research:

1. Measure the apparent reaction kinetics in a three-phase slurry batch reactor and develop a model of the mass transfer with reaction of oxygen into the slurry.

2. Qualitatively understand the mechanisms of crystal growth and subsequently develop the framework for modelling this process.

3. Recommend a reactor design which will provide the best control of the goethite particle size.

C. Research Accomplishments

The process used in the formation of goethite consists of two basic steps. In step one, $Fe(OH)_2$ is precipitated by mixing solutions of NaOH and $FeSO_4$ in the absence of oxygen. Once the $Fe(OH)_2$ has been precipitated, the slurry is oxidized with an oxygen containing gas. The important chemical reactions can be written as follows:

Step 1: Precipitation

$$FeSO_{4(aq)} + 2\ NaOH_{(aq)} \text{ (excess)} \ <=======> \ Fe(OH)_{2(solid)} + 2\ Na^{+} + SO_4^{2-}$$

Step 2: Oxidation

$$O_{2(g)} <=======> O_{2(aq)}$$

$$\left.\begin{array}{l} Fe(OH)_{2(solid)} + OH^{-} <=======> Fe(OH)_3^{-}{}_{(aq)} \\ Fe(OH)_3^{-}{}_{(aq)} + 1/4\ O_2 \text{ ----------> } \alpha\text{-}FeOOH_{(solid)} + OH^{-} + 1/2\ H_2O \end{array}\right\} \text{Desired}$$

$$Fe(OH)_{2(solid)} + 1/4\ O_2 \text{ ----------> (vigorous) } \delta\text{-}FeOOH_{(solid)} + 1/2\ H_2O \qquad \text{Undesired}$$

The mechanism which results in the formation of goethite (α-FeOOH) apparently proceeds through the liquid phase oxidation of a dissolved ferrous complex (2). Vigorous oxidation of the $Fe(OH)_2$ slurry either through extreme agitation or the use of H_2O_2 results in the formation of δ-FeOOH. This δ-FeOOH is apparently formed from the heterogeneous oxidation of $Fe(OH)_2$ and results in an oxidized platelet of the same morphology as the initial $Fe(OH)_2$ precipitate. Further support of the solution phase mechanism is gained by noting that appreciable Ostwald ripening of the precipitate occurs over the first 3-4 hours after precipitation. The ripened precipitate is heterogeneously oxidized at conditions which fresh precipitate forms needles (suggesting that the concentration of ferrous complex is lower, allowing oxygen to reach the $Fe(OH)_2$ solid surface).

The oxidation reaction rates at various conditions have been measured in an agitated batch reactor. The reactor is operated in a batch gas, batch slurry mode and the gas absorption rate is measured by measuring the gas pressure change. By degassing the liquid with no reactant present, the mass transfer coefficient for the slurry can be independently measured.

Figure 1 shows the independently measured mass transfer coefficient (thick, solid line) for the slurry, k_La, along with reaction rate data at two particle loadings. The horizontal lines above and below k_La represent ± one standard deviation from the mean k_La value. Even at these low particle loadings, the oxidation reaction does not occur to

any appreciable extent in the bulk slurry. Data at higher particle loadings and various NaOH concentrations have been taken and show essentially the same results.

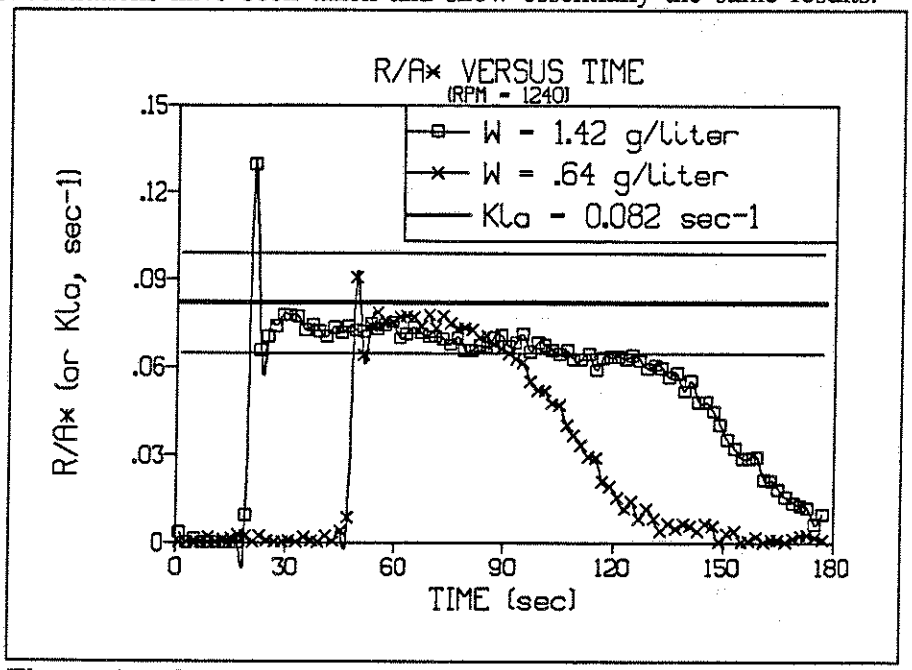

Figure 1: Graph showing that even at low particle loading, the apparent reaction rate data are simply the rate of mass transfer of oxygen into the slurry.

A possible explanation of these phenomena can be made using simple film theory (3). For an instantaneous gas-liquid reaction occurring in the liquid film adjacent to the gas-liquid interface, the following diagram applies:

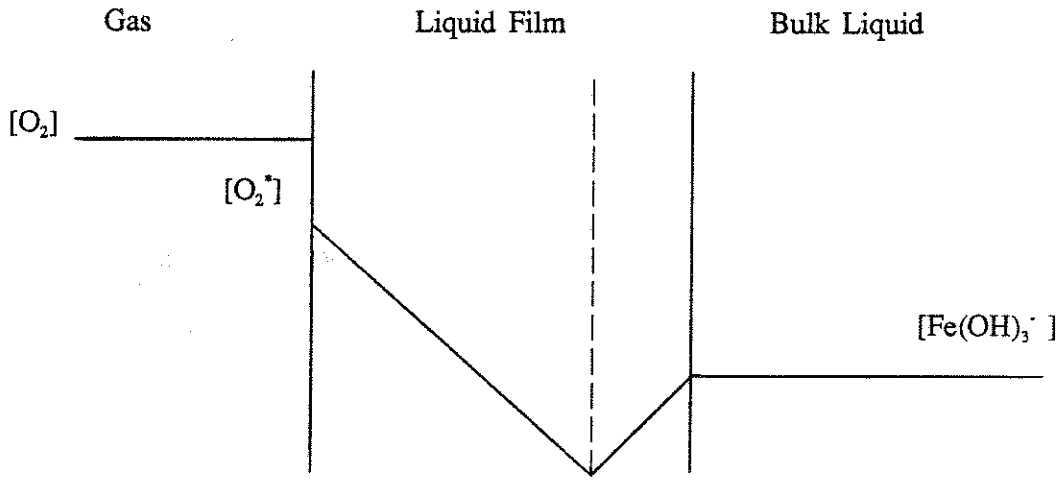

Reaction Rate, $$R = k_L a[O_2^*] \left\{ 1 + \frac{D_{Fe}\,[Fe(OH)_3^-]}{z\,D_{O2}\,[O_2^*]} \right\}$$

In the above rate expression, the D's are diffusivities, k_La is the mass transfer coefficient, and z is the stoichiometric coefficient (z = 4). The *'s denote equilibrium concentrations. When $[Fe(OH)_3^-] << [O_2^*]$, then $R \approx k_La[O_2^*]$. It is expected that when the overall reaction rate exceeds the maximum dissolution rate of the particles, the reaction will move to the solid surface. Since the actual $[Fe(OH)_3^-]$ is $\approx 10^{-5}$, it is difficult if not impossible to accurately measure this concentration in the slurry. More data are currently being taken at lower mass transfer coefficients to see if any enhancement of the reaction rate can be measured.

Once a better understanding of the oxidation reaction has been gained, and the reaction rate can be predicted based on known operating conditions, the question of how this rate impacts the crystallization process still remains. Based on data published in the literature (4), it is possible to show a correlation between the particle size and reaction rate. This data seems to support the notion that it is the oxidation reaction that controls the super-saturation of ferric species in the slurry. Only recently was this observation documented in the open literature (5). Thus, the oxidation process is a film process occurring at the gas-liquid interface, while the crystallization process is primarily a bulk process.

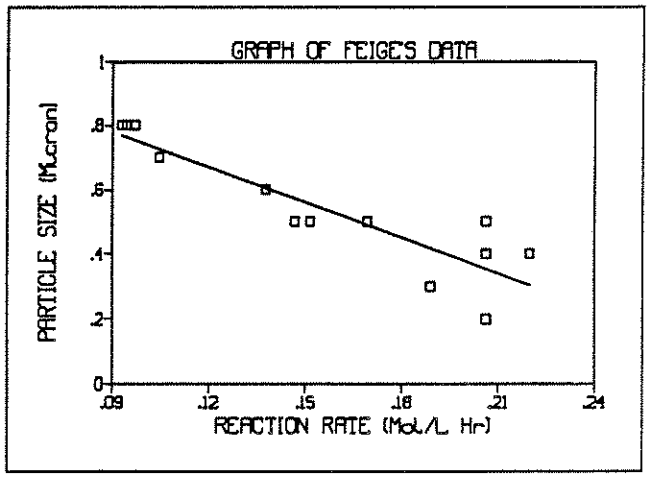

Figure 2: Graph showing the relationship between reaction rate and mean particle length.

D. Future Work

Additional work in this area will be concentrated on developing a better understanding of the apparent reaction kinetics. This will involve experimental work with further model development. The ideal result will be a model which can predict when the reaction moves to the particle surface. Once a better understanding of the reaction process is developed, an improvement in reactor design may be achieved.

E. Bibliography

1. O'Connor, D. L., 'The Crystal Growth of α-FeOOH (Goethite) in Aqueous Solution at High pH', D. Sc. proposal, Washington University, 1988.
2. Misawa, T., K. Hashimoto, and S. Shimodaira, 'The Mechanism of Formation of Iron Oxide and Oxyhydroxides in Aqueous Solutions at Room Temperature', Corrosion Science, 14, 131, 1974.
3. Danckwerts, P. V., *Gas-Liquid Reactions*, McGraw-Hill, New York, 1970.
4. Feige, M., M. Lorenz, and K. Stopperka, 'Reaktionsbedingungen und Teilchengrobe von α-FeOOH', Lakokrasochnye Materialy i ikh Primenenie, 5, 7, 1984.
5. Sada, E., H. Kumzawa, and M. Aoyama, 'Reaction Kinetics and Controls of Size and Shape of Goethite Fine Particles in the Production Process by Air Oxidation of Alkaline Suspension of Ferrous Hydroxide', Chem. Eng. Comm., 71, 73, 1988

MODELING THE PROCESS CYCLE OF THERMOPLASTIC COMPOSITES WITH EXPERIMENTAL VERIFICATION

A. Problem Definition

In order to fabricate a thermoplastic polyimide (Avimid[1] K-III) composite of high quality, models describing the process (so-called master model) are required for understanding and controlling the process. The master model includes submodels involving kinetics, viscosity, devolatilization, heat transfer, consolidation, and void formation and growth.

A submodel for describing the devolatilization of thermoplastic polyimide composites has been proposed [1]. The devolatilization process is absolutely necessary because the polyimide composite is produced in situ by the reaction of an aromatic diethylester diacid with an aromatic diamine dissolved in a high-boiling solvent such as N-methyl-2-pyrrolidone. The solvent and by-products such as ethanol and water should be removed to fabricate a void-free thermoplastic polyimide composite. It is assumed that the mass transfer limited model and Darcy's Law are valid in the development of the governing equations for the devolatilization model. A submodel for the consolidation process has also been proposed using soil consolidation theory [2].

This project addresses the problems of devolatilization and consolidation of thermoplastic polyimide composites in terms of modeling and experimental verification.

B. Research Objectives

1. Address the crack formation and healing phenomena. Develop and experimentally verify a submodel for crack formation and healing.

2. Experimentally verify a submodel for devolatilization.

3. Experimentally verify a submodel for resin flow (consolidation).

C. Research Progress and Results

1. Resin Pressure Measurements

A schematic of the apparatus for measuring resin pressure is shown in Figure 1. A laboratory press was utilized in the middle of which a rectangular consolidation cell ($4.8 \times 4.8 \times 2$ *inches*) made of Plexiglas was placed. The applied pressure can be determined by the dead weight placed on the plunger. Miniature pressure transducers (Kulite Semiconductor Products) were used whose positions could be changed as desired.

[1]Trademark of Du Pont Co.

A data acquisition system was developed to process the electrical signals from the miniature pressure transducers. A System 200 personal computer was used to digitally record the resin pressure measurements. The pressure transducers were connected to the PC via 3B-18 signal conditioners (Analog Devices). The signal conditioners were then attached to the universal data acquisition board which contained the A/D converter. Four data points per second for each pressure transducer were recorded and averaged.

1.1 Effect of Bleeder Capacity

A consolidation experiment with the bleeder was performed to examine the effect of bleeder capacity. The bleeder used was Airweave N-10 which is a nonwoven fabric and lighter than a typical glass bleeder. The height of the unidirectionally aligned carbon fiber bed was 16 mm and the fiber volume fraction, V_f, was 0.45. Three miniature pressure transducers were positioned at the bottom (tool surface), middle point, and top (below the bleeder), respectively.

Figure 2 shows the resin pressure change as a function of time at three different positions for the case of two layers of Airweave N-10. The resin pressures at the bottom and in the middle are continuously decreasing and the boundary pressure at the bleeder-composite interface is almost constant after jumping slightly on application of the load. Figure 3 shows the resin pressure-position profile as a function of consolidation time. It can be seen that the resin pressure profiles are nonlinear and the pressure gradients at the boundary are decreasing with time.

In order to examine whether or not a pressure gradient in the horizontal direction (parallel to the fiber axis) occurs the resin pressures in this direction were measured. A pronounced pressure gradient in the horizontal direction was detected which means that the bleeder ply consolidation experiment must be considered as two-dimensional flow.

In order to investigate the effect of bleeder capacity on the resin pressure, the number of layers of Airweave N-10 was reduced to one, all other parameters being kept the same. Figure 4 shows the resin pressure change as a function of time. The resin pressure at the bottom continuously decreases. However, the resin pressure in the middle of the fiber bed initially decreases and increases later. This phenomenon can be explained as follows: The flow pattern is initially two-dimensional until the layer of Airweave N-10 becomes saturated with oil. When the bleeder becomes saturated, horizontal flow becomes dominant. Figure 5 shows the resin pressure profiles in the vertical direction as a function of time. It is noteworthy that the resin pressure profiles are nonlinear. The observed maximum in the pressure profiles at larger times (the 20 and 25 minute curves) is due to a saturated bleeder which makes the horizontal flow dominant at that point in time.

In order to further examine the effect of a bleeder, no bleeder was used. This experiment can be referred to as a compression molding. The resin pressures at

three different positions along the vertical direction were measured as a function of time as shown in Figure 6. It was observed that the oil is squeezed and overflows on the caul plate when the fiber bed consolidates. The resin pressure below the caul plate is as high as that at the bottom and at the middle point and becomes higher after 10 *min*. From these measurements, it is clear that the pressure gradient in the vertical direction is negligible when no bleeder is introduced. This implies that there are pressure gradients in the horizontal direction which induce the resin flow.

From the comparison of Figure 6, Figure 4 and Figure 2, it seems that the bleeder capacity plays an important role in determining the flow pattern.

1.2 Effect of Applied Pressure

The effect of the applied load on the resin pressure was investigated. The consolidation pressure was increased from 0.7 psig to 1.9 psig. Figure 7, when compared with Figure 2, shows that the resin pressures decrease more quickly due to the increased load. The resin pressure profiles are also found to be nonlinear.

2. Comparison with Model Predictions

The resin flow through a fiber bed with the bleeder under a constant load was found to be two-dimensional in the vertical and horizontal (parallel to the fiber alignment) direction. The governing equation for one-dimensional consolidation with two-dimensional flow (x, z directions) is shown elsewhere [2] and the analytical solution is given by

$$p_r(x,z,t) = \frac{16\sigma_0}{\pi^2}\sum_{p=0}^{\infty}\sum_{q=0}^{\infty}\left[\frac{(-1)^q}{(2p+1)(2q+1)}\right]\left\{\sin\left[\frac{(2p+1)\pi x}{a}\right]\cos\left[\frac{(2q+1)\pi z}{2c}\right]\right\}$$

$$\left\{\exp\left(-\frac{k_x}{\eta m_v}\left[\frac{(2p+1)^2\pi^2}{a^2}+\frac{(2q+1)^2\pi^2}{4(k_x/k_z)c^2}\right]t\right)\right\} \qquad (1)$$

Figure 8 shows the comparison between the measured resin pressure change (the same as Fig. 2) and that predicted from Dave et al. [2] resin flow model. The parameters used for the model calculation are shown in Figure 8. There is an acceptable agreement between the measured and predicted resin pressure. The agreement might be improved with a more rigorous simulation which considers the time-dependent properties and the moving boundary.

D. Future Work

1. Completion of TGA/Mass Spectroscopy experiment.
2. Verification of crack formation and healing.
3. Verification of a devolatilization submodel including completion of measurements of gas pressure and temperature profiles.

4. Demonstration of usefulness of the verified model in selection of a desirable process cycle.

E. List of References

1. S. J. Choi, "Modeling Devolatilization of Thermoplastic Polyimide Composites," D. Sc. Proposal, Dept. of Chem. Eng., Washington University, Apr. 1988.

2. R. Dave, J. L. Kardos and M. P. Dudukovic, "A Model for Resin Flow During Composite Processing: Part 1 - General Mathematical Development," *Polymer Composites,* 8, 29 (1987).

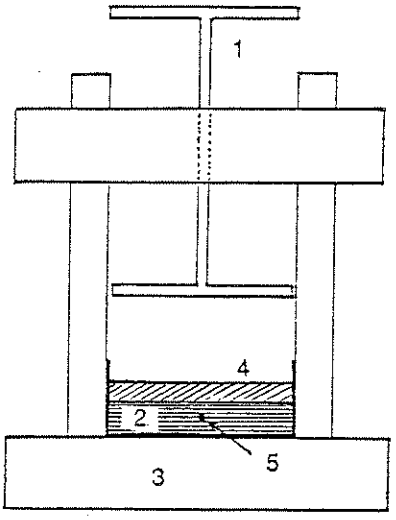

1. Plunger
2. Fiber Bed
3. Lab Press
4. Bleeder
5. Miniature Pressure Transducer

Figure 1: Schematic of a resin pressure measurement cell.

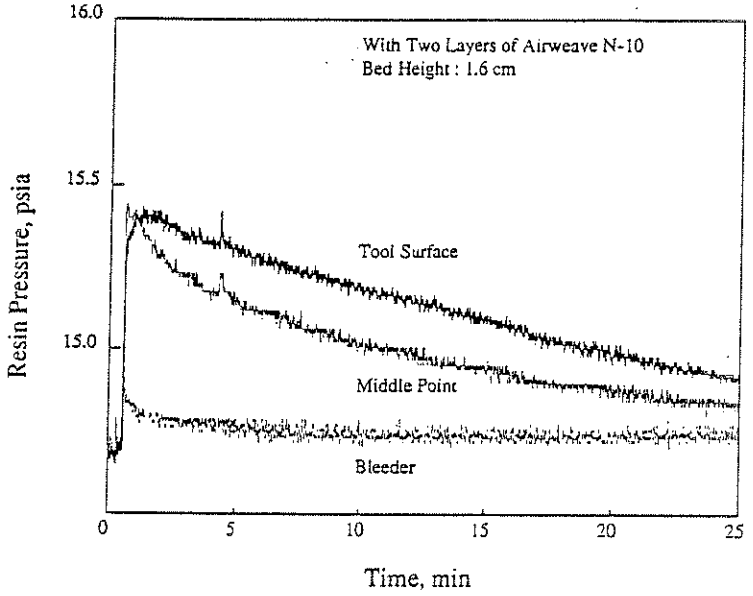

Figure 2: Resin pressure change as a function of time with two layers of Airweave N-10.

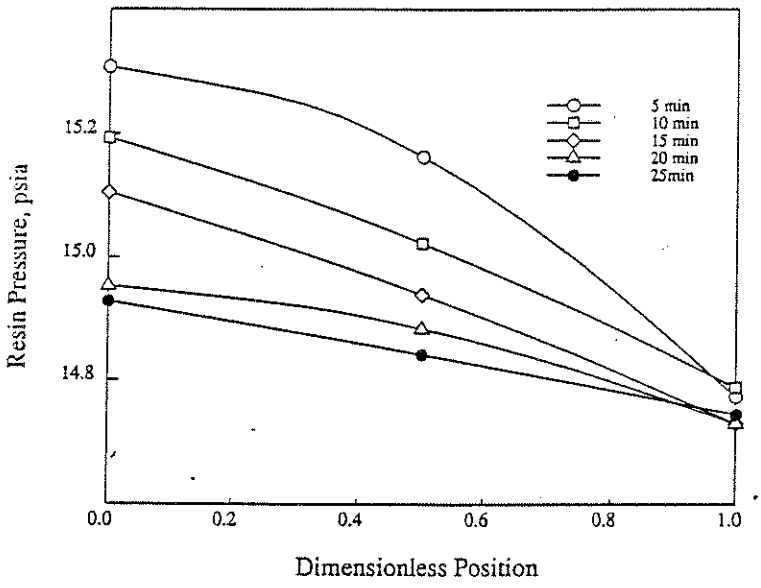

Figure 3: Resin pressure distributions as a function of vertical position with two layers of Airweave N-10.

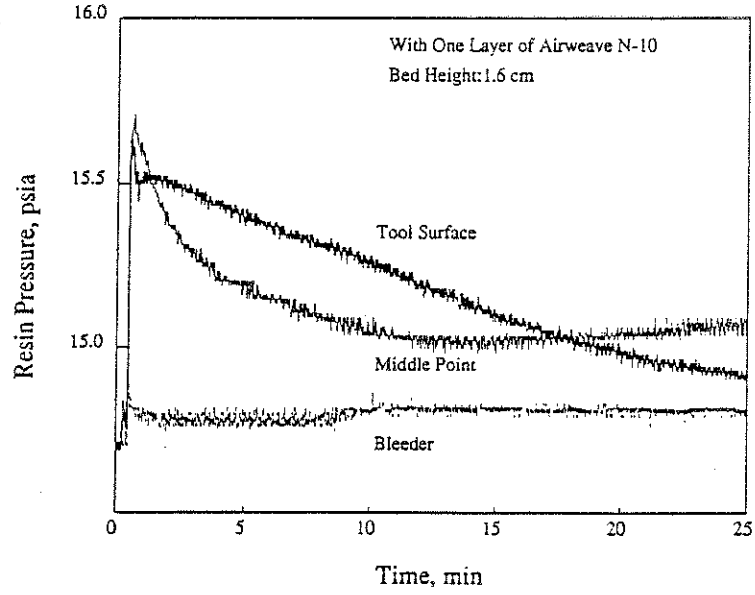

Figure 4: Resin pressure change as a function of time with one layer of Airweave N-10.

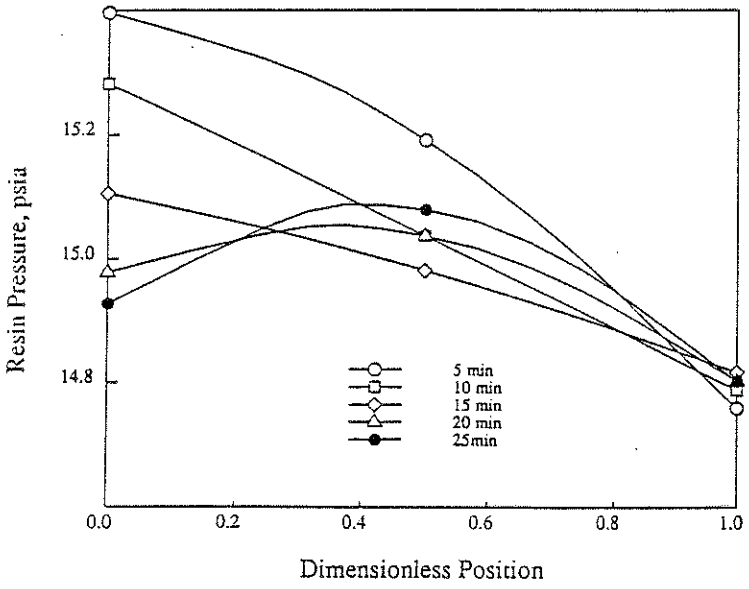

Figure 5: Resin pressure-position (vertical) distributions as a function of time with one layer of Airweave N-10.

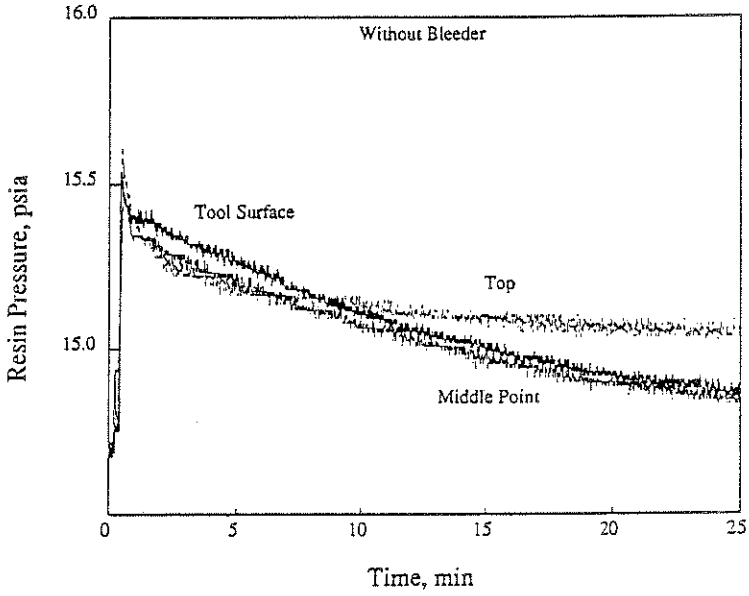

Figure 6: Resin pressure change as a function of time without a bleeder.

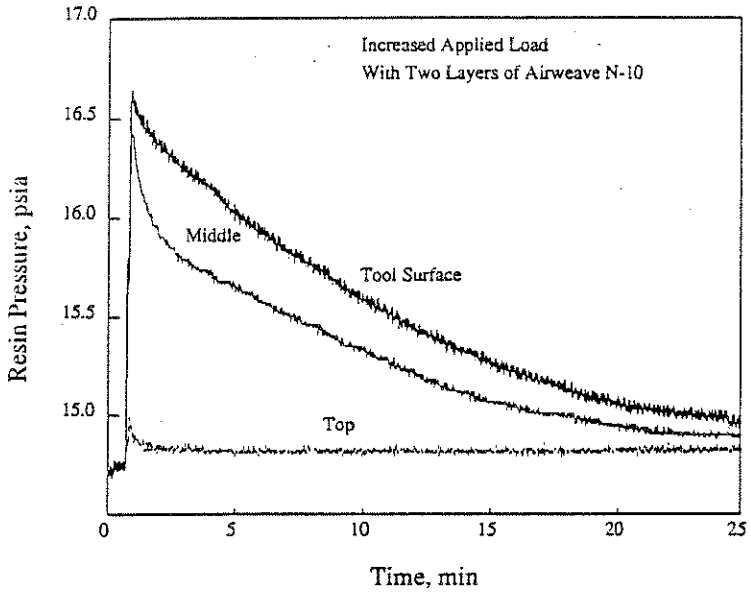

Figure 7: Resin pressure change as a function of time with two layers of Airweave N-10 and the increased consolidation load in the vertical direction.

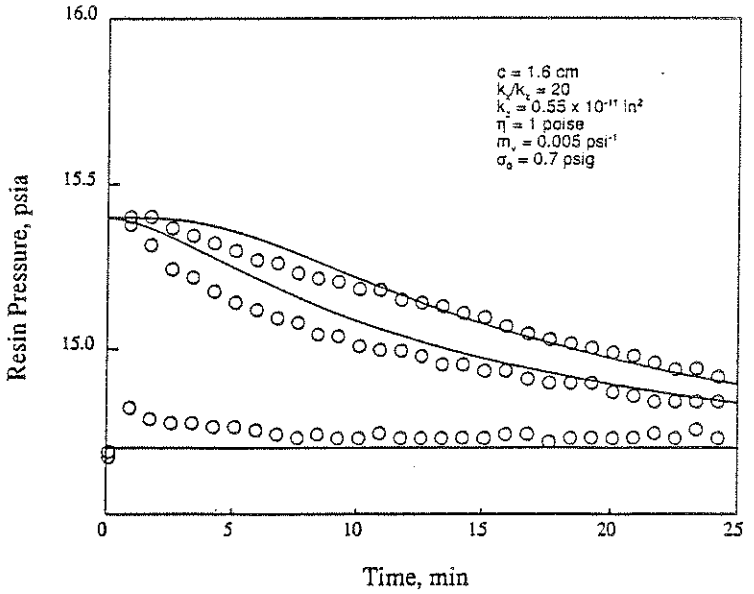

Figure 8: Comparison between the measured resin pressure change in the vertical direction and that predicted from Dave et al. [2] resin flow model (solid lines-model; circles-experiment).

MODELING OF DEVOLATILIZATION OF THERMOPLASTIC (POLYIMIDE) COMPOSITES

A. Problem Definition

High performance structural composite materials, containing continuous fibers and polymer matrices, are in demand in the aerospace industry. The occurrence of voids and undesirable resin composition gradients in the final products are most frequent manufacturing problems which cause part rejection.

Thermoplastic composites have several advantages over thermosetting composites such as: high thermal decomposition temperature, strong mechanical strength, short processing cycles, tolerance of solvents and environment. However, composite processing technology of fiber reinforced thermoplastic materials is very immature compared to thermoset technology. Unlike the thermosetting composite processing, where environmentally absorbed water is a critical factor in the formation of voids, absorbed moisture is only a minor contribution to the formation of voids in the thermoplastic composite (polyimide processing). Avimid K-III polymer (DuPont Co.) is amorphous, linear chain, condensation polyimide, which is produced from polyimide precursor solution by the reaction of aromatic diethyl ester diacid with aromatic diamine in the presence of solvent NMP (N-Methyl-2-Pyrrolidinone). The solvent in the initial prepreg in necessary to ensure the wettability and adherence of the resin to the fibers. The reaction proceeds with loss of water, ethanol, and solvent to form the imide ring. Volatile species (H_2O, CH_3CH_2OH and NMP) are evolved at the bleeder as polymerization takes place.

It is believed that a scientific understanding of the release of volatiles and the formation of voids within polyimide matrix composites is a prerequisite to their extensive use in aircraft primary structures and in other applications. Requirements for higher temperature-capable, damage-tolerant composite materials are driving designers to consider thermoplastic polyimides as viable alternatives to state-of-the-art thermoset bismaleimides. However, if these design opportunities are to become reality, polyimide composite processing must be improved substantially.

B. Research Objectives

The overall objective of this research is to study the formation, growth, and transport of voids during a condensation polymerization process in the presence of fiber reinforcement. The purpose of the current work is to present the framework of a model for the devolatilization of polyimides as a function of cure cycle, and to demonstrate its usefulness for scale-up and cure cycle selection. The specific objectives for this research are:

- Formulate a model for the devolatilization process of thermoplastic composites.
- Predict the effects of the major variables on the product quality, such as heating rate, vacuum cycle, composite thickness. Investigate the key model parameters effects on model performance, i.e. the gas phase permeability and the mass transfer coefficient at the liquid/gas interface.
- Experimentally determine the key model parameters

- Verify the model prediction with experimental results.

C. Research Accomplishments

The system under consideration is a porous medium consisting of three phase as shown in Figure 1. The solid phase σ (fiber) is considered as inert; liquid phase β (resin) is assumed to be stationary because of its high viscosity; gas phase γ (volatiles) is assumed to be continuous, with transport occurring by diffusion and convection. The complex geometry of the porous medium makes it difficult to solve the transport equations. A different set of governing equations will arise for each phase and there is no way of knowing a priori in which phase an arbitrary point lies. In order to achieve solvable equations which are valid throughout the composite, the point equations need to be volume averaged to include the effect of each phase on the whole. Thus the method of local volume averaging is used for modeling the devolatilization process.

Since the ratio of thickness/length is very small, a one dimensional model is employed. The mathematical model is developed for one dimensional heat, mass, and momentum transfer based on local volume averaging. The model consists of seven coupled partial differential equation: heat balance on laminate; overall mass balance on liquid phase; species mass balances on water, ethanol and NMP; mass balance on active group in monomer and polymer chains; overall mass balance on gas phase (pressure). The evaporation rate of the ith volatile component is calculated locally by:

$$\dot{m}_i = K_m A_\beta (\gamma_i \phi_i P_i^{sat} - Y_i P) \tag{1}$$

where K_m is the mass transfer coefficient at the interface between the liquid and vapor phase, A_β is the interfacial area for mass transfer per unit volume of the composite, γ_i is the activity coefficient of the ith volatile component, ϕ_i is the volume fraction of species i in the liquid phase, P_i^{sat} is the saturation vapor pressure of pure component i, Y_i is the molar fraction in the gas phase and is estimated by:

$$Y_i = \frac{\dot{m}_i / M_{Wi}}{\sum_{i=1}^{3} \dot{m}_i / M_{Wi}} \tag{2}$$

Here $\dot{m}_i$ is the liquid-gas local volatilization flux of component i and M_{Wi} is the molecular weight of i. The mass flux for the ith component at the bleeder is $V_\gamma \rho_{\gamma i}$. Darcy's law is employed to compute the gas velocity V_γ.

A finite element collocation method based on the method of lines was utilized to solve the seven coupled partial differential equations. Several packages have been tested and the DPDE subroutine in the IMSL package (1983) was chosen for simulation due to its efficiency and accuracy.

Figure 2 shows the model predictions for the cumulative mass fluxes of volatiles at the bleeder for the heating rate of $0.5°K/min$ to the maximum temperature of $360°C$, laminate thickness of 0.64 cm, initial vacuum of $50mmHg$ and full vacuum of $20mmHg$ starting at $115°C$ (corresponding to industrial practice). The cumulative mass fluxes at the bleeder based on an overall mass balance result in the following total evaporation amount per unit area: $W_{H_2O} = 1.365 \times 10^{-2} g/cm^2$,

$W_{CH_3CH_2OH} = 3.494 \times 10^{-2} g/cm^2$ and $W_{NMP} = 6.534 \times 10^{-2} g/cm^2$. This is in excellent agreement with Figure 2. Comparing Figure 2 with Figure 3, which presents the experimental results taken under the same process conditions, it is evident that the model predictions are in good agreement with the experimental evidence.

The computed pressure profiles through the laminate are shown in Figure 4. It is seen from this figure that uneven distributed mesh points, with more mesh points concentrated near the bleeder, should be utilized in order to represent the pressure gradients well near the bleeder. The pressure gradient determines the mass flux at the bleeder. Figure 5 illustrates the normalized pressure (P/P_{VAC0}) at the tool surface as a function of cure cycle for the cases of both constant initial vacuum (50 $mmHg$) and full vacuum (20 $mmHg$, applied starting from $T = 115\,^{\circ}C$). Figure 6 shows the dimensionless temperature profile through the laminate ($T_0 = 300\,^{\circ}K$). The maximum temperature difference between the tool surface and the laminate surface is less than $10\,^{\circ}K$ for the laminate thickness of $0.64cm$.

Figure 7 illustrates the effect of full vacuum on the cumulative mass fluxes at the bleeder. One concludes from this figure that full vacuum ($20mmHg$) is not necessary for removing H_2O and CH_3CH_2OH because the first term inside the parentheses of equation (1) is dominant. However, full vacuum at later stages of devolatilization is required to remove the solvent NMP, otherwise some solvent will be left inside the laminate.

The effects of heating rates and composite thickness on cumulative fluxes were also investigated. It is formed that if the heating rate is too fast for a thick laminate, the volatiles, especially the solvent NMP, will not be evaporated at low temperatures before the composite viscosity builds up. This results in some solvent or by-products being left in the composite after devolatilization. This should be avoided by decreasing the heating rate. However, the heating rate should not be too small since this will increase the time necessary for the devolatilization process. On the other hand, a slow heating rate is desirable to avoid the formation of large voids since large amount of volatiles in a thick laminate may cause bulk flow of gas phase. Thus, heating rate and void formation has to be balanced.

D. Further Research Plan

- Experimentally determine the key model parameters, such as the gas phase permeability and the mass transfer coefficient at the gas/liquid interface as a function of cure cycle.
- Justify Darcy's law validity for volatiles flow
- Recommend the best cure cycle for processing the thermoplastic composites

Bibliography

1. J. L. Kardos, M. P. Duduković, Yubo Yang and I. S. Yoon, "Processing Science of Thermoplastic Composites: Condensation Reaction Void Modeling", Air Force Contract *No. F33615-85-C-5046*, Seventh Quarterly Interim Report, Materials Research Laboratory, Washington University, St.Louis, MO., October 1988; Eighth Quarterly Interim Report, January 1989.

2. Kurz, J. E., G. D. Deucker, A. R. Mallow, F. R. Muncaster, and J. L. Kardos "Processing Science of Thermoplastic Composites", Air Force Contract *No. F33615-85-C-5046*, Fourteenth Quarterly Interim Reports, Air Force Materials Laboratory, Wright-Patterson AFB, 1 October 1988 - 31 December 1988.

3. Wedgewood, A. R., "Autoclave Processing of Condensation Polyimide Composites Based on Prepregs of Avimid K-III", 19th International SAMPE Technical Conference, Vol. 19, 420 (1987)

4. Flory, P. J., *Principles of Polymer Chemistry*, Cornell University, Ithaca (1953)

5. Biesenberger, I. A. and D. H. Sebastian, *Principles of Polymerization Engineering*, John Wiley and Sons, New York (1983)

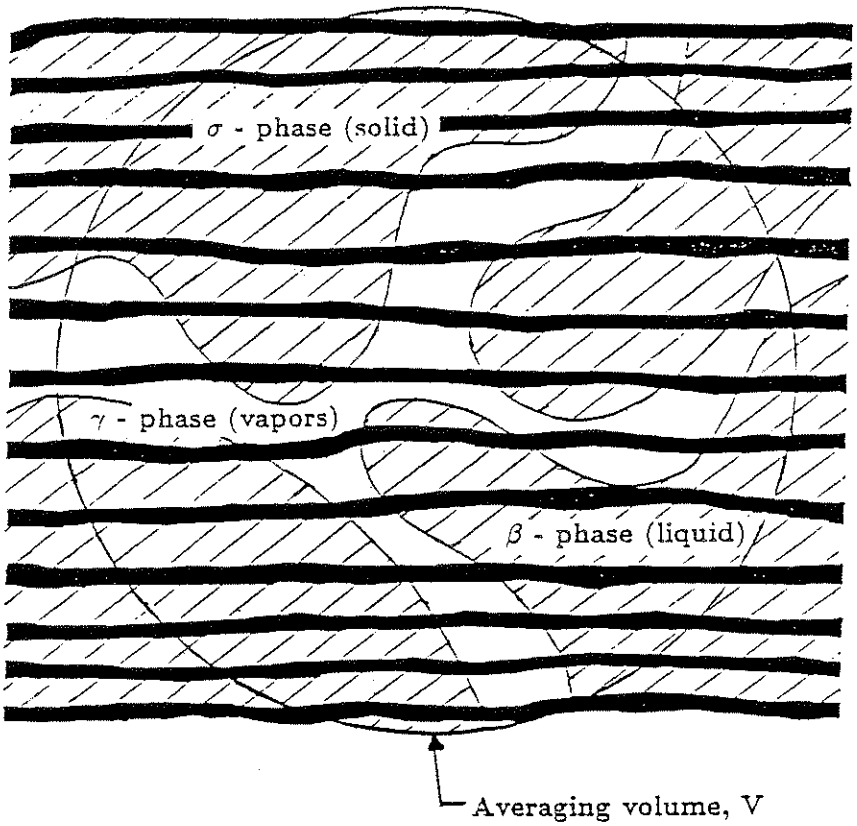

Figure 1. Schematic of Three Phase System

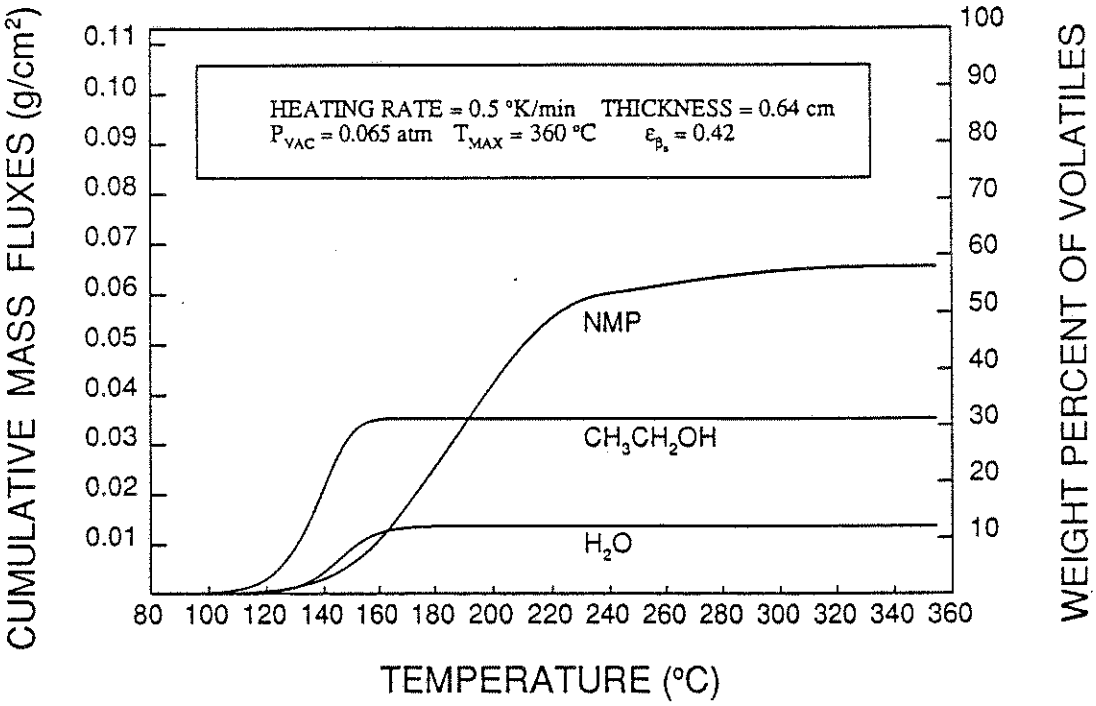

Figure 2. Model Predictions of Cumulative Mass Fluxes at the Bleeder

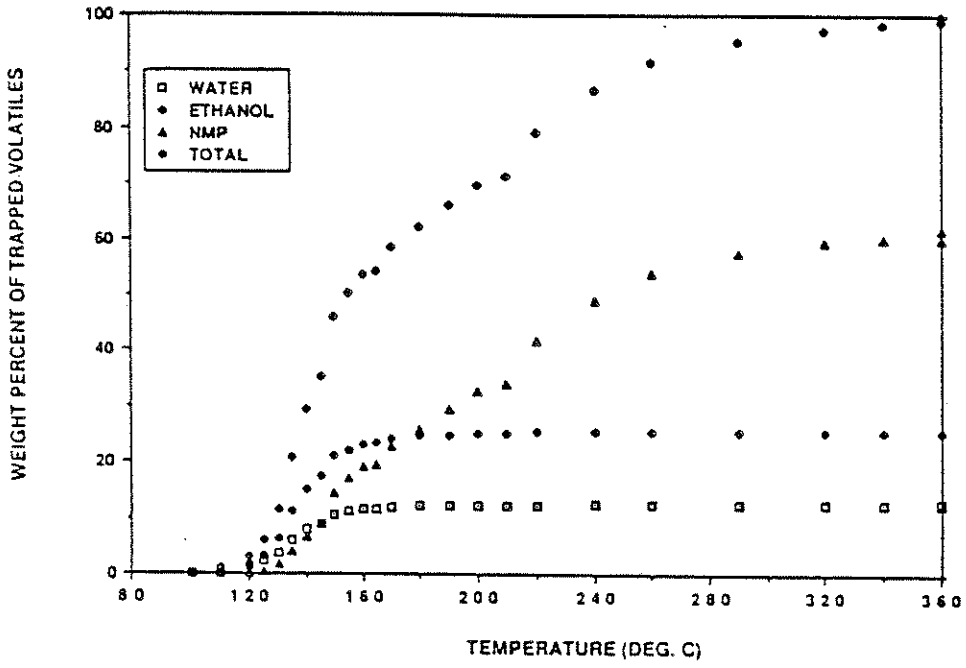

Figure 3. Experimental Results of Cumulative Mass Fluxes at the Bleeder under the Same Conditions as in Figure 2

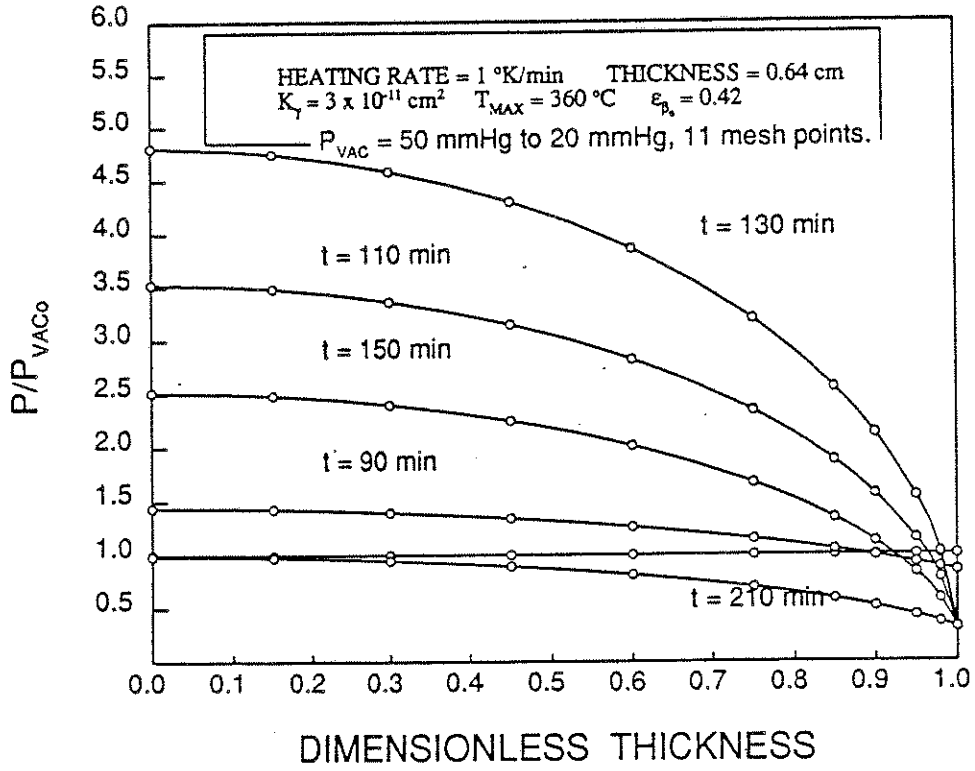

Figure 4. Computed Pressure Profiles along the Laminate as a Function of Temperature

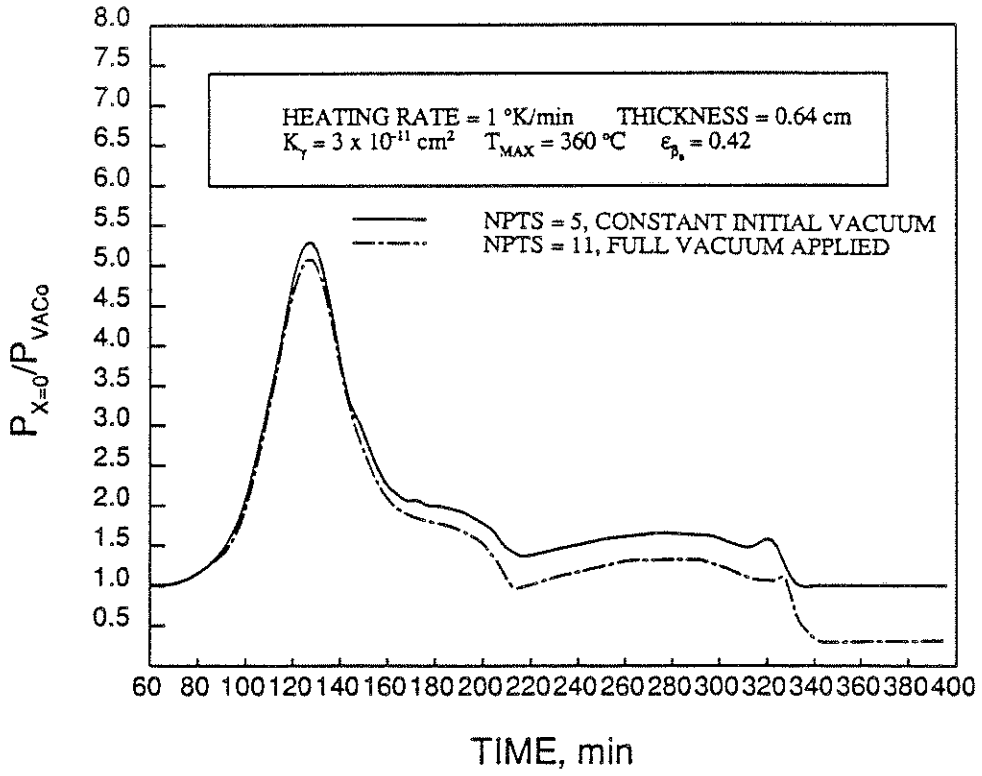

Figure 5. Computed Pressure Profiles at the tool Surface as a Function of Time

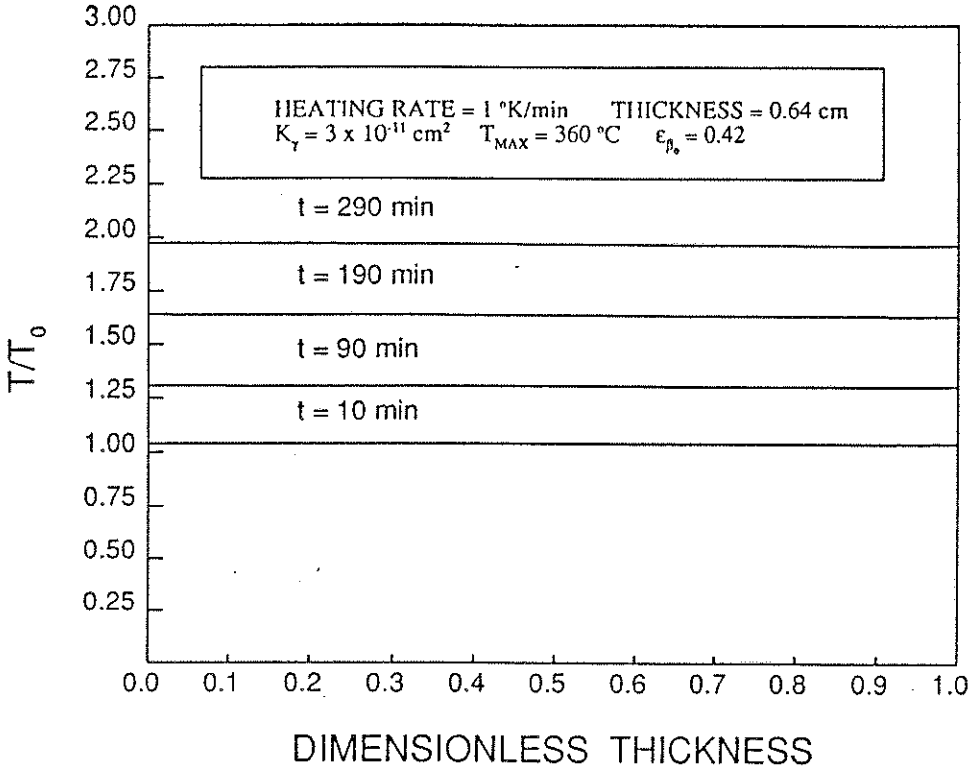

Figure 6. Temperature Profile along the Laminate

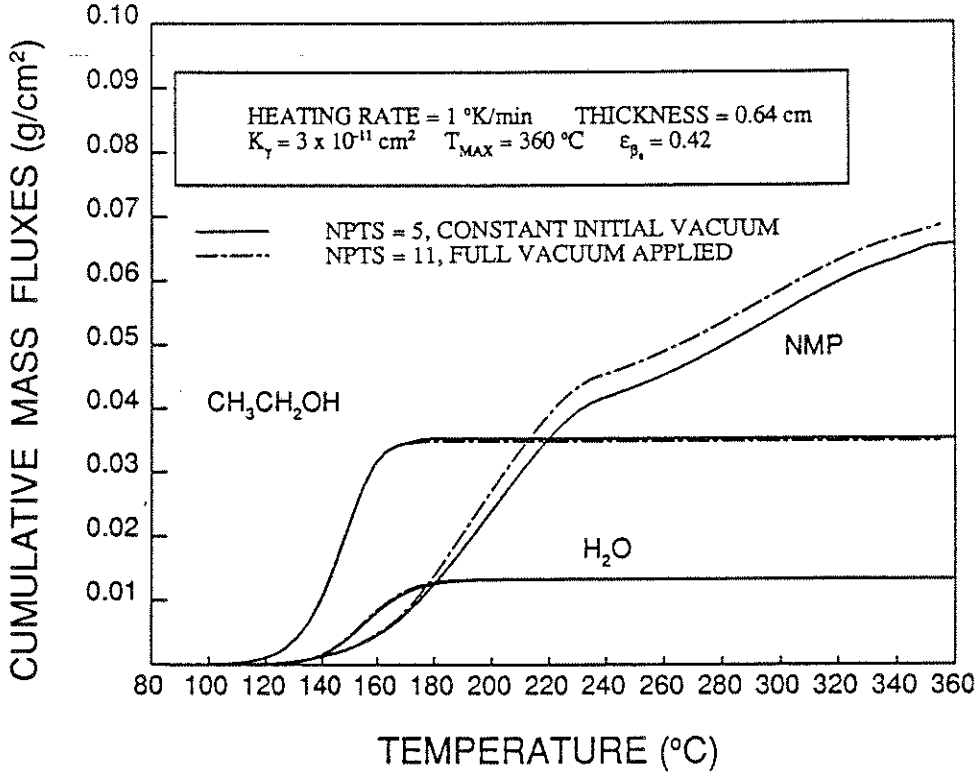

Figure 7. Cumulative Mass Fluxes at the Bleeder as a Function of Vacuum Cycle

AREA III. EXPERT SYSTEMS AND CONTROL

The emphasis is on introducing and testing expert systems into various reaction engineering tasks.

The goal is to examine the utility in reaction engineering of the latest advances in computer-expert system-artificial intelligence technology.

STRUCTURE AND IMPLEMENTATION OF A KNOWLEDGE-BASED SYSTEM FOR CATALYTIC REACTOR DESIGN

A. Problem Definition

In the design of a catalytic reactor, the design engineer can typically start with a number of different catalysts for which to carry out a particular reaction(s) to produce some desired product(s). His job is to pick the catalyst, the reactor type, the reactor dimensions, and the reactor conditions which will be the most profitable.

In order to reliably and accurately accomplish this task, one must determine the physical properties which are pertinent to the reaction system and the reactor type chosen, and how these properties affect the reactor performance. Typically, the needed model properties and their effects are determined from cited work of others and by experimentation. The needed model parameters and their effects unfortunately can not be generalized for all systems, and therefore they must be (re)determined for each new reactor design.

A well-directed project will minimize the amount of experimentation and work that needs to be done to characterize the reactor. A poorly directed project will add to the time and the difficulty of the design, and quite often to a poorly designed reactor. The direction for these projects is usually based upon personal , company and/or colleagues knowledge of and experience in the design process.

The knowledge required for reactor design is widely scattered in the literature. Most textbooks approach reactor design from a fundamental perspective. The need for numerical calculations preclude the development of a manual that can be used easily by practicing engineers. Companies try to resolve this problem by designating some individuals as experts in this area. However, there are problems because experts may not be readily available. This results in increased expenditures in the design stage and sometimes an inferior quality design.

B. Research Objectives

The objective of this project is to assemble, organize and implement a knowledge-based computer system which will aid and direct the engineer in the design process of catalytic reactors with the goal of a more efficient and knowledge directed process. The knowledge for the expert system will come from literature and the experience and knowledge of Dr. Dudukovic, Dr. Mills and Dr. Ramachandran. Other peoples' input will be sought and added as the project progresses.

C. Research Accomplishments

Presently, the information and the knowledge needed to construct the expert

system is being gathered and organized. For the first stage in the development of the expert system, a proto-type expert system concentrating on the design of the trickle-bed reactor is being developed. From the prototype expert system, we hope to show the viability of this project and to gain insight on how to organize and develop the system on a grander scale (i.e incorporate more reactor types or add more detail to the prototype system).

The proposed system is currently organized into eight sections interrelated (shown below). The below organization is temporary and probably will be changed and updated as the project develops.

1. Selection and characterization of the catalyst
2. Determination of the reaction mechanism and intrinsic kinetics
3. Characterization of the the fluids (gas and liquid) physical and transport properties
4. Preliminary design of an experimental reactor
5. Analysis of the experimental data from the laboratory reactor
6. Suggested additional studies to be done based upon the above data analysis
7. Scale-up of the experimental reactor to either pilot plant or full scale
8. Trouble shooting and operating suggestions for the reactor

Note that each of the above sections may require considerable input from the user. This input may be in the form of experimental results or the solution of a mathematical or modelling problem. Therefore, this system is not being built with the goal of eliminating experiments and the need for engineering knowledge, expertise and creativity, but with the idea of directing and making more efficient use of these entities. It should also help reduce the chance of overlooking some possibly important design considerations.

D. Future Work

Develop a proto-type expert system for the design of trickle-bed reactors. Based upon the prototype system, develop a full-scale expert system.

KNOWLEDGE-BASED CONTROL IN MANUFACTURE OF COMPOSITE MATERIALS

A. Problem Definition

Operation and control of composite manufacturing typically relies on experience of operators. This causes problems in the quality and cost of the product, because people do not make decisions consistently. Problems also arise when experienced operators leave their job and take their knowledge about the process away. Expert system technology provides some solutions to these problems by conserving expertise of experienced operators in the knowledge base which can be used repeatedly. Previous understanding of the process can also be cast into the form of mathematical models and integrated into the expert control system to simulate the process. The power of the computer can thus be fully utilized to provide decision making support to the operators.

B. Research Objectives

The objective of this project is to build, implement and test a knowledge-based control system for the manufacturing of polymer composites via pultrusion and autoclave processes. Specifically, research will focus on the following:

1. Develop a mathematical model for numerical simulation of the process.
2. Develop a general architecture for the knowledge-based control system.
3. Extract knowledge through numerical simulation of the process.
4. Implement the knowledge-based control system.

C. Research Progress and Results

So far, the focus of this project has been partly on obtaining a good understanding of pultrusion and autoclave processes through the development of mathematical models and numerical simulation using these models. The heat transfer and curing reaction model given by Han et al. (1986) in the pultruded materials has been extended to simulate the unsteady state response of the process. Similar formulation for heat transfer in the die is also added to the model. Figure 1 and 2 give some simulation results of the pultrusion process. The mathematical model of the autoclave process is based on formulations of Dave (1986). This model can predict temperature and resin conversion distributions in the composite laminate as function of position and time. Thickness and viscosity changes are also simulated. Typical results from this simulation are given in Figure 3 and 4.

Progress has also been made in developing an architecture for the knowledge-based control system. The architecture developed in this project is an extension of the concept of a blackboard model originally proposed by Hayes-Roth (1986). A scheme of the architecture is given in Figure 5. The mathematical model and past experiences in operating the process are integrated in this hybrid symbolic/numeric reasoning architecture.

D. Future Work

Perspective goals of this project in the following period are:

1. Extract knowledge about the process through simulation study.
2. Build the knowledge-based control system using a C-based expert system shell.
3. Test the knowledge-based control system.

E. References

Dave, R., "Computer Aided Processing of Composites", D. Sc. Thesis, Washington University (1986).
Han, C. D. and Lee, D. S., "Development of a Mathematical Model for the Pultrusion Process", Polymer Engineering and Science, 26(6), 393 (1986).
Hayes-Roth, B., "A Blackboard Architecture for Control", Artificial Intelligence Journal, 26, 251 (1986).

Figure 1.
Composite Curing Using Pultrusion

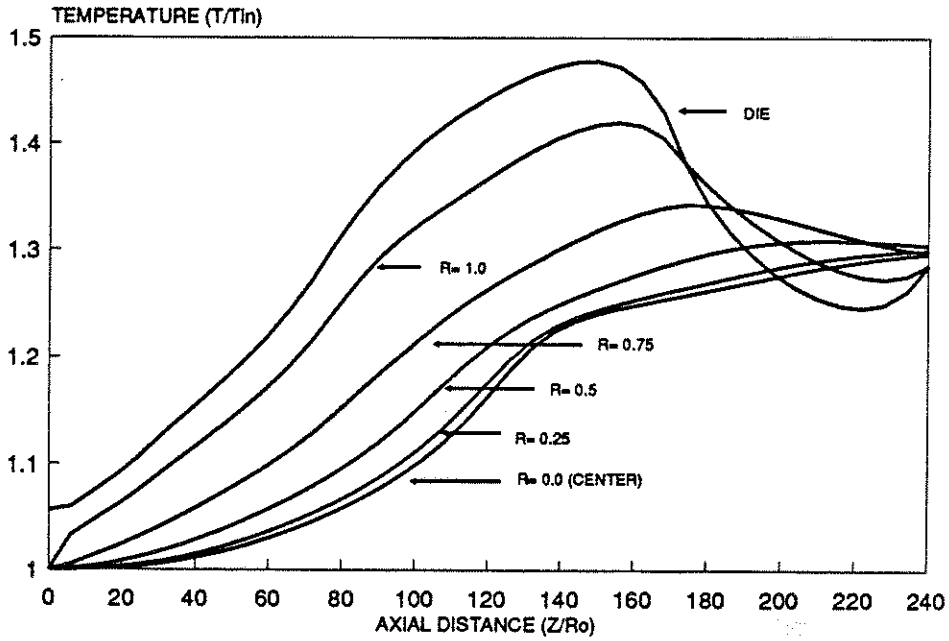

Figure 2.
Composite Curing Using Pultrusion

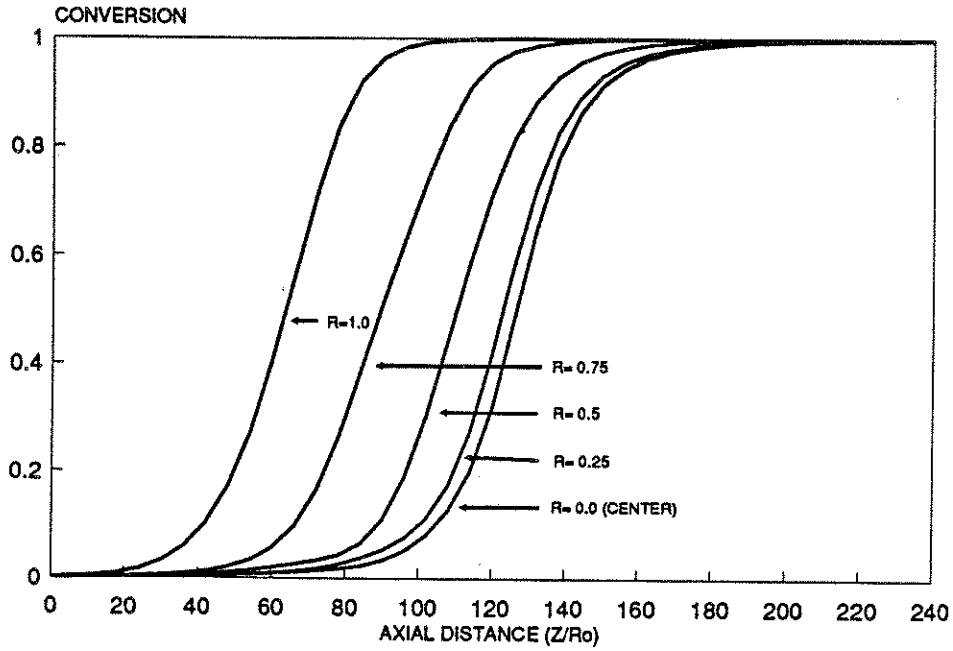

Figure 3.
Composite Curing Using Autoclave Process

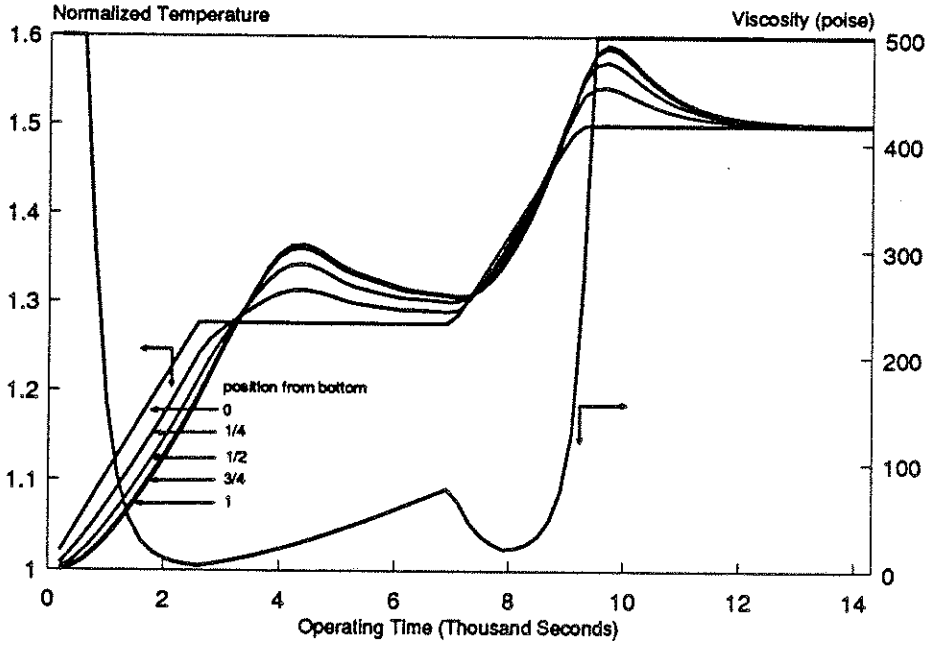

Figure 4.
Composite Curing Using Autoclave Process

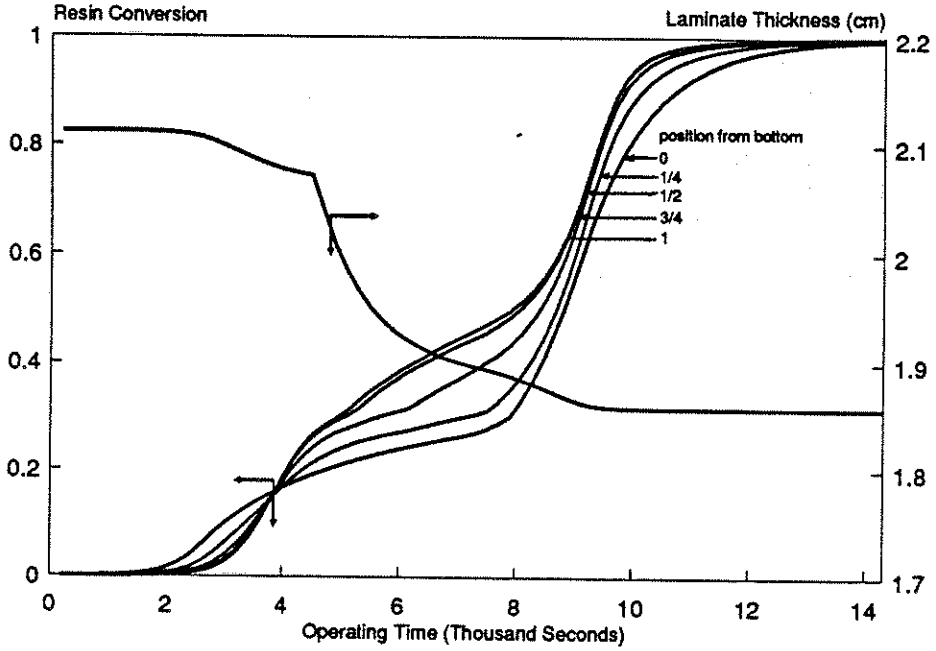

Figure 5.
Knowledge-Based Control System

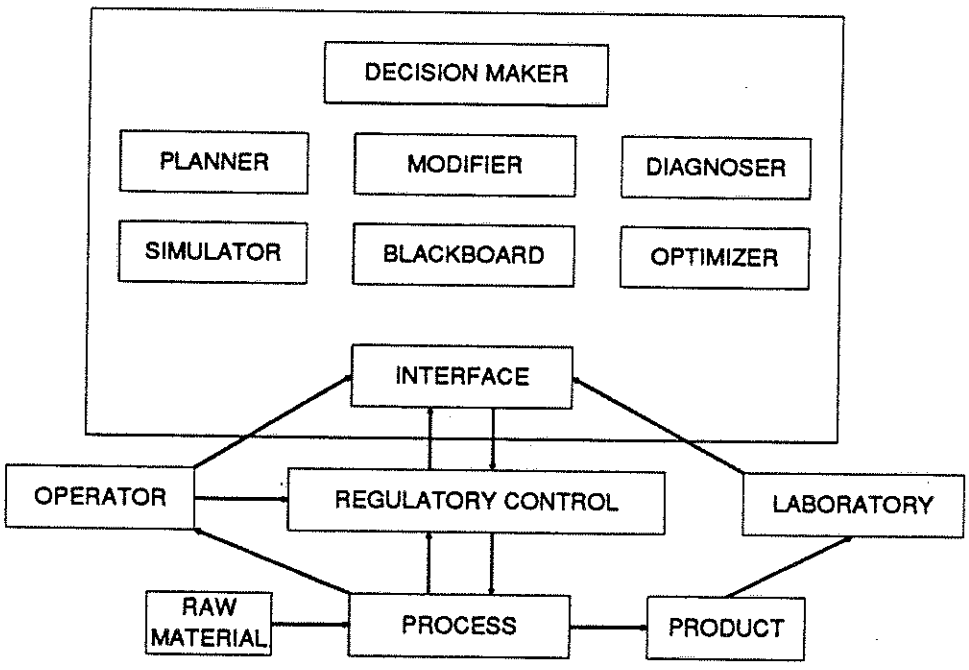

APPLICATION OF GENETIC ALGORITHMS AND NEURAL NETWORKS IN PROCESS CONTROL

A. Problem Definition

A lot of work is being done in developing expert systems to aid process control, especially for complex and ill-defined processes. One major problem that hinders the application and development of expert systems is the difficulty of knowledge acquisition. The traditional method of knowledge acquisition - joint efforts of knowledge engineers and experts - is quite lengthy and inefficient. This suggests the possible assistance from automatic knowledge acquisition. In addition, large records of operating data and some mathematical simulation information are available for a lot of processes. Considerable amount of knowledge can be explored by manipulating the past data and utilizing the simulation information. This suggests learning from examples, or inductive learning.

Among all the inductive learning methods, genetic algorithms and artificial neural networks are known for their adaptive nature. This is an attractive feature, especially with complex and ill-defined processes for which our knowledge is incomplete or even uncertain.

Genetic algorithms seek improved performance by sampling areas of a solution space with high probability of success. The algorithms combine some string manipulation similar to the mechanics of natural genetics and a survival-of-the-fittest mechanism.

Artificial neural networks provide subsymbolic processing and knowledge representation. The networks use patterns of activity distributed over a large network composed of simple neuron-like processing elements locally interacting through a set of weighted connections.

Both genetic algorithms and neural networks promise the ability to adapt and continue learning to improve performance.

B. Research Objectives:

The objective of this research project is to synthesize, implement and test the application of genetic algorithms and neural networks to assist knowledge acquisition for expert system development. Specifically, research will focus on the following:

1. Select the most suitable genetic algorithm and neural network to fit our process control application.
2. Implement and test the algorithm and network.
3. Modify and improve the algorithm and network to make it applicable and effective for a wide range of processes.

C. Research Accomplishments:

So far, the focus of this project has been on obtaining a good and broad understanding of genetic algorithms and neural networks. A simple genetic algorithm has been implemented to control a pure, inertial object in a frictionless, one-dimensional domain.

D. Future Research Plan

The prospective goals of this project are:

1. Modify the implemented genetic algorithm to control a more realistic and complex problem.
2. Implement, test and modify a suitable neural network.

E. References:

Goldberg, D., "Genetic Algorithms in Search, Optimization & Machine Learning," Addison-Wesley, Inc., 1989.
Rumelhart, D. E. and McClelland, J. L., "Parallel Distributed Processing," Vol.1, The MIT Press, 1986.
Hoskins, J. C. and Himmelblau, D. M., "Artificial Neural Network Models of Knowledge Representation in Chemical Engineering," Comput. Chem. Engng. Vol.12, No.9/10, 1988.

AUTOMATIC KNOWLEDGE ACQUISITION PROCEDURES FOR PROCESS AND QUALITY CONTROL USING ROUTINE DATA

A. Problem Definition

Expert system is defined as a computer program which can function as an expert in the specific area of the real world. One of the first publicized expert systems, MYCIN, devised by E. Shortliff (1976) at Stanford University, has been used successfully in medical diagnosis. Since then, the development of expert systems has been sprouting in many areas (Hunt, 1986), such as SECHS in chemical synthesis, HODGKINS in medical diagnosis, IDT in Computer faults, DENDRAL in chemistry, et al. But so far, few commercial expert systems are visible in the market (Parnas, 1988).

Expert systems, traditionally, are the creation of joint efforts of knowledge engineers and experts. Knowledge engineers who have the full knowledge of hardware and software of computer systems, would elicit expertise in a specific area from experts. To effectively acquire knowledge from experts such as process engineers, and foremen, knowledges engineers need to attain a certain level of expertise. At least, they must fully understand the terminologies of process engineering including transport phenomena, reaction engineering, etc. Besides experts tend to simplify or to give a statement without an explanation. As a result, the knowledge acquisition is fragile and requires many iterations. In the chemical engineering domain, the operation and control philosophy of each process is unique and hard to generalize. Obviously, automatic knowledge acquisition ,which is also called machine learning, can be of great help in building a knowledge base for the use of expert control systems, particularly for those ill-defined processes.

On the other hand, since the Distributed Control Systems (DCS) have been implemented in plants, large records of operating data are available on storage. Considerable process-dependent knowledge can be explored by manipulating and analyzing those operational routine data with the help of relational database management, statistics and inductive methods. This automatic knowledge acquisition process can be conducted off-line by batch operation to use computer idle time, say, in the evening or weekend.

To demonstrate how to acquire knowledge automatically, the autoclave process is used as an example.

B. Research Objectives

1) To investigate machine learning techniques in eliciting knowledge from routinely collected data. In computer science, the above form of acquiring knowledge is called learning from examples (Cohen & Feigenbaum, 1982). Four kinds of algorithms have been used in the way of learning from examples: namely induction, statistical correlation, genetic algorithm, and neural network. This report focuses on the first two kinds of techniques, i.e. induction and statistical correlation.

2) To investigate how to link a machine learning module (MLM) with a knowledge base module (KBM) as shown in Figure 1. There are three phases of interactions between them. The first phase is to pass generated knowledge by MLM to KBM. The different techniques used in MLM could generate different forms of knowledge. It is necessary to convert those various forms into a production rule (or other forms) which are adopted to represent knowledge in KBM. Also, there are several expertise domains existing in KBM. It might be necessary to classify generated knowledge before storing in KBM. The second phase is to utilize the existing knowledge in KBM to help acquire knowledge in MLM by routinely collected data. The last phase is to resolve the conflict

if the newly generated knowledge in MLM is contradictory to the present knowledge in KBM.

C. Research Progress and Results

Some progress has been made on the first objective of this project. Three different kinds of induction algorithms were programmed in the C programming language to acquire knowledge from the data which were generated by a simulator of an autoclave process. The first algorithm called ID3 (Quinlan, 1986) uses a concept derived from information theory to generate a decision tree. It would need a little extra effort to convert a decision tree into a set of production rules. PRISM (Cendrowska, 1987), another induction algorithm, generates a set of production rules directly. Both algorithms can handle qualitative data only. Therefore, a data type conversion is needed to acquire knowledge using these two algorithms when quantitative data are collected from an autoclave simulator (Wu, 1989). To overcome this restriction, Breiman et al. (1984) presented the CART algorithm which generates a binary decision tree. The basic algorithm is similar to that of ID3.

The autoclave process is used to manufacture composite materials by curing fiber reinforced thermosetting resin matrix prepregs. The curing cycle as well as operating parameters of this batch process are usually predetermined. Due to a broad variation of raw prepregs, it is difficult to set the operating parameters properly. To search for the optimum setting of parameters for a given prepreg matrix, a training set, which consists of routine data with the parameters given below in Table 1, is provided. In order to be used by ID3 and PRISM, the operational range of temperatures t_0, t_1, t_2, and a pressure P_r, during various parts of the cycle, which are operating parameters shown in Figure 2, is divided into several subranges and are designated as I, II, III, IV.

operation parameter	I	II	III	IV
t_0 (°K)	300-314	315-329	330-344	345-360
t_1 (°K)	368-372	373-397	398-412	413-428
t_2 (°K)	430-444	445-459	460-474	475-490
P_r (atm)	1.5-1.9	2-2.9	3-3.5	

Table 1 : The conversion of quantitative data to qualitative data

Good product is defined by absence of bubbles, i.e. small void size, composite thickness within the certain range, and very high degree of curing. Quantitatively, we set these measures of product quality as follows: D_b (the diameter of gas bubble which is assumed spherical) < 0.06cm, 1.685 cm < L (final thickness of composite) < 1.75 cm, and α (the extent of curing) > 0.999. The results using the three induction algorithms, ID3, PRISM, and CART to get the good product, are shown in Figure 3, Table 2, and Figure 4 respectively.

In order to have more comprehensive rules, further generalization of rule-sets is necessary. Rules after being trimmed are shown in Table 3. The final sets of rules by the three algorithms are very similar. We almost obtain the same final set of rules in ID3 and PRISM except that Rule 2 in ID3 has a superfluous term.

Scrutinizing the generalized rules by PRISM in Table 3, several conclusions can be reached for the operation of this given prepreg matrix. 1) The operation parameter t_0 is not important for quality control. 2) The proper combination of the elevated temperatures t_1 & t_2 will reduce the sensitivity to the applied pressure P_r, because the elaborate selection of t_1 and t_2 can smooth the growth of bubble size and the conversion of reaction which would increase the viscosity of composite and consequently confine the growth of bubble without a high applied pressure. 3) Otherwise, as described by Rule 1 & 4, where the first elevated temperature t_1 or the second elevated temperature t_2 is so high that bubble grows very fast, a high applied pressure is necessary.

From the above demonstration, the results of this work are simply summarized as follows. Induction methods can be used to explore the relationship between operating parameters and product quality. Among the existing algorithms, PRISM and CART are suggested to be used for qualitative and numerical data sets, respectively.

D. Future Work

1. The algorithm of acquiring knowledge by statistical correlation method is under investigation. The data used in this algorithm involves time domain.
2. The integration of knowledge generated in machine learning module with knowledge base module in expert systems is to be studied.

E. Bibliography

Breiman, L., Friedman, J. H., Olshen, R. A. & Stone, C. J., "Classification and Regression Trees," Wadsworth, Inc., 1984.

Cendrowska, J., "PRISM: An Algorithm for Inducing Modular Rules," in Int. J. Man-Machine Studies, 27, 1987, pp. 349-370.

Cohen, P. R. & Feigenbaum, E. A., "The Handbook of Artificial Intelligence," Vol III, Addison-Wesley, Inc., 1982.

Hunt, V. D., "Artificial Intelligence and Expert System Sourcebook," Chapman & Hall, 1986.

Quinlan, J. R., "Induction of Decision Trees," in Machine Learning 1(1), 1986, pp. 81-106.

Parnas, d. L., "Why Engineers Should not Use Artificial Intelligence," in INFOR, 26(4), 1988.

Wu, H. T., "Simulation of Autoclave Process," Technical Report, Department of Chemical Engineering, Washington University in St. Louis, 1989.

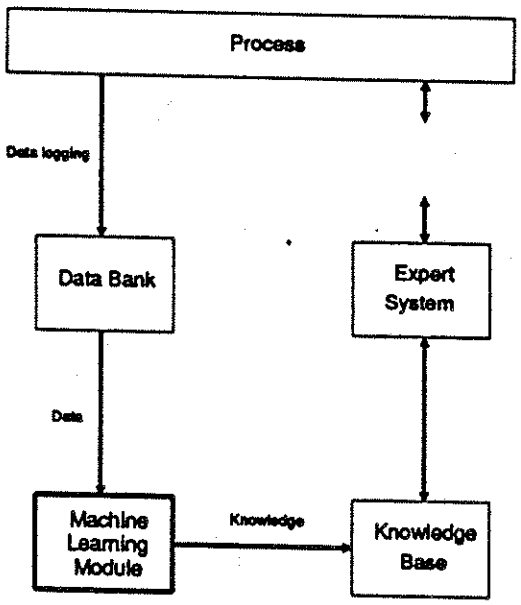

Figure 1: Schematic of an expert system

Rule #	IF	THEN
1	t_2 = III & P_T = II	Good
2	t_2 = IV & P_T = II	Good
3	t_2 = III & P_T = III	Good
4	t_2 = IV & P_T = III	Good
5	t_1 = III & t_2 = II	Good
6	t_1 = II & t_2 = III	Good
7	t_1 = II & t_2 = IV	Good
8	t_1 = III & t_2 = III	Good
9	t_1 = III & t_2 = IV	Good
10	t_1 = IV & t_2 = II & P_T = II	Good
11	t_1 = IV & t_2 = II & P_T = III	Good
12	t_2 = I	No good
13	t_1 = II & t_2 = II	No Good
14	t_1 = I & t_2 = II	No Good
15	t_1 = IV & P_T = I	No Good
16	t_1 = I & P_T = I	No Good

Table 1: Rules generated by PRISM

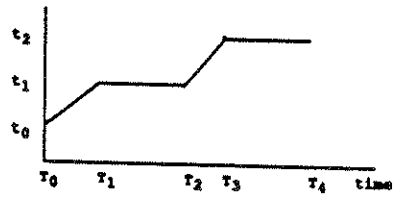

Figure 2: A predetermined cycle of Autoclave process

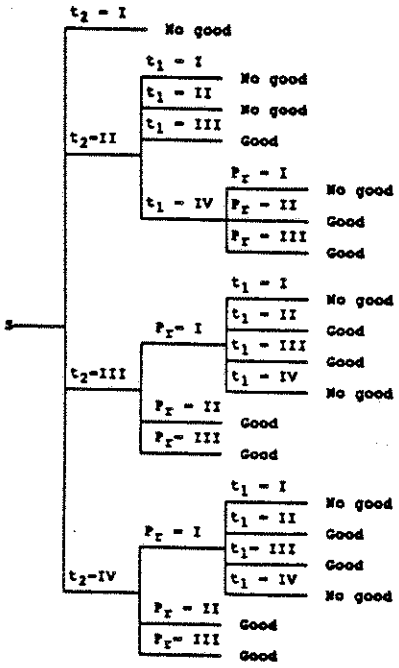

Figure 3: The decision tree generated by ID3

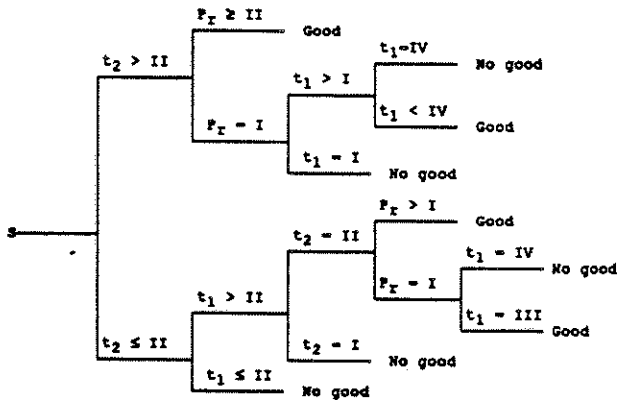

Figure 4: The decision tree generated by CART

Rule #	IF	THEN
1	$t_2 \geq$ III & $P_r \geq$ II	Good
2	II≤ t_1 ≤III & $t_2 \geq$ III & Pr = I	Good
3	t_1 = III & t_2 = II	Good
4	t_1 = IV & t_2 = II & $P_r \geq$ II	Good
	(By ID3)	
1	$t_2 \geq$ III & $P_r \geq$ II	Good
2	II≤ t_1 ≤III & $t_2 \geq$ III	Good
3	t_1 = III & t_2 = II	Good
4	t_1 = IV & t_2 = II & $P_r \geq$ II	Good
	(By PRISM)	
1	$t_2 \geq$ III & $P_r \geq$ II	Good
2	II≤ t_1 ≤III & $t_2 \geq$ III & Pr = I	Good
3	$t_1 \geq$ IV & t_2 = II & $P_r \geq$ II	Good
4	t_1 = III & t_2 = II & P_r = I	Good
	(By CART)	

Table 2: The final generalized rules

MODEL ACCURACY CONSIDERATIONS IN MODEL-BASED CONTROL

A. Problem Definition

Recently, due to the availability of on-line process computers and the increased demand for productivity and efficiency in manufacturing, several computer-based algorithms have been developed. The main attention is now focused on model uncertainty. To cope with this difficulty, many researchers emphasize the design of robust controllers. Since we can never know the exact model in detail, it is necessary to have robust controllers as a means of coping with the uncertainty. However, making controllers insensitive to the model uncertainty causes the performance to deteriorate. Most practical engineers have some knowledge about the characteristic of the process and would agree that developing and validating a suitable model is the most reasonable approach to improve the quality of the control system. It is worth reconsidering this approach because of the increased demand on automatic control systems in industry.

B. Research Objectives

The purpose of this project is to develop criteria for improving model accuracy based on statistical methods. To make this research more practical, the model accuracy should be considered from the following aspects:

(1) Process model structure
Suitable model structure can be different according to the requirements of the control strategy used. It is necessary to establish a common criterion for evaluating the accuracy different model types.

(2) The quality of input disturbances or operating conditions
To maximize confidence in parameter estimates, suitable input disturbances are essential.

(3) Measurement selection and error detection
Generally, a choice of measurements is available to control engineers. There is a question of where, how many, and what kind of sensors to use. Another issue is error detection. Measurements are not totally random. We have to detect such undesired measurements and minimize their effect.

(4) Decision making
Developing and validating process models is expensive. We have to consider the trade-off associated with the cost of improving the model accuracy and the economic return from it.

C. Research Accomplishments

C1. Model discrimination
A common criteria for model discrimination is based on factorial design of experiments to get a wide variety of data and then comparing the goodness of fit. Box (1963,1967) proposed another method based on information theory. For a test system, temperature profile in a metal rod heated at one end, our studies show that the factorial design can lead to erroneous conclusion regarding model accuracy. The criterion developed by Box is shown to be superior.

C2. The accuracy of parameter estimates
Suitable input disturbances and data-selection are necessary for achieving the desired accuracy of parameter estimates. We developed a new criterion considering the above two points (selective elimination design). The changes of estimated parameters in the heated bar process using selective elimination design are shown in Fig.1 (In this simulation example, bias is added at the specific location.). The effect of bias on the estimated parameters, namely, heat transfer coefficient and surrounding temperature, can be reduced with this algorithm.

C3.Measurement selection
We are investigating the best location of measurements when we are given a number of sensors. The variance of the errors in the parameters can be used to place the sensors.

D.FUTURE RESEARCH PLAN

(1) Developing criteria for decision making in model-based control systems using sensitivity analysis

(2) Application to other process examples

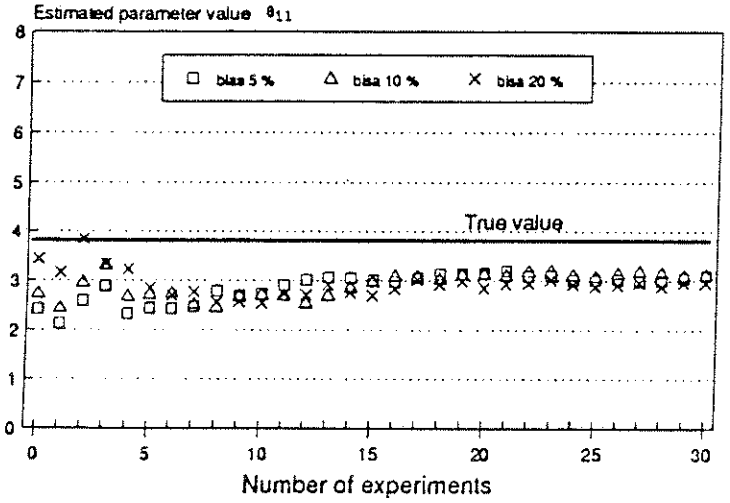

Fig.1 Effect of biased data on the parameter estimate
using selective elimination design
(θ_{11} = heat transfer coefficient)

E. BIBLIOGRAPHY

(1) Box,G.E.P.;Hunter,W.G. " Sequential Design of Experiments for Nonlinear Models " Proc. IBM Sci. Comput. Symp. Statist., IBM,White Plains,NY,1963.
(2) Box,G.E.P.;Hill,W.G. " Discrimination among Mechanistic Models " Techometrics,1967,9,57.
(3) Bard,Y. Nonlinear Parameter Estimation, Academic Press, NY,1974.

CURRENT FUNDING

The external support of CREL during the period covered by this report (June 1, 1988 through May 31, 1989) was derived from various sources.

Industrial participation fees were essential in supporting the research in all areas. They amounted to $120,000.

Rotating packed-bed research was supported by a continuing NSF grant at $60,000/year.

Control and expert system project was supported by an NSF grant of $66,000/year and a supplemental NSF undergraduate research grant of $7,200.

CURRENT STAFF (1988/89)

During the period covered by this report (June 1, 1988 through May 31, 1989) the following individuals have been associated with the various projects in the laboratory.

A. Faculty

Dr. Milorad (Mike) Duduković, Professor and Director
Dr. Babu Joseph, Associate Professor
Dr. P. A. Ramachandran, Associate Professor
Dr. G. Gao, Visiting Scholar
Dr. Y. B. Yang, Research Associate

B. Graduate Students

M. Al Dahhan
A. Bašić
S. J. Choi
N. Devanathan
D. Dorsey
H. Erk
P. Hanratty
R. Holub
K. Kage
V. Kalthod
D. O'Connor
S. Pirooz
D. Shieh
J. Turner
H. T. Wu
Y. B. Yang
I. S. Yoon

INDUSTRIAL ADVISORY BOARD (1988/89)

L. P. Bosanquet	Monsanto
G. Vaporciyan	Shell Development
J. Cropley	Union Carbide
H. Hensley	Phillips Petroleum
R. E. W. Jansson	Monsanto
M. Joshi	Eastman - Kodak
F. Krambeck	Mobil
F. X. Mayer	Exxon
P. L. Mills	Autoclave Engineers
B. L. Tarmy	Exxon
P. Wanser	British Petroleum

CREL PUBLICATIONS AND PRESENTATIONS

A. PAPERS AND CHAPTERS

1. "A Numerical Study of Approximation Methods for Solution of Linear and Nonlinear Diffusion-Reaction Equations with Discontinuous Boundary Conditions", P. L. Mills, S. Lai, M. P. Dudukovic and P. A. Ramachandran, Comp. Chem. Eng., 12(1), 37-53 (1988).

2. "Determination of Binary Gas Diffusion Coefficients in Spherical Porous Media by Steady and Unsteady-State Analysis of Single Pellet Reactor Data", S. P. Waldram, P. L. Mills and M. P. Dudukovic, Mathl. Comp. Modeling, 11, 38-42 (1988).

3. "Approximation Methods for Linear and Nonlinear Diffusion-Reaction Equations with Discontinuous Boundary Conditions", P. L. Mills, S. Lai, M. P. Dudukovic and P. A. Ramachandran, SIAM J. Sci. Stat. Comput., 9(2), 271-288 (1988).

4. "A Finite Element Solution for Diffusion and Reaction in Partially Wetted Catalysts with Power-Law Kinetics", P. L. Mills, S. Lai, M. P. Dudukovic and P. A. Ramachandran, Ind. Eng. Chem. Res., 27, 191-199 (1988).

5. "Modeling Hysteresis Phenomena in Systems of Multiple Slits: Application of the Principle of a Minimum Rate of Entropy Production at Steady-State", R. A. Holub, P. A. Ramachandran and M. P. Dudukovic, Mathl. Comput. Modeling, 11, 26-31 (1988).

6. "Voids in Composites", J. L. Kardos, R. Dave and M. P. Dudukovic, in The Manufacturing Science of Composites - IV (Gutowski, T. G., ed.), ASME, NY, 1988, pp. 41-48.

7. "The Effect of Flow on Mixing and Performance of Radial Flow Electrochemical Reactors", F. B. Thomas, P. A. Ramachandran, M. P. Dudukovic and R. E. W. Jansson, Chem. Eng. Science, 43, 2013-2018 (1988).

8. "Laminar Radial Flow Electrochemical Reactors I. Flow Fields", F. B. Thomas, P. A. Ramachandran, M. P. Dudukovic and R. E. W. Jansson, J. Appl. Electrochemistry, 18, 768-780 (1988).

9. "Deconvolution of Noisy Tracer Response Data by a Linear Filtering Method", P. L. Mills and M. P. Dudukovic, AIChE J., 34, 1752-1756 (1988).

10. "Simulation of Fixed-Bed Gas-Solid Reactors Using an Adaptive-Spline Collocation Method", A. Bhattacharya and B. Joseph, Comp. Chem. Engr. 12(4), 351-353 (1988).

11. "Integrated Model Based Control of Multivariable Nonlinear Systems", B. Joseph, S. S. Jang and H. Mukai, Proceedings IFAC Workshop on Model Based Process Control, Am. Automatic Control Council (1988).

12. "Mathematical Modeling of Chemical Engineering Systems by Finite Element Analysis Using PDE/PROTRAN", P. L. Mills and P. A. Ramachandran, Comp. Math. Applic., 15, 769 (1988).

13. "Catalytic Hydrodesulfurization of a Specialty Agricultural Chemical Intermediate", S. J. Tremont, P. L. Mills and P. A. Ramachandran, Chem. Eng. Sci., 43, 2221 (1988).

14. "Modeling and Guidelines for the Autoclave Process", R. S. Dave, J. L. Kardos, and M. P. Duduković, Adv. Materials in Future Transp. Design SP 754, SAE Techn. Paper Series 881180, 1-9 (1988).

B. BOOKS

1. B. Joseph: Real-Time Personal Computing for Data-Acquisition and Control. Prentice Hall, New Jersey, 1988.

C. PRESENTATIONS

1. "Radial Flow Electrochemical Reactors", B. Thomas, M. P. Duduković and P. A. Ramachandran, ISCRE 10, Basel, Switzerland, August, 1988.

2. "Modeling of the Komatsu Decomposer for Production of Polycrystalline Silicon, Y. B. Yang, and M. P. Duduković, AIChE Annual Meeting, Washington, D.C., November, 1988, paper 38f.

3. "Hydrodynamics of Trickle-Bed Reactors: A Diagnostic Model for Phase Maldistribution", R. Holub, M. P. Duduković and P. A. Ramachandran, AIChE Annual Meeting, Washington, D.C., November, 1988, paper 45a.

4. "Modeling of the Aerosol Reactor for Production of Polycrystalline Silicon", Y. B. Yang and M. P. Duduković, AIChE Annual Meeting, Washington, D. C., November, 1988, paper 62j.

5. "Temporal Analysis of Products (TAP): An Experimental and Modeling Study of TAP Microreactor Performance", P. L. Mills, B. S. Zou, J. T. Gleaves and M. P. Duduković, AIChE Annual meeting, Washington, D.C., November, 1988, paper 124f.

6. "The Use of Expert System Technology for Batch Process Control: An Evaluation of Some Tools", B. Joseph, B. Allen and H. T. Wu, AIChE National meeting, Houston, April, 1989.

7. "Architecture of a Knowledge-Based Control System for Batch Manufacturing Process, H. T. Wu and B. Joseph, AIChE One-Day Symposium, St. Louis, April, 1989.

8. "A Review of Procedures for Automatic Knowledge Acquisition Using Routine Data in Process and Quality Control, D. Shieh and B. Joseph, AIChE One-Day Symposium, St. Louis, April, 1989.

D. SHORT COURSES OFFERED BY CREL

1. "Reaction Engineering for Multiphase Reactors"
   P. L. Mills, M. P. Dudukovic and P. A. Ramachandran
   3-day short course offered through the AIChE Continuing Education Program

Summer AIChE Meeting	-	Denver, August, 1988
Annual AIChE Meeting	-	Washington, D.C., November 1988
Spring AIChE Meeting	-	Houston, April, 1989
Summer AIChE Meeting	-	Philadelphia, August, 1989
Annual AIChE Meeting	-	San Francisco, November, 1989

2. "Microcomputers for Data Acquisition and Control"
   B. Joseph
   3-day short course offered through the AIChE Continuing Education Program and in Modified Version on Washington University Campus

Summer AIChE Meeting	-	Denver, August, 1988
Annual AIChE Meeting	-	Washington, D.C., November, 1988
Spring AIChE Meeting	-	Houston, April, 1989
Upjohn Company	-	Michigan, November, 1988
Washington University	-	St. Louis, March and May, 1989

E. D. SC. THESES

1. D. Dorsey, "Oxygen Transport in Czochralski Growth of Single Crystal Silicon", D.Sc. Thesis, Washington University, St. Louis, MO, December, 1988.

2. Y. B. Yang, "Transport-Kinetic Effects in Manufacture of Polycrystalline Silicon", D.Sc. Thesis, Washington University, St. Louis, MO, December, 1988.

F. D. SC. PROPOSALS

1. D. O'Connor, "The Crystal Growth of α-FeOOH (Goethite) in Aqueous Solution at High pH", D.Sc. Proposal, Washington University, St. Louis, MO, August, 1988.

2. S. Pirooz, "Modeling of Direct Current Plasma Processes", D.Sc. Proposal, Washington University, St. Louis, MO, November, 1988.

3. B. S. Zou, "Quantification of the TAP Experiments", D.Sc. Proposal, Washington University, St. Louis, MO, December, 1988.

G. M. S. THESES

1. K. Kage, "Model Accuracy Considerations in Model Based Control", M.S. Thesis, Washington University, St. Louis, MO, May, 1989